View metadata, citation and similar papers at core.ac.uk
brought to you by CORE
provided by edoc

STRUCTURE ELUCIDATION OF THE WATER-SOLUBLE ORGANIC CARBON FRACTION IN ATMOSPHERIC AEROSOLS BY MASS SPECTROMETRY

Inauguraldissertation

zur
Erlangung der Würde eines Doktors der Philosophie
vorgelegt der
Philosophischen-Naturwissenschaftlichen Fakultät
der Universität Basel

von

Fernando Romero

aus Birsfelden (BL)

Basel 2006

Genehmigt von der Philosophisch-Naturwissenschaftlichen Fakultät
auf Antrag von

Prof. Dr. Michael Oehme
Prof. Dr. Johannes Stähelin

Basel, den 6. Juni 2006

Prof. Dr. Hans-Jakob Wirz
Dekan

The present thesis was carried out under the supervision of Prof. Dr. M. Oehme in the laboratories of the Organic Analytical Chemistry at the University of Basel in Switzerland.

ACKNOWLEDGMENTS

First I would like to express my sincere gratitude to Prof. Dr. M. Oehme for his supervision, advice, support and inspiration as well as for his confidence to let me work in generous freedom. Thanks for giving me the possibility to work with modern analytical techniques.

All dear present and former work mates in Basel: Anita Ciric, Dorrit Griesshaber, Jana Hüttig, Klauser Lucia, Langlois Ingrid, Reth Margot, Sonja Skopp, Stephan Brombacher, Elie Fux, Saverio Iozza, Alexander Kotz, Sven Heekmann, Fabian Stapf, Simon Trinkler and Zdenek Zencak thanks for a phantastic working environment and cheerful private experiences.

A special thank goes to Mathias Jecklin for his valuable scientific contributions to this thesis during his stage in our laboratories.

I would also to acknowledge Dr. M. Baumann from the meteorological station in Binningen as well as M. Camenzind of the "Lufthygieneamt beider Basel" for providing the sampled aerosol filters for this thesis. Moreover, I would like to thank Mathias Wild (Basilea Pharmaceutica Ltd., Basel) for the experiments on the TOF-MS.

Thanks to Prof. Dr. H. Puxbaum for stimulating scientific discussions and for providing me with material and equipment.

Thanks to Dr. J. Figueiredo and Dr. S. Sack for letting me carry out experiments on their equipment at Syngenta AG (Basel).

Finally, I would also thank my parents, Asunción Fernández Pérez and Fernando Romero Navarro and all my friends for their support over all the years of this thesis.

TABLE OF CONTENTS

ABBREVIATIONS

ACN	Acetonitrile
CID	Collision induced dissociation
CCN	Cloud condensation nuclei
EC	Elemental carbon
EI	Electron ionisation
ESI	Electrospray ionisation
FA	Fulvic acids
FTICR	Fourier transform ion cyclotron mass spectrometer
GC	Gas chromatography
GC-MS	Gas chromatography coupled with mass spectrometry
HA	Humic acids
HPLC	High performance liquid chromatography
HULIS	Humic-like substances
IT	Ion trap mass spectrometer
LC-MS	Liquid chromatography coupled with mass spectrometry
MeOH	Methanol
MS	Mass spectrometry
MS-MS	Tandem mass spectrometry
MS^n	Consecutive multiple fragmentation
m/z	Mass-to-charge ratio
OC	Organic carbon
PAH	Polycyclic aromatic hydrocarbons
PC	Principal component
PCA	Principal component analysis
PTFE	Polytetrafluoroethylene
PM_{10}	Aerosols with a diameter ≤10 μm
$PM_{2.5}$	Aerosols with a diameter ≤2.5 μm
PM_1	Aerosols with a diameter ≤1 μm
R^2	Correlation coefficient
SAX	Strong ion exchange sorbent
SIM	Single ion monitoring
SPE	Solid phase extraction
TC	Total organic carbon
TOF-MS	Time of flight mass spectrometry
TMAH	Tetramethyl ammonium hydroxide
WINSOC	Water-insoluble organic carbon
WSOC	Water-soluble organic carbon

SUMMARY

Atmospheric aerosols can act as cloud condensation nuclei (CCN) and scatter or absorb light thus influencing many important processes in the atmosphere. The CCN activity of atmospheric aerosols depends mainly on the water solubility of their chemical components. Besides inorganic salts also polar and water-soluble organic compounds are responsible for the water solubility of atmospheric aerosols. Humic-like substances (HULIS) constitute a major part of the water-soluble organic carbon (WSOC) fraction of atmospheric aerosols and may thus be largely involved in cloud condensation processes. However, hitherto little is known about the chemical composition and structure of HULIS.

Structure elucidation was performed by different mass spectrometric techniques of the WSOC fraction and specially of HULIS from atmospheric aerosols collected in the city of Basel. HULIS were cleaved into smaller substructures by thermochemolysis using tetramethylammonium hydroxide (TMAH). The simultaneously methylated substructures were separated by gas chromatography and detected by mass spectrometry (GC-MS). Furthermore, composition and fragmentation behaviour of HULIS were studied by liquid chromatography coupled to ion trap multiple mass spectrometry ($LC\text{-}MS^n$).

Structure elucidation of the WSOC fraction by thermochemolysis GC-MS

Solid phase extraction (SPE) was applied to separate the HULIS from the rest of the WSOC and inorganic compounds. Analysis of HULIS by thermochemolysis GC-MS revealed that aliphatic monocarboxylic acids (C_9, C_{10}, C_{12}, C_{14}, C_{16} and C_{18}), aliphatic dicarboxylic acids ($C_{4\text{-}10}$), mono-, di- and trihydroxylated benzoic acids, as well as benzenedicarboxylic and benzenetricarboxylic acids were the main substructures. However, HULIS could not be completely analysed by thermochemolysis GC-MS. A dark brownish residue persisted after thermochemolysis. Its chemical composition remained unknown, since no further structural information could be retrieved by pyrolysis.

Reference compounds such as fulvic acids, humic acids and lignin were analysed by thermochemolysis GC-MS as well. Their substructures were very similar to those of HULIS, which indicated fossil fuel burning or combustion of lignin containing biomass as possible sources. Moreover, thermochemolytical degradation of model compounds containing ester and ether groups was investigated. Aromatic esters, and esters with aliphatic and aromatic partial structures degraded easily. However, aromatic ethers and ethers with aliphatic and aromatic partial structures were less prone to cleavage. In conclusion, HULIS probably contain aromatic esters, and esters with aliphatic and aromatic partial structures rather than aromatic ethers and ethers with aliphatic and aromatic partial structures.

Principal component analysis was used to compare the fingerprint patterns in the thermochemograms of HULIS taken at different sampling dates. A seasonal variation of the composition was observed. HULIS composition of spring, summer and autumn samples seemed to be similar. However, HULIS from November, December, January and February were completely separated from the rest. Hydroxylated aromatic carboxylic acids were more abundant in the HULIS of these filter samples. Aliphatic dicarboxylic acids seemed to be typical for HULIS in spring, summer and autumn filter samples.

Structure elucidation of the WSOC fraction by LC-MS

WSOC was separated into five fractions using a HPLC column containing a 300 Å pore size reversed stationary phase. Mass spectrometry revealed that HULIS in fractions I-IV consisted of polar compounds of lower mass with a mass distribution between *m/z* 100-400 and a maximum at *m/z* 240. HULIS in fraction V were less polar substances of higher mass with a mass distribution between *m/z* 100-900 and a maximum at *m/z* 500.

MS^2 and MS^3 spectra showed that carboxylic and hydroxyl moieties were predominant functional groups of HULIS. Moreover, fragment *m/z* 97 was detected in most MS^2 and MS^3 spectra. TOF-MS and deuterium exchange experiments identified *m/z* 97 as HSO_4^-. These experiments supported the existence of sulphate covalently bound to

HULIS. Furthermore, a loss of -80 u (SO_3) was observed in the fragment spectra. However, it could not be clearly associated to sulphonated or sulphated HULIS as both sulphonation and sulphatation of HULIS are possible in the atmosphere.

Quantification of sulphate covalently bound to HULIS was performed by source fragmentation of HULIS detecting HSO_4^- as *m/z* 97. Combined concentrations in fractions I-V were similar to other polar organic compounds common in atmospheric aerosols. A slight seasonal trend was observed with higher concentrations in winter and summer than in spring and autumn. However, the trend might be within the normal fluctuation of the concentrations. Concentrations of inorganic HSO_4^- did not correlate with those of organosulphates, which indicated that sulphatation reaction of HULIS does not only depend on the amount of sulphate in the atmospheric aerosol, but on other factors such as temperature, solar irradiation, acidity of other chemical components present in aerosols.

Combined structural information obtained by thermochemolysis GC-MS and LC-MS allowed to propose defined structures for lower mass HULIS based on 2-3 substructures as well as for higher mass HULIS with 3-4 substructures. In addition, sulphate is covalently bound. The mass distributions of the postulated substructures were in good agreement with the recorded full scan spectra of HULIS.

1 INTRODUCTION

1.1 Atmospheric aerosols

An aerosol is a system of small solid or liquid particles suspended in a gas. Aerosols are also called particulate matter, aerosol particles or simply particles. They have to be very small to remain dispersed in air for longer periods. Atmospheric aerosols are well visible as dust, smoke or fume. Under certain meteorological conditions a very intense haze called smog is generated in big urban agglomerations due to heavy pollution by anthropogenic aerosols and other combustion gases. Moreover, atmospheric aerosols scatter sunlight, which is observable as a reddish light during sunset.

Large amounts of aerosols have an important effect on atmospheric processes including our climate (Seinfeld and Pandis, 1998). Moreover, health is affected by elevated concentrations (Brimblecombe, 1996). Especially water-soluble organic compounds are thought to be mainly responsible for climatic and health effects (Novakov and Corrigan, 1996). Detailed knowledge about the chemical composition of the water-soluble fraction of atmospheric aerosols is therefore of major interest.

In the following chapters the sources of atmospheric aerosols, and their effects on climate and health are explained. Moreover, sampling techniques for atmospheric aerosols are discussed. Finally, a general overview of the chemical composition of atmospheric aerosols is given.

1.1.1 Size of atmospheric aerosols

The size of atmospheric aerosols affects atmospheric transport and deposition, as well as the environment and health. Size is usually given in micrometers [μm]. In figure 1-1 the size and nomenclature for atmospheric particles are shown. The smallest particles are called Aitken particles (ca. 0.001-0.1 μm). Most of these are secondary particles

produced from chemical reactions in the atmosphere (see secondary aerosols). The majority of the mass of particulate material in the atmosphere consists of large and giant particles between 0.1 and 10 μm diameter. Coarse particles have a diameter of more than 10 μm (Brimblecombe, 1996).

A different classification system for aerosols in the atmosphere is given by sampling with impactors. Particles with a diameter of equal or less than 10 μm are termed PM_{10}. They comprise part of the giant and all of the large and Aitken particles. PM_{10} are of special concern because of their ability to enter the respiratory system (chapter 1.1.4; Brimblecombe, 1996; Hutzinger, 1995; Seinfeld and Pandis, 1998).

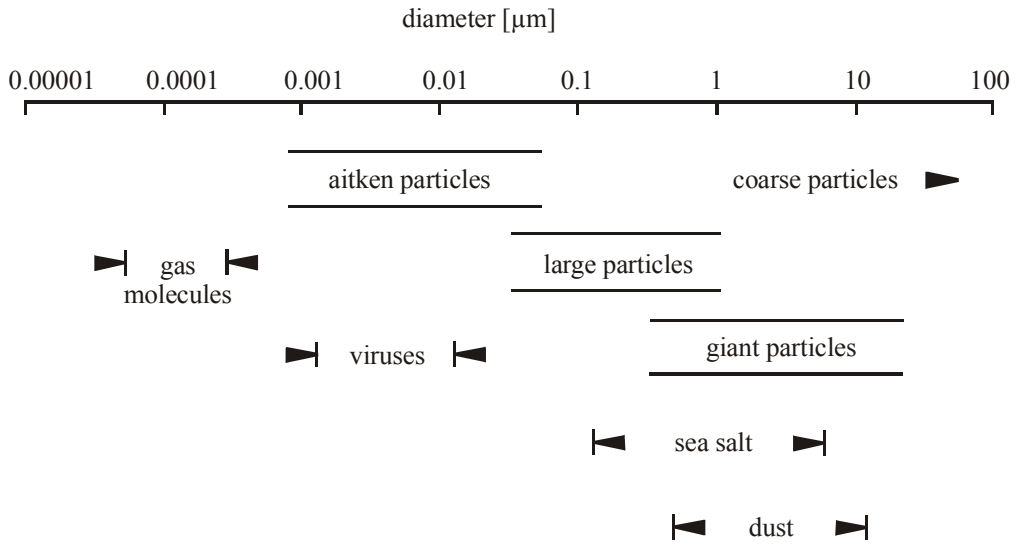

Figure 1-1. Size and nomenclature for atmospheric particles (Brimblecombe, 1996).

1.1.2 Sources of atmospheric aerosols

Primary Aerosols

Aerosols that are directly emitted into the atmosphere, are called primary aerosols. Sources for primary aerosols can be both biogenic and anthropogenic. The importance of the source depends on its location and the emission duration.

Oceans constitute a large and continuous source of biogenic primary aerosols. Bubbles from braking waves are the major source for sea salt aerosols. The production of bubbles occurs in the white foam caps, which cover about 2% of the sea surface. The bubbles usually burst at the top of the foam. Sea water droplets are then generated, which evaporate leading to concentrated sea salt droplets or little crystals of sea salt (Brimblecombe, 1996; Gelencsér, 2004; Hutzinger, 1995).

The suspension of dusts from dry areas is an important source of particles. Much of the mineral dust is very coarse and will quickly deposit (figure 1-2). However, finer atmospheric aerosols can be transported over long distances, e.g. dust from the Sahara is occasionally found in Europe (Brimblecombe, 1996; Gelencsér, 2004; Hutzinger, 1995).

Bioaerosols are particles of different biological origin, e.g. bacteria, pollen, fungal spores, viruses, fragments of insects, and other components of bioorganisms. Among bioorganisms, bacteria are most common in atmospheric aerosols. Furthermore, plants have been observed to emit particles directly into the atmosphere. In autumn the decay of leafs produces large amounts of particulate material. Different sources as well as meteorological conditions can cause strong variation in concentrations of bioaerosols (Brimblecombe, 1996; Gelencsér, 2004; Hutzinger, 1995).

During biomass combustion large amounts of small primary particles are generated. Forest fires can be strong local sources, emitting several tonnes of smoke per hectare. Not only the amount of released primary particles is important, but also the area they can disperse in the atmosphere (Brimblecombe, 1996; Gelencsér, 2004; Seinfeld and Pandis, 1998).

Erupting volcanoes are a further source of primary particulate matter, even if their emission is not continuous. However, once erupted, volcanoes can represent a source of very large amounts of particulate material in the atmosphere (Brimblecombe, 1996; Hutzinger, 1995).

Comet and meteorite debris are another source of biogenic primary aerosols. Extraterrestrial particles are found to a great extent in polar regions. Their total contribution to the atmosphere is rather small. However, a very large meteorite impact such as in Tunguska (Siberia in 1908) is able to introduce large quantities of dust into the atmosphere (Brimblecombe, 1996; Hutzinger, 1995).

Fossil fuel burning constitutes a large anthropogenic source for primary aerosols. Coal burning is with 70% the largest anthropogenic source of the global carbonaceous aerosol emission from fossil fuel sources. Vehicular emissions make up 20%. In addition, emission of particles from aircrafts is of high importance, since they are released in the upper atmosphere, where they have long residence times (Gelencsér, 2004).

Secondary aerosols

Secondary aerosols are formed by chemical reactions in the atmosphere. Formation mechanisms are complex. One possibility is shown in figure 1-2.

The main source of secondary aerosols is the atmospheric oxidation of SO_2 to sulphate and of NO_2 to nitrate. Sulphur and nitrogen containing gases are generated both biogenically and anthropogenically. Oxidation of these precursors occurs in the gas phase and in liquid droplets. Non-volatile products are formed, which either condense onto primary aerosol particles (nucleation range, figure 1-2) or form new condensation particles, which in turn coagulate to larger particles (accumulation range, figure 1-2).

Another important source of secondary aerosols is the generation of semi-volatile compounds by photooxidation of anthropogenic hydrocarbons and biogenic volatile organic compounds such as terpenes. The semi-volatile compounds condense and form new condensation growth particles coagulating to larger particles (accumulation range, figure 1-2).

Secondary oxidation processes can be very fast and can occur within seconds from the moment of emission of the primary particle. Secondary aerosol formation can even start much before condensation of primary particles happens. Therefore, the differentiation between primary and secondary aerosols is often very difficult and sometimes even impossible (Gelencsér, 2004; Hutzinger, 1995).

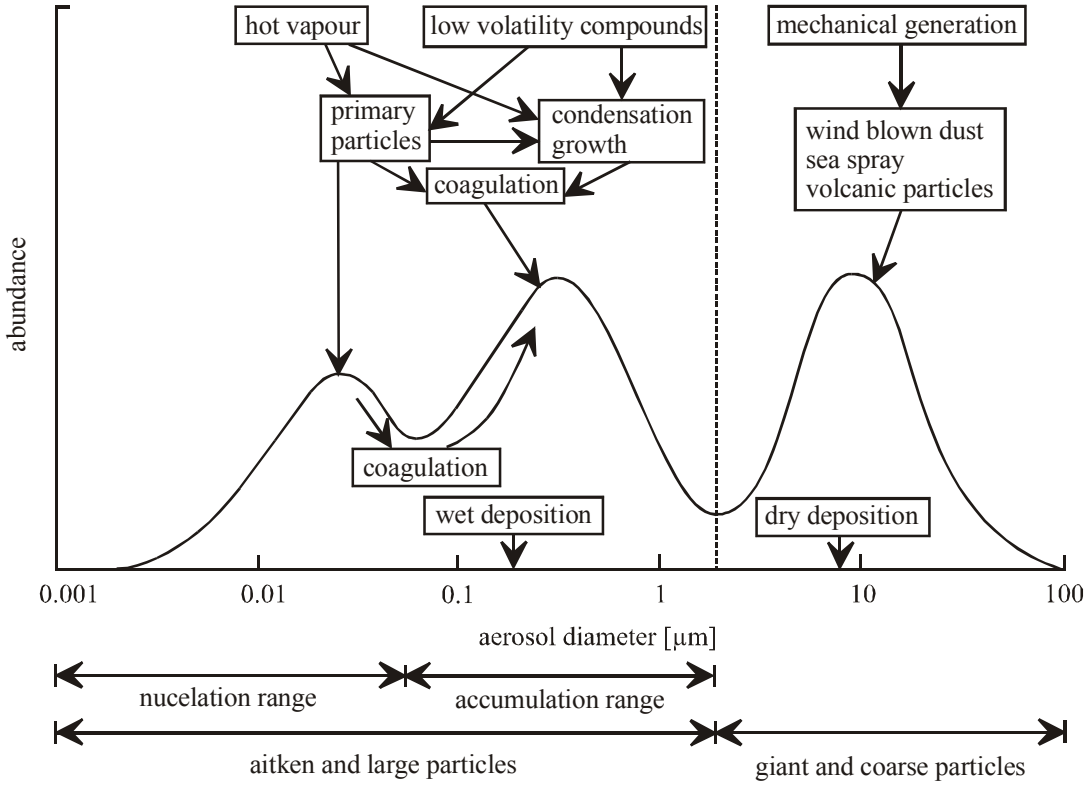

Figure 1-2. Schematic diagram of a typical size distribution and formation mechanisms of atmospheric aerosol (Hutzinger, 1995).

Aerosol sinks

Aerosols are removed from the atmosphere by two processes. Aitken particles will rapidly diffuse into cloud droplets or coagulate to large and giant particles (figure 1-2). This means that large and giant particles will accumulate in the air, because of their long residence times in the atmosphere (figure 1-2). They absorb water and are removed from the atmosphere by rainfall (wet deposition). Coarse particles will have a limited lifetime in the atmosphere and are rapidly deposited (dry deposition) (Brimblecombe, 1996; Hutzinger, 1995).

1.1.3 Effects on climate

Visibility is reduced in polluted atmospheres due to scattering and absorption of light by particulate matter affecting the radiation balance of the Earth. Moreover, atmospheric aerosols can influence cloud formation. Influences of aerosols on the climate are differentiated into direct and indirect effects.

Direct effects – absorption and scattering

Direct effects mean change of the solar radiation reaching the surface of the Earth by scattering and absorbing of atmospheric aerosol particles. The net effect of aerosols on the radiation balance depends on the relative amount of light scattered back to space versus the amount absorbed by the aerosols. Experimental and theoretical results suggest that scattering of light dominates. Overall, atmospheric particles tend to cool down the atmosphere, reducing the effects of greenhouse gases. Currently, a global cooling effect of ca. -0.5 to -2.0 Wm^{-2} is assumed (Brimblecombe, 1996; Hutzinger, 1995; Jacobson *et al.*, 2000; Seinfeld and Pandis, 1998).

Indirect effect - Cloud condensation nuclei

Supersaturation of water vapour of several hundred percent is necessary for the formation of water droplets in particle free air. Particles are thus essential for cloud formation in the atmosphere. Aerosol particles, which are capable of initiating drop formation are called “Cloud Condensation Nuclei” (CCN). Supersaturation of less than 2% is needed for cloud droplet formation in the presence of CCN. Aerosol particles can act as CCN depending on size, hygroscopicitiy and chemical composition. Hence, CCN are able to modify the cloud characteristics such as droplet number, droplet size and cloud lifetime. An increased emission of aerosols to the atmosphere generates a higher concentration of CCN, which in turn provokes a higher concentration of droplets with smaller radii in clouds. The result is an increased reflection of solar radiation from these clouds back to space and hence a cooling effect (Novakov and Corrigan, 1996; Novakov and Penner, 1993; Seinfeld and Pandis, 1998).

1.1.4 Effects on health

The size of particles influences their transfer into the lung. In figure 1-3 the deposition of various particle size fractions is shown in different parts of the respiratory tract. Only the smallest can enter the lung. Dissolution of solid material can occur, followed by transfer into the blood. Moreover, very small particles may mimic viruses, increasing physiological stress, and hence the probability of illness or death (Brimblecombe, 1996; Hutzinger, 1995).

A correlation between concentration of fine particles and illness or mortality has been found (Brimblecombe, 1996). Studies of the World Health Organisation reported that PM_{10} and particularly $PM_{2.5}$ in indoor air generated by biomass burning might have potential effects on human health. Particulate matter may aggravate asthma, cause respiratory infections, chronic bronchitis and other chronic pulmonary diseases (Bruce *et al.*, 2000; Tesfaigzi *et al.*, 2002). However, the health effects of extensive outdoor atmospheric pollution by industries, wood heating and traffic should not be underestimated.

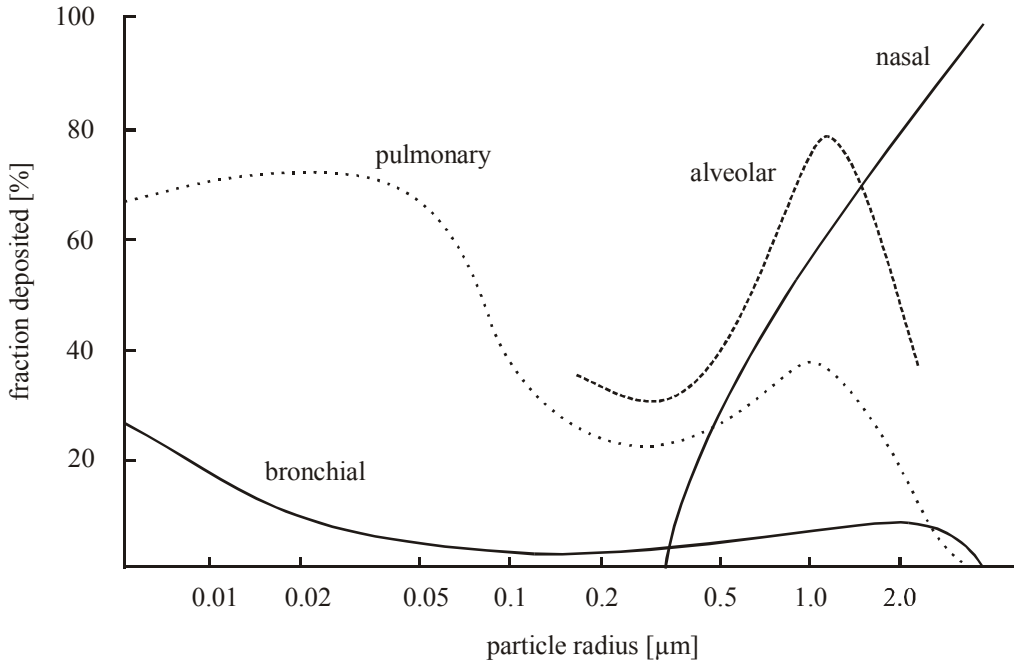

Figure 1-3. Fractions of particles of different size deposited in various parts of the respiratory tract (Brimblecombe, 1996).

1.1.5 Aerosol sampling

Several devices such as gravity collectors, cyclones, electrostatic precipitators and wet scrubbers can be used to collect aerosols (Hutzinger, 1995). However, a series of disadvantages make them not well suitable for accurate aerosol size sampling. These are poorly definable size cut-off or poor collection efficiencies for small aerosols like PM_{10}. Generally, impactors and filters are preferred.

Particle size sampling by Impactors

In an impactor the particle containing gas is passed through a acceleration nozzle, where particles are accelerated. The air stream is sharply deflected at the nozzle exit, so that particles larger than a certain size (the impactor's cut-off size) impact and stay on the collection surface. Smaller particles escape and follow the deflected air flow. Important parameters determining the cut-off size are the gas flow rate (Q), the nozzle diameter (W) and the position of the impactor plate (S) (figure 1-4).

Teflon filters and aluminium sheets are used as impaction surface for collection of particles. If impactors are used only as size cut-off device, the collection surface has to be coated with sticky material (e.g. common grease or silicone grease) to prevent particle bouncing. Impactors provide a very sharp size cut-off with very little contamination by larger particles (Hutzinger, 1995; Jacobson *et al.*, 2000). However, chemical contamination can occur by the grease applied to collect the larger particles. Impactors are used either to collect aerosols on the impaction plate or to size the particles, which are to be collected on a subsequent filter.

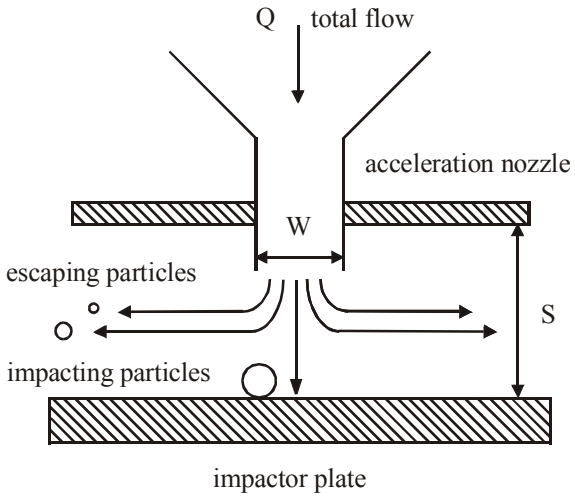

Figure 1-4. Schematic diagram of a conventional impactor. Particles exceeding a certain size cannot follow the gas flow and are separated from it by impaction on the plate (Hutzinger, 1995).

Filtering

Filtration is most widely used for particle sampling. It is considered as the most reliable, efficient and economical method removing particulate matter from gases. Atmospheric aerosols are usually collected on glass or quartz fibre filters. Possible organic contaminations can be removed by pre-heating. Filters can have collection efficiencies of more than 99%, down to a particle size of 0.3 μm. Fine particles are not trapped, if the filter pores are larger than the size of the dust. Therefore, the collection efficiency for small particles will be low, as long as not enough larger particles are deposited building up a dust layer, which is able to retain fine particles (Hutzinger, 1995).

Sampling of PM_{10}

Collection of PM_{10} is often carried out by a high volume sampler. It sizes aerosols by an impactor. The PM_{10} are collected on a glass or quartz fibre filter. Filters can be changed by an autosampler or manually. The main variable is the air flow, which controls the cut-off of the impactor. Usually high air volumes of typically 30 m^3/h are pumped through the collector by a turbine pump. $PM_{2.5}$ and PM_1 can also be collected

by installing an impactor with the corresponding cut-off. A scheme of a PM_{10} high volume sampler is shown in figure 1-5.

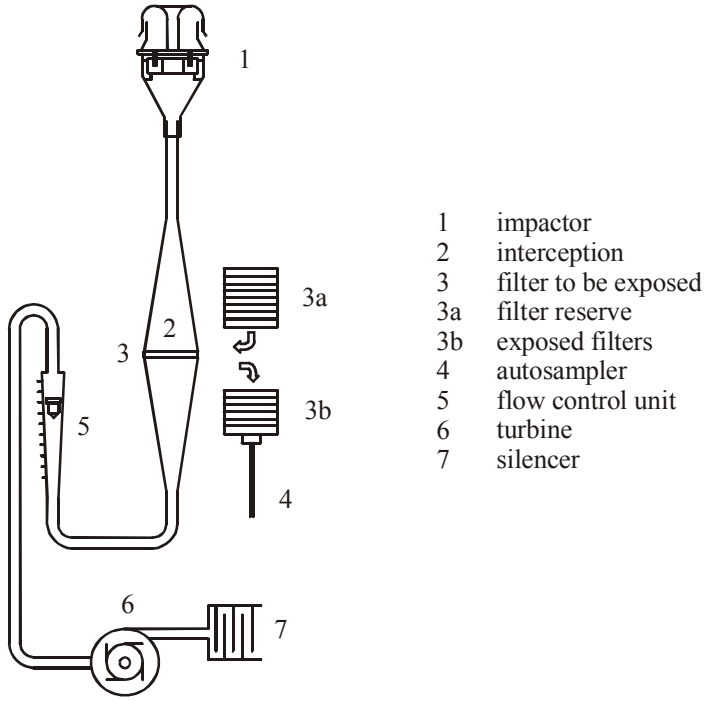

Figure 1-5. Scheme of PM_{10} high volume sampler (DHA 80, Digitel AG).

1.1.6 Chemical composition of atmospheric aerosols

Inorganic compounds

Inorganic ions contribute about 50% to the total number of chemical species in atmospheric aerosols (figure1-6). Sulphate (SO_4^{2-}) is the most abundant anion and adds between 20 and 30% (0.8-13 ng/m^3) to the total aerosol mass (Zappoli *et al.*, 1999). Sulphate is either directly generated from sea spray or by oxidation of SO_2 in the atmosphere. SO_2 is emitted by combustion of sulphur containing fuel. A further large SO_2 source are erupting volcanoes (Brimblecombe, 1996). Nitrate (NO_3^-) contributes 16% (~9 ng/m^3) to the aerosols mass (Zappoli *et al.*, 1999) and is mainly generated by oxidation of nitrogen oxides (NO_x) in the atmosphere (Hutzinger, 1995). Nitrogen oxides are also formed by fuel combustion. Other anions such as Cl^-, Br^- and I^- are found as well (Zappoli *et al.*, 1999). They are released from the sea. Ammonium

(NH_4^+) is the most abundant cation (10% of the average mass, 3 ng/m^3). Na^+, K^+, Ca^{2+} and Mg^{2+} are present in smaller quantities (2-14% of the average mass balance, 0.2-2.1 ng/m^3) and summarised as other ions in figure 1-6.

A large number of trace elements are also present in atmospheric aerosols: Ag, Al, As, Ba, Cd, Ce, Co, Cr, Cs, Cu, Fe, Hf, La, Ni, Pb, Sb, Sr, V, W and Zn (Hutzinger, 1995; Pike and Moran, 2001). Concentrations of typical anthropogenic trace elements at remote and urban sites vary between 0.012-110 ng/m^3 for Pb, 0.001-0.170 ng/m^3 for Cd, and 2.5-13.0 ng/m^3 for Zn (Pike and Moran, 2001).

Silicon is the most abundant element on Earth after oxygen. It is present as silica or silicates. Silicates are found in atmospheric aerosols due to dispersion of mineral dust. Average concentrations of around 10 ng/m^3 were measured for soluble silicates (silicic acid and low polymerised silicates). The average of the total silicate amount (soluble silicates and complex silicate polymers) was found to be around 0.6 µg/m^3 (Giacomelli *et al.*, 1999).

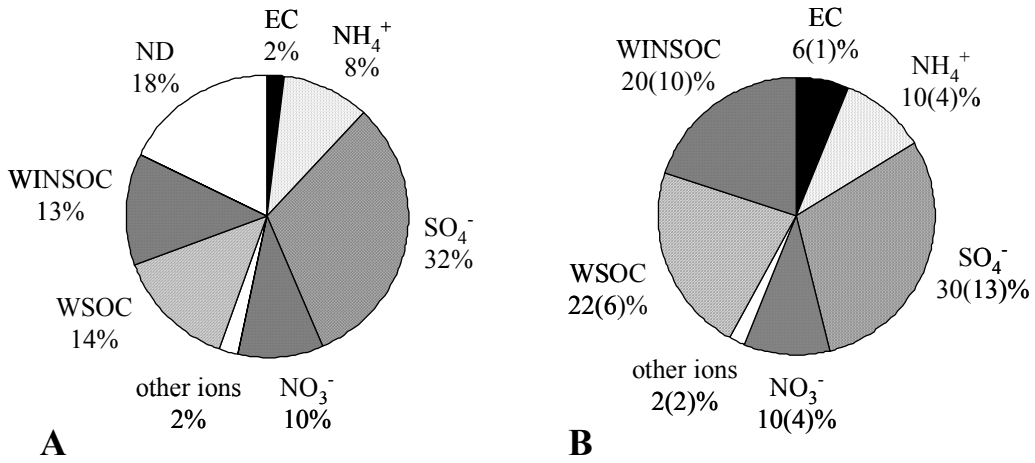

Figure 1-6. (**A**) Average mass balance of atmospheric aerosols at K-puszta (Hungary) (Zappoli *et al.*, 1999) and (**B**) distribution of inorganic ions and carbon in the fine atmospheric aerosol at Jungfraujoch (Switzerland). (EC – elemental carbon; WSOC – water-soluble organic compounds; WINSOC – water-insoluble organic compound; ND – not determined) (Krivacsy *et al.*, 2001). Trace elements were not taken into account. Insoluble silicates may be part of the not determined fraction.

Biological matter

Biological matter is ubiquitous in atmospheric aerosols. It derives from bacteria, pollen, yeasts and moulds (chapter 1.1.2). Concentrations of bacteria and yeast are in the range of 100-500 CFU (colony forming unit). For moulds it varies between 2000 and 3000 CFU (Fuzzi *et al.*, 1997).

A possibility to assess biological matter in atmospheric aerosols is the analysis of proteins and cellulose. Protein concentrations in atmospheric aerosols were around 0.1 $\mu g/m^3$ in alpine areas and up to 1.1 $\mu g/m^3$ in urban areas (Franze *et al.*, 2005). Moreover, concentrations between 50-400 pg/m^3 were found for dissolved free aminoacids over the Pacific Ocean (Matsumoto and Uematsua, 2005). Kunit and Puxbaum (1996) quantified cellulose in urban atmospheric aerosols. Concentrations were between 0.1 and 1.0 $\mu g/m^3$. Cellulose constitutes around 0.1 to 2% of the total aerosol mass, depending on sampling site and season.

Classification of organic matter

Total Carbon (TC) is usually divided into two subgroups. The first one is called Organic Carbon (OC) and is defined as the carbon fraction that evaporates under heating (up to 500 °C) in the presence of pure Helium. OC may include individual semi-volatile organic compounds. The second subgroup is called elemental carbon (EC), black carbon (BC), graphitic carbon or soot. The definitions are operational and depend on the analytical method used.

A different approach to classify organic matter in atmospheric aerosols is based on extraction with either organic, rather nonpolar solvents or pure water. Two fractions are obtained: the water-insoluble organic carbon (WINSOC) fraction and the water-soluble organic carbon (WSOC) fraction. The remaining carbon is classified as elemental carbon (EC) (figure 1-7).

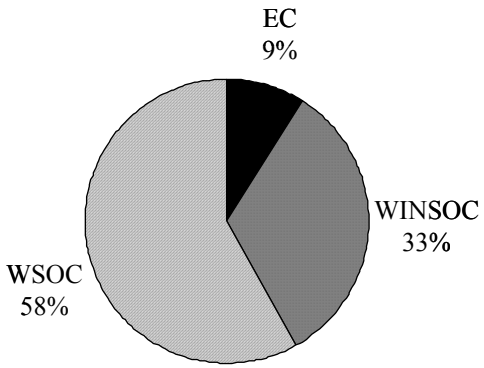

Figure 1-7. Average distribution of carbon in atmospheric aerosol samples. (EC – elemental carbon; WSOC – water-soluble organic carbon; WINSOC – water-insoluble organic carbon) (Kiss *et al.*, 2000).

Water-insoluble organic carbon

The WINSOC fraction is obtained by extraction with *n*-hexane, dichloromethane, acetone (Zappoli *et al.*, 1999) or benzene (Fraser *et al.*, 1999). The additional use of acetone and *iso*-propanol extracts not only polar, but also possibly water-soluble compounds. A sharp separation between water-insoluble and water-soluble carbon is therefore not possible. The water-insoluble organic carbon fraction can be up to 13-20% of the total aerosol mass (figure 1-6) or 33% of the total carbon content (figure 1-7).

A large number of rather nonpolar organic compounds was found. Mainly *n*-alkanes, wax alkanes, PAHs, *n*-alkanones, terpenoids, *n*-alkanols, sterols and phenols were identified in a concentration range of 10-1000 ng/m^3 (Bin Abas and Simoneit, 1996; Rogge *et al.*, 1993; Simoneit, 2002). Very specific organic compounds are emitted during biomass combustion, such as triterpenoids, resin acids and lignin-derived compounds (Fine *et al.*, 2002; Simoneit *et al.*, 1993). The composition of the WINSOC fraction can vary considerably depending on sampling location and emission source (e.g. motor vehicle exhaust and biomass burning; Fraser *et al.*, 1999; Simoneit, 2002).

Water-soluble organic carbon

The WSOC fraction comprises all ionic, polar and less polar organic compounds which are extractable with water. WSOC contributes up to 14-22% to the total aerosol mass (figure 1-6) or 58% to the total carbon content (figure 1-7). A large part of the WSOC has not been identified yet, thus being still subject of research.

First studies showed that the bulk of WSOC consisted of compounds with oxygen containing functional groups such as alcohols, carbonyls and carboxylates attached to aromatic as well as to aliphatic moieties (Duarte *et al.*, 2005; Kiss, 2002; Krivacsy *et al.*, 2001; Zappoli *et al.*, 1999).

Single polar and/or ionic compounds were detected and quantified. Mainly aliphatic monocarboxylic acids (C_9-C_{18}/C_{30}, 2-100 ng/m^3), aliphatic dicarboxylic acids (C_2-C_9, 1-50 ng/m^3), aromatic carboxylic and polycarboxylic acids (1-60 ng/m^3), alcohols (C_{12}, C_{14}, C_{16}, 2-15 ng/m^3), diterpenoid acids (1-20 ng/m^3), and small aldehydes and ketones were present (Graham *et al.*, 2002; Limbeck and Puxbaum, 1999; 2000; Rogge *et al.*, 1993). A large number of sugars (0.2-50 ng/m^3) and anhydrosugars (0.1-250 ng/m^3) were found by Graham *et al.* (2002). Levoglucosan was most abundant (1200-6900 ng/m^3) among anhydrosugars. Furthermore, some phenolic derivates, different esters of benzoic acid, olefinic mono- and dicarboxylic acids, methylated carboxylic acids and hydroxylated carboxylic acids were detected. A general overview about the WSOC fraction given by Saxena and Hildemann (1996).

Macromolecular compounds with a molecular weight between 100 and 1000 u were found in the WSOC fraction of atmospheric aerosols. They were present as well in fog and cloud water, which are supposed to contain dissolved material from atmospheric aerosols. Hydroxylic and carboxylic functional groups seem to be attached to a backbone of aromatic and aliphatic moieties (Cappiello *et al.*, 2003; Feng and Möller, 2004). These macromolecular compounds were found to have very similar physical-chemical properties as fulvic and humic acid. Therefore, the macromolecular compounds were called “Humic Like Substances” (HULIS). HULIS may constitute around 25% of the WSOC (Fuzzi *et al.*, 2002).

1.2 State of WSOC characterisation

Atmospheric aerosols are often sampled as PM_{10} or $PM_{2.5}$ on glass or quartz fibre filters using a high-volume sampler. WSOC is extracted with pure water by ultrasonication or by shaking of the filter (Havers *et al.*, 1998; Krivacsy *et al.*, 2001). The extract contains a mixture of inorganic compounds and WSOC. Different approaches are applied to isolate HULIS from other components of the WSOC fraction. One possibility consists in using cellulose and ion exchange resins for separation as described by Havers *et al.* (1998). Another approach isolates HULIS by solid phase extraction with a C_{18} reverse phase (Krivacsy *et al.*, 2001; Varga *et al.*, 2001). However, since the chemical characterisation of HULIS is far from being complete, no standardised extraction method is available.

Spectroscopic characterisation of WSOC was performed by UV-Vis, fluorescence and infrared spectroscopy. However, only information about the bulk of the WSOC was obtained (Duarte *et al.*, 2005). Proton nuclear magnetic resonance spectroscopy (^{1}H NMR) yielded more detailed information about abundant chemical moieties of the fraction (Decesari *et al.*, 2001; Fuzzi *et al.*, 2001). However, only few single compounds could be identified (Decesari *et al.*, 2000; Suzuki *et al.*, 2001). The complex composition of the WSOC fraction clearly limited the possibilities of its spectroscopic characterisation.

Polar or ionic organic compounds are difficult to separate by GC. Derivatisation of the ionic and polar moieties is often needed. Derivatisation of carboxylic acids and hydroxy compounds to their methylester and methoxy analogues is very common. Ionic and polar compounds from atmospheric aerosols were derivatised with diazomethane (Rogge *et al.*, 1993) or BF_3 in methanol (Limbeck and Puxbaum, 1999).

However, these derivatisation methods are rather smooth. Derivatisation by tetramethylammonium hydroxide (TMAH) is able to cleave additionally ester and ether bonds, yielding the methylesters and methoxy compounds of the cleavage products. Derivatisation with TMAH can be performed online (inside the GC injector)

avoiding the loss of volatile organic compounds. It has been applied to HULIS from winter and summer atmospheric aerosols from a remote area giving a first insight into this structural composition (Gelencser *et al.*, 2000). However, composition of HULIS in atmospheric aerosols from urban sites has not been investigated by this method so far. Moreover, geographical and seasonal variations in HULIS composition are of interest.

Chromatographic separation of the very polar and ionic organic compounds in the WSOC fraction was impossible using conventional HPLC columns containing a C_{18}-coated stationary phase. They eluted within the dead volume of the column (2001; Krivacsy *et al.*, 2000). Furthermore, chromatographic separation of HULIS was difficult and a part of the HULIS seemed to irreversibly adsorb on the column. Size exclusion chromatography and C_{18} stationary phases with large pores offered a possibility to overcome these problems as shown for fulvic and humic acids (Mukai and Ambe, 1986; Persson *et al.*, 2000).

LC-MS is a useful tool for structure elucidation of polar or ionic compounds. Full scan spectra of WSOC were recorded with electrospray ionisation in the negative mode. An ion distribution between *m/z* 100-1000 with a maximum at *m/z* 300 was present (Kiss *et al.*, 2000; Krivacsy *et al.*, 2001). Moreover, collision induced dissociation (CID) fragment spectra of single masses in fog water were recorded with a triple quadrupole (MS-MS) and compared with model compounds (Cappiello *et al.*, 2003). However, detailed structural information of WSOC and HULIS obtained by CID fragmentation is still missing. Moreover, no ion trap mass spectrometry has been applied to the structure elucidation of WSOC so far. Ion traps offer enhanced possibilities for structure elucidation, due to multiple fragmentation (MS^n).

1.3 Aim of the work

WSOC and inorganic compounds are responsible for the water solubility of atmospheric aerosol, which affects their ability as CCN. Especially HULIS as a major component of the WSOC are of interest. A detailed chemical characterisation of the WSOC and particularly of HULIS, would contribute to a better understanding of atmospheric and climatic processes.

This work had the aim to obtain more structural information about WSOC and especially about HULIS in urban atmospheric aerosols of ≤10 μm diameter (PM_{10}). The applicability of electrospray ionisation ion trap mass spectrometry (ESI-MS^n) and thermochemolysis GC-MS should be tested and further developed for structure elucidation of HULIS.

Substructures and fragmentation behaviour of HULIS should be investigated by consecutive fragmentations with an ion trap mass spectrometer (MS^n) and electrospray ionisation (ESI). Application of liquid chromatography should provide separation of HULIS from inorganic salts and other WSOC. The combination of liquid chromatography and mass spectrometry would offer considerable advantages compared to off-line methods concerning isolation and detection of HULIS as well as its structural characterisation.

Cleavage of HULIS by their ester and ether bonds into smaller methylated substructures should be studied by thermochemolysis using tetramethylammonium hydroxide (TMAH). The methylated fragments should be well amenable to separation by GC. Detection by electron ionisation mass spectrometry (EI-MS) in the full scan mode should allow identification of the methylated substructures by comparing their full scan mass spectra with a database. Identified substructures should allow to draw conclusions from the macromolecular structure of HULIS. Furthermore, seasonal variations in the chemical composition of HULIS should be investigated by fingerprinting.

1.4 References

Bin Abas, M. R. and Simoneit, B. R. T., 1996: Composition of extractable organic matter of air particles from Malaysia: Initial study, *Atmos. Environ.* **30**, 2779-2793.

Brimblecombe, P., 1996: *Air composition & chemistry*, Cambridge University Press, Cambridge.

Bruce, N., Perez-Padilla, R. and Albalak, R., 2000: Indoor air pollution in developing countries: a major environmental and public health challenge, *Bull. World Health Organ.* **78**, 1078-1092.

Cappiello, A., De Simoni, E., Fiorucci, C., Mangani, F., Palma, P., Trufelli, H., Decesari, S., Facchini, M. C. and Fuzzi, S., 2003: Molecular Characterization of the Water-Soluble Organic Compounds in Fogwater by ESI-MS/MS, *Environ. Sci. Technol.* **37**, 1229-1240.

Decesari, S., Facchini, M. C., Fuzzi, S. and Tagliavini, E., 2000: Characterization of water soluble organic compounds in atmospheric aerosol: a new approach, *J. Geophys. Res.* **105**, 1481-1489.

Decesari, S., Facchini, M. C., Matta, E., Lettini, F., Mircea, M., Fuzzi, S., Tagliavini, E. and Putaud, J.-P., 2001: Chemical features and seasonal variation of fine aerosol water-soluble organic compounds in the Po Valley, Italy, *Atmos. Environ.* **35**, 3691-3699.

Duarte, R. M. B. O., Pio, C. A. and Duarte, A. C., 2005: Spectroscopic study of the water-soluble organic matter isolated from atmospheric aerosols collected under different atmospheric conditions, *Anal. Chim. Acta* **530**, 7-14.

Feng, J. and Möller, D., 2004: Characterization of Water-Soluble Macromolecular Substances in Cloud Water, *J. Atmos. Chem.* **48**, 217-233.

Fine, P. M., Cass, G. R. and Simoneit, B. R. T., 2002: Chemical Characterization of Fine Particle Emissions from the Fireplace Combustion of Woods Grown in the Southern United States, *Environ. Sci. Technol.* **36**, 1442-1451.

Franze, T., Weller, M. G., Niessner, R. and Pöschl, U., 2005: Protein Nitration by Polluted Air, *Environ. Sci. Technol.* **39**, 1673-1678.

Fraser, M. P., Cass, G. R. and Simoneit, B. R. T., 1999: Particulate organic compounds emitted from motor vehicle exhaust and in the urban atmosphere, *Atmos. Environ.* **33**, 2715-2724.

Fuzzi, S., Decesari, S., Facchini, M. C., Matta, E. and Mircea, M., 2001: A simplified model of the water soluble organic component of atmospheric aerosols, *Geophys. Res. Lett.* **28**, 4079-4082.

Fuzzi, S., Facchini, M. C., Decesari, S., Matta, E. and Mircea, M., 2002: Soluble organic compounds in fog and cloud droplets: what have we learned over the past few years?, *Atmos. Environ.* **64**, 89-98.

Fuzzi, S., Mandroli, P. and Perfetto, A., 1997: Fog droplets - an atmospheric source of secondary biological aerosol particles, *Atmos. Environ.* **31**, 287-290.

Gelencsér, A., 2004: *Carbonaceous Aerosol*, Springer, Dordrecht.

Gelencser, A., Meszaros, E., Blazso, M., Kiss, G., Krivacsy, Z., Molnar, A. and Meszaros, E., 2000: Structural Characterisation of Organic Matter in Fine Tropospheric Aerosol by Pyrolysis-Gas Chromatography-Mass Spectrometry, *J. Atmos. Chem.* **37**, 173-183.

Giacomelli, M. C., Largiuni, O. and Piccardi, G., 1999: Spectrophotometric determination of silicate in rain and aerosols by flow analysis, *Anal. Chim. Acta* **396**, 285–292.

Graham, B., Mayol-Bracero, O. L., Guyon, P., Roberts, G. C., Decesari, S., Facchini, M. C., Artaxo, P., Maenhaut, W., Köll, P. and Andreae, M. O., 2002: Water-soluble organic compounds in biomass burning aerosols over Amazonia 1. Characterization by NMR and GC-MS, *J. Geophys. Res.* **107**, 1-15.

Havers, N., Burba, P., Klockow, D. and Klockow-Beck, A., 1998: Characterisation of Humic-Like Substances in Airborne Particalte Matter by Capillary Electrophoresis, *Chromatographia* **47**, 619-624.

Havers, N., Burba, P., Lambert, J. and Klockow, D., 1998: Spectroscopic Characterization of Humic-Like Substances in Airborne Particulate Matter, *J. Atmos. Chem.* **29**, 45-54.

Hutzinger, O., (Ed.), T. Kouimtzis and C. Samara, (Eds.) 1995. Airborne Particulate Matter. In: The Handbook of Environmental Chemistry, Berlin, Springer.

Jacobson, M. C., Hansson, H.-C., Noone, K. J. and Charlson, R. J., 2000: Organic Atmospheric Aerosols: Review and State of the Science, *Rev. Geophys.* **38**, 267-294.

Kiss, G., 2002: Characterization of water-soluble organic matter isolated from atmospheric fine aerosol, *J. Geophys. Res. ICC* **107**, 1-1-1-8.

Kiss, G., Gelencser, A., Hoffer, A., Krivacsy, Z., Meszaros, E., Molnar, A. and Varga, B., 2000: Chemical Characterisation Of Water Soluble Organic Compounds In Tropospheric Fine Aerosol, *Proc. Conf. on Nucleation and Atmospheric Aerosols*, 761-764.

Krivacsy, Z., Gelencser, A., Kiss, G., Meszaros, E., Molnar, A., Hoffer, A., Meszaros, T., Sarvari, Z., Temesi, D., Varga, B., Baltensperger, U., Nyeki, S. and Weingartner, E., 2001: Study on the Chemical Character of Water Soluble Organic Compounds in Fine Atmospheric Aerosol at the Jungfraujoch, *J. Atmos. Chem.* **39**, 235-259.

Krivacsy, Z., Hoffer, A., Sarvari, Z., Temesi, D., Baltensperger, U., Nyeki, S., Weingartner, E., Kleefeld, S. and Jennings, S. G., 2001: Role of organic and black carbon in the chemical composition of atmospheric aerosol at European background sites, *Atmos. Environ.* **35**, 6231-6244.

Krivacsy, Z., Kiss, G., Varga, B., Galambos, I., Sarvari, Z., Gelencser, A., Molnar, A., Fuzzi, S., Facchini, M. C., Zappoli, S., Andracchio, A., Alsberg, T., Hansson, H.-C. and Persson, L., 2000: Study of humic-like substances in fog and interstitial aerosol by size-exclusion chromatography and capillary electrophoresis, *Atmos. Environ.* **34**, 4273-4281.

Kunit, M. and Puxbaum, H., 1996: Enzymatic determination of the cellulose content of atmospheric aerosols, *Atmos. Environ.* **30**, 1233-1236.

Limbeck, A. and Puxbaum, H., 1999: Organic acids in continental background aerosols, *Atmos. Environ.* **33**, 1847-1852.

Limbeck, A. and Puxbaum, H., 2000: Dependence of in-cloud scavenging of polar organic aerosol compounds on the water solubility, *J. Geophys. Res.* **105**, 19857-19867.

Matsumoto, K. and Uematsua, M., 2005: Free amino acids in marine aerosols over the western North, *Atmos. Environ.* **39**, 2163-2170.

Mukai, H. and Ambe, Y., 1986: Charaterization of a humic acid-like brown substance in airborne particulate matter and tentative identification of its origin, *Atmos. Environ.* **20**, 813-819.

Novakov, T. and Corrigan, C. E., 1996: Cloud condensation nucleus activity of the organic component of biomass smoke particles, *Geophys. Res. Lett.* **23**, 2141-2144.

Novakov, T. and Penner, J. E., 1993: Large contribution of organic aerosols to cloud-condensation-nuclei concentrations, *Nature* **365**, 823-826.

Persson, L., Alsberg, T., Kiss, G. and Odham, G., 2000: On-line size-exclusion chromatography/electrospray ionisation mass spectrometry of aquatic humic and fulvic acids, *Rapid Commun. Mass Spectrom.* **14**, 286-292.

Pike, S. M. and Moran, S. B., 2001: Trace elements in aerosol and precipitation at New Castle, NH, USA, *Atmos. Environ.* **35**, 3361-3366.

Rogge, W. F., Mazurek, M. A., Hildemann, L. M., Cass, G. R. and Simoneit, B. R. T., 1993: Quantification of urban organic aerosols at a molecular level: identification, abundance and seasonal variation, *Atmos. Environ.* **27A**, 1309-1330.

Saxena, P. and Hildemann, L. M., 1996: Water-Soluble Organics in Atmospheric Particles: A Critical Review of the Literature and Application of Thermodynamics to Identify Candidate Compounds, *J. Atmos. Chem.* **24**, 57-109.

Seinfeld, J. H. and Pandis, S. N., 1998: *Atmospheric Chemistry and Physics*, Wiley-Interscience, New York.

Simoneit, B. R. T., 2002: Biomass burning - a review of organic tracers for smoke from incomplete combustion, *Appl. Geochem.* **17**, 129-162.

Simoneit, B. R. T., Rogge, W. F., Mazurek, M. A., Standley, L. J., Hildemann, L. M. and Cass, G. R., 1993: Lignin Pyrolysis Products, Lignans, and Resin Acids as Specific Tracers of Plant Classes in Emissions from Biomass Combustion, *Environ. Sci. Technol.* **27**, 2533-2541.

Suzuki, Y., Kawakami, M. and Akasaka, K., 2001: ^{1}H NMR Application for Characterizing Water-Soluble Organic Compounds in Urban Atmospheric Particles, *Environ. Sci. Technol.* **35**, 2656-2664.

Tesfaigzi, Y., Singh, S. P., Foster, J. E., Kubatko, J., Barr, E. B., Fine, P. M., McDonald, J. D., Hahn, F. F. and Mauderly, J. L., 2002: Health Effects of Subchronic Exposure to Low Levels of Wood Smoke in Rats, *Toxicol. Sci.* **65**, 115-125.

Varga, B., Kiss, G., Ganszky, I., Gelencser, A. and Krivacsy, Z., 2001: Isolation of water-soluble organic matter from atmospheric aerosol, *Talanta* **55**, 561-572.

Zappoli, S., Andracchio, A., Fuzzi, S., Facchini, M. C., Gelencser, A., Kiss, G., Krivacsy, Z., Molnar, A., Meszaros, E., Hansson, H.-C., Rosman, K. and Zebühr, Y., 1999: Inorganic, organic and macromolecular components of fine aerosol in different areas of Europe in relation to their water solubility, *Atmos. Environ.* **33**, 2733-2743.

2 STRUCTURE ELUCIDATION OF THE WSOC FRACTION BY THERMOCHEMOLYSIS GC-MS

2.1 Introduction

Atmospheric aerosols can influence processes in the atmosphere by acting as cloud condensation nuclei (CCN) and by scattering or absorbing light as described in the introduction. The activity of atmospheric aerosols as CCN depends mainly on the polarity and the water solubility of their components. Besides inorganic salts also polar and water-soluble organic compounds contribute to the water solubility of atmospheric aerosols. The water-soluble organic carbon (WSOC) fraction accounts for 20-70% of the total organic carbon in atmospheric aerosols (Saxena and Hildemann, 1996). Humic-like substances (HULIS) constitute around one quarter of the WSOC and are known to be macromolecular polycarboxylic acids (Fuzzi *et al.*, 2002). However, hitherto little is known about the chemical composition and structure of HULIS.

Thermochemolysis GC-MS is an established method for generation of fingerprints and qualitative characterisation of structurally complex macromolecular compounds. Tetramethylammonium hydroxide (TMAH) is used as a reaction and derivatisation agent for soft online cleavage and derivatisation of the analyte at low temperatures (200-400 °C) avoiding thermal degradation. Hydroxyl and carboxylic acid groups react to methoxyl groups respectively methyl esters. In addition, ester and ether bonds are cleaved. The resulting alcohols and carboxylic acids are methylated as well. They are separated by GC and identified by MS. Identification of derivatised cleavage products provides valuable structural information allowing elucidation of part of the analyte. Moreover, no previous derivatisation step is needed, thus minimising errors due to manipulation and loss of volatile compounds. Thermochemolysis is the method of choice, if as much as possible information about the original structure has to be maintained.

Thermochemolysis GC-MS was applied to a large variety of materials such as synthetic and natural resins, lipids, lignin, polysaccharides and proteins (Challinor, 2001). Moreover, it is an established method for generating fingerprints of complex polymeric materials in the fields of forensic science, petroleum chemistry, polymer chemistry and soil chemistry, enabling to see differences in sample compositions. Humic acid (Davies *et al.*, 2001; Martin *et al.*, 1995) and fulvic acid (Martin *et al.*, 1994) from soil and water have been successfully investigated by thermochemolysis GC-MS. Furthermore, characterisation of organic matter from natural water and quantification of some of its thermochemolytical products were carried out by Frazier *et al.* (2003) gaining structural information about humic and fulvic acids. Consequently, thermochemolysis GC-MS should also be applicable to HULIS.

The first application of thermochemolysis GC-MS to organic matter in atmospheric aerosols from a remote area was performed by Gelencser *et al.* (2000). However, thermochemolysis GC-MS should provide additional information about the chemical and structural composition of HULIS from other sampling locations such as urban areas. This should enable a better assessment of the water solubility of HULIS and their contribution to cloud condensation processes. Moreover, seasonal variations in the chemical composition of HULIS have not been studied yet. A comparison of the seasonal variations might provide indications for the origin of HULIS.

2.2 Experimental

2.2.1 Chemicals and solvents

4-Phenoxyphenol, 4-phenoxybenzoic acid, 11-phenoxy undecanoic acid, 2(3)-(tetrahydrofurfuryloxy)-tetrahydropyran, 4-methylphenylester benzoic acid and palmitinpalmitate were purchased from Aldrich (Switzerland). Benzylbenzoate and di-*iso*-decylphthalate were obtained from Fluka (Switzerland) and used as model compounds (≥95% quality). Benzoic acid, 3-hydroxybenzoic acid, butanedioic acid and 1,2-benzenedioic acid of ≥97% quality were supplied by Fluka (Switzerland). Tetramethylammonium hydroxide pentahydrate (TMAH) (>97% quality) was purchased from Sigma (Switzerland). Humic acid (Aldrich, Switzerland), Nordic aquatic fulvic acid (International Humic Substances Society, IHSS, USA) and hydrolytic lignin (Fluka, Switzerland) were used as references. Acetonitrile (ACN, Multisolvent, HPLC) was purchased from Scharlau (Spain) and methanol (MeOH, Pestipur) was obtained from SDS (France). Water was processed by an Elgastat Maxima HPLC water purification unit (Elga Ltd., UK). Helium of 99.996% (Carbagas, Switzerland) was used for GC.

2.2.2 Aerosol filter samples

Exposed quartz fibre filters (Ø 150 mm, QF 20, Schleicher & Schuell, Germany) were provided by the "Lufthygieneamt beider Basel" (Liestal, Switzerland). A DHA-80 high volume sampler (Digitel AG, Switzerland) was used at flow rate of 30 $m^3 h^{-1}$. The sampling period was 24 h. Particulate matter ≤10 μm (PM_{10}) was collected on non-pretreated quartz fibre filters. Blanks were checked for unloaded non-pretreated filters. Unknown compounds were detected at the detection limit. However, they did not interfere, as analytes in real samples were >100 times more abundant.

Quartz fibre filters from the city of Basel (47° 32' N, 7° 35' E) were exposed at Zürcherstrasse, Feldbergstrasse and St. Johanns-Platz. Filters from the motorway A2 were loaded close to Muttenz (47° 31' N, 7° 39' E) at the entrance of the city of Basel.

The filter number, date, location and amount of collected PM_{10} of all examined quartz fibre filters are shown in table 2-1.

Table 2-1. Filter number, date, location and amount of collected PM_{10} of the quartz fibre filters exposed in the city of Basel and at motorway A2 close to Basel.

Filter-No.	Date of exposition	Location	mg of collected PM_{10} *)
Urban filters			
U1	28.01.2003	Zürcherstrasse	9.2
U2	02.02.2003	St. Johann	21.9
U3	13.02.2003	St. Johann	25.6
U4	06.03.2003	St. Johann	16.1
U5	25.03.2003	St. Johann	33.8
U6	17.04.2003	Zürcherstrasse	24.7
U7	11.05.2003	Zürcherstrasse	17.0
U8	31.05.2003	Zürcherstrasse	14.7
U9	02.06.2003	Zürcherstrasse	16.6
U10	23.06.2003	Zürcherstrasse	17.0
U11	21.07.2003	Feldbergstrasse	16.1
U12	05.08.2003	Feldbergstrasse	24.0
U13	14.08.2003	Feldbergstrasse	22.2
U14	10.09.2003	Feldbergstrasse	17.8
U15	19.09.2003	Feldbergstrasse	27.9
U16	05.10.2003	Feldbergstrasse	10.4
U17	06.10.2003	Feldbergstrasse	13.4
U18	17.10.2003	Feldbergstrasse	23.9
U19	06.11.2003	Feldbergstrasse	34.6
U20	19.11.2003	Feldbergstrasse	16.0
U21	09.12.2003	Feldbergstrasse	31.2
U22	14.12.2003	Feldbergstrasse	8.1
Motorway filters			
M1	15.01.2003	A2	39.6
M2	07.05.2003	A2	32.4
M3	25.06.2003	A2	28.3
M4	13.08.2003	A2	27.9
M5	19.10.2003	A2	38.3
M6	10.12.2003	A2	44.3

*) gravimetric determination

2.2.3 Extraction of WSOC and isolation of HULIS

The isolation of HULIS from exposed quartz fibre filters (U1-U22 and M1-M6) consisted of two extraction steps. First, the WSOC fraction was extracted. HULIS were isolated from the rest of WSOC by solid phase extraction (SPE).

Extraction of WSOC

Half of a sampled quartz fibre filter was cut into small pieces with a metallic pizza cutter. The pieces were transferred to a 100 ml flask (Schott, Germany). 26 ml of water were added and the solution was shaken overnight with a bench top shaker. The resulting grey slurry of quartz fibres and water was filtered through a glass fibre filter (GF 55, Ø 25 mm, Schleicher & Schuell, Germany, preheated at 275 °C) with a nitrocellulose membrane filter underneath (NC 03, Ø 25 mm, 0.025 µm pore size, Schleicher & Schuell, Germany, no pretreatment) using a filtration apparatus with a perforated PTFE coated stainless steal filter support (Selectron-GV, Schleicher & Schuell, Germany). The filtration apparatus was washed and preheated at 270 °C before usage. Moreover, the apparatus and the filters were rinsed with water before each filtration. The filtered raw extracts were clear and yellowish for all filters investigated.

Solid-phase extraction of HULIS

The yellowish raw extract was further cleaned by SPE. New SPE cartridges (C_{18}, end-capped, 500 mg sorbent mass, 3 ml reservoir volume, International Sorbent Technology, UK) were washed consecutively with 6 ml of ACN, 3 ml of MeOH, 3 ml of H_2O, 3 ml of 0.01 M HCl, 3 ml of H_2O and 6 ml of ACN. The cartridge was rinsed with 6 ml of ACN, and conditioned with water before every application.

4 ml of the yellowish raw extract were acidified with 1 ml of 0.01 M HCl to ca. pH 5. The total of 5 ml was transferred to the cartridge. The retained brownish material was washed with 1 ml of 0.01 M HCl and 3 ml of H_2O. The effluent consisting of 5 ml of the raw extract and 4 ml of the washing solution contained inorganic and polar organic compounds and were used for further analysis (polar compound fraction).

The HULIS fraction was obtained by eluting the retained brownish material consecutively with 3 ml of ACN, 3 ml of MeOH and 3 ml of ACN. It was concentrated to dryness by a gentle stream of air at 40 °C and redissolved in 100 µl of ACN and 100 µl of MeOH.

2.2.4 Instrumentation

A flash-pyrolyser (CDS 121, Pyroprobe, Chemical Data Systems Inc., USA) was used for thermochemolysis and pyrolysis. Products from thermochemolysis or pyrolysis were separated by gas chromatography and detected by mass spectrometry. A 1800B GCD Plus gas chromatograph/mass spectrometer (Hewlett-Packard, USA) was used with a DB-1701 GC-column (length 10 m, i.d. 0.18 µm and film thickness 0.4 µm, J&W Scientific, USA) at a flow of 1 ml/min (He) in the splitless mode. It was programmed from 35 °C (3 min) to 280 °C (3 min) at 4 °C/min (method 1) or from 18 °C (1 min) to 280 °C (3 min) at 4 °C/min (method 2). The temperature of 18 °C was achieved by cooling down the column oven with dry ice. Electron ionisation was carried out at 70 eV. The mass spectrometer was operated in full scan mode in the mass range of *m/z* 33-450 at 1.9 scans/sec. The injector was run at 300 °C and the interface temperature was set to 280 °C.

A blank of the GC injector and the pyrolyser probe was taken before each real-sample measurement. The quartz wool (Chromatography Research Supplies Inc., USA) was preheated in an oven at 600 °C for 12 h. Quartz tubes (length 255 mm, outer diameter 2.5 mm, inner diameter 1.9 mm; CDS Analytical Inc., USA) were preheated with a gas burner and filled with quartz wool. 20 µl of the polar compound fraction or the HULIS fraction were then placed onto the glass wool. 20 µl of a 2% or 20% TMAH solution in MeOH were added. The loaded quartz tube was placed into the coil of the pyrolyser probe and dried at 50 °C outside the injector. The probe was then introduced into the modified injector and heated at 360 °C for 20 s. Thermochemolytical products were transferred onto the column in the splitless mode at 1 ml/min. A scheme of the modified injector and an expanded view of the pyrolyser probe are given in figure 2-1.

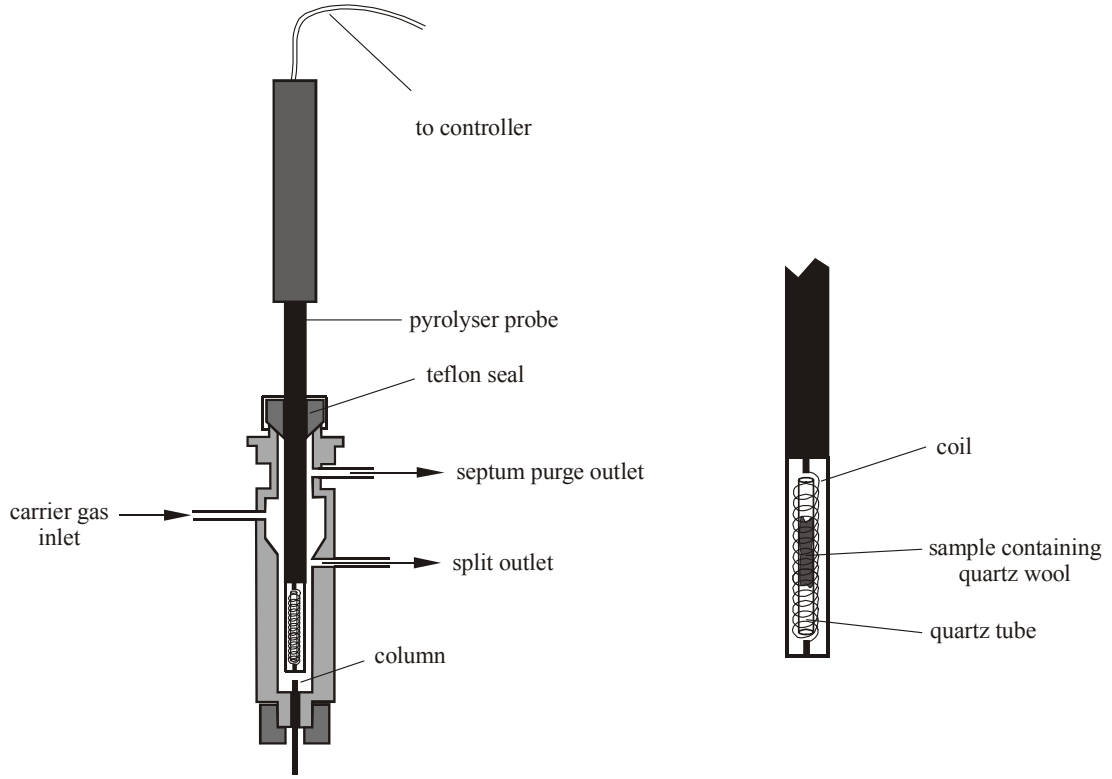

Figure 2-1. Scheme of a split/splitless injector modified for thermochemolysis and pyrolysis (left). Expanded view of the pyrolyser probe (right).

Chromatographic data were recorded with a MS ChemStation (Hewlett Packard, USA). Background subtraction was performed for better visualising chromatograms and improving quality of full scan mass spectra. Identification of unknown compounds was carried out by comparing full scan mass spectra with a library (NIST 2002 reference library, USA). Identification criteria for unknown compounds were set as follows. Matching values ≥90 were considered as very high, proving normally the identity of the unknown compound. Values between 80-90 indicated a good agreement of the proposed compound with the unknown. Values between 70-80 pointed to a lower agreement, inviting to caution. Values below 70 were not considered.

Cluster analysis and factor analysis were performed with data obtained by thermochemolysis GC-MS. For this purpose the statistics software Statistica (Version 5.5, 1999 Edition, StatSoft Inc., USA) was employed.

2.3 Results and discussion

2.3.1 Thermochemolysis of HULIS

Isolation of HULIS

The SPE clean-up separated HULIS (HULIS fraction) from other polar organic and inorganic compounds (polar compound fraction). The separation method for HULIS was adapted from a two-step fractionation method described by Varga *et al.* (2001). Macromolecular HULIS were expected to be less polar under neutral conditions (pH 7) and consequently more retained on a C_{18} SPE cartridge than polar organic and inorganic compounds. However, the acidity of the raw extracts ranged between pH 5-7. Therefore all raw extracts were acidified to pH 5 to obtain a reproducible separation of the HULIS.

Separation of WSOC into a HULIS and a polar compound fraction was checked by a mixture of butanedioic acid, benzoic acid, 3-hydroxybenzoic acid and 1,2-benzenedioic acid. These acidic polar compounds should not be retained on the C_{18} SPE. They were expected to be mainly present in the polar compound fraction. This was the case for butanedioic acid, benzoic acid and 1,2-benzenedioic acid (89-94%). However, about 80% of 3-hydroxybenzoic acid was found in the HULIS fraction. Consequently, the presence of polar organic compounds in the HULIS fraction could not be completely excluded. In addition, separation of HULIS was visually controlled. The retained brownish HULIS layer was washed until it started to migrate through the sorbent (after 1 ml 0.01 M HCl and 3 ml H_2O). Then, this fraction was eluted with MeOH and ACN.

Both the experimental verification above and the visual control showed that HULIS were well separated from most other polar organic compounds. However, a complete isolation of HULIS could not be proven.

Enrichment by a strong anion exchange (SAX) SPE was tried alternatively as typically applied to fulvic acid. The brownish HULIS were retained very well. However, they were only eluted by strong bases, which in turn degraded part of the SAX resin. When neutralising the eluate, the dissolved resin precipitated. HULIS were probably not eluted, but transferred together with the resin. HULIS seemed to be irreversibly adsorbed to the SAX resin making an isolation impossible.

Another approach would have been acidic precipitation as applied to humic acid (Mukai and Ambe, 1986). However, acidic precipitation was not applicable to the atmospheric HULIS fraction, since large amounts of aerosols would have been needed, to obtain a filterable precipitate.

Thermochemolytical products of the HULIS fraction and the polar compound fraction

As indicated in the introduction (chapter 2.1), thermochemolysis is a soft method for fragmentation of macromolecular compounds, since the cleavage products are methylated simultaneously. Lower temperatures were used to reduce thermal stress of the analyte and to minimise production of CO_2. However, thermal degradation of excessive TMAH occurred during thermochemolysis. Large amounts of trimethylamine eluted first. Trimethylamine and CO_2 were main background compounds. The background covered the chromatographic signals as shown in figure 2-2. Background subtraction was necessary for a better visualisation of the thermochemograms and made database matching possible.

Furthermore, reproducibility of the thermochemolytical method was checked. The HULIS fraction of filter U9 was re-analysed four times. The visual control of the thermochemograms stated a good reproducibility. In addition, comparison of the fingerprints of the four thermochemograms by cluster analysis and principal component analysis proved the good reproducibility (chapter 2.3.6).

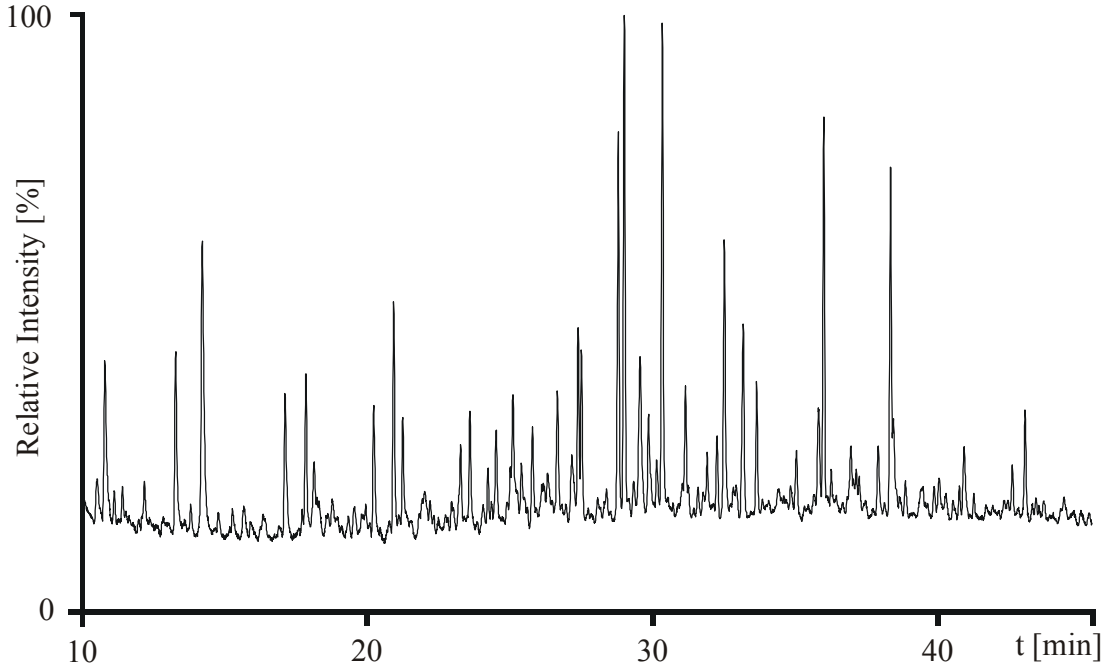

Figure 2-2. Thermochemogram without background subtraction of the HULIS fraction of filter U21 obtained with 2% TMAH. EI, full scan mode, mass range *m/z* 35-350 (100% = 3.4 x 10^6 counts). The mass signals of CO_2 and trimethylamine were present as background in the full scan spectrum. The same background subtracted thermochemogram is shown in figure 2-3.

Thermochemolysis of the HULIS fraction was performed for filters U1-U22 and M1-M6 (table 2-1). Moreover, thermochemograms of the polar compound fraction of filters U10, U21 and M5 were registered for comparison. The thermochemograms of the HULIS fraction and the polar compound fraction of filter U21 are shown in figure 2-3 as an example. The thermochemograms varied with sampling time and date. The type of the detected compounds was nearly the same for most filters. Mainly intensity variation was observed. A detailed discussion of the chromatographic patterns of HULIS fractions is given in chapter 2.3.6. A summary of all underivatised aliphatic and aromatic compounds found in the HULIS fractions and polar compound fractions is given in table 2-2. The corresponding structures are presented in figure 2-4.

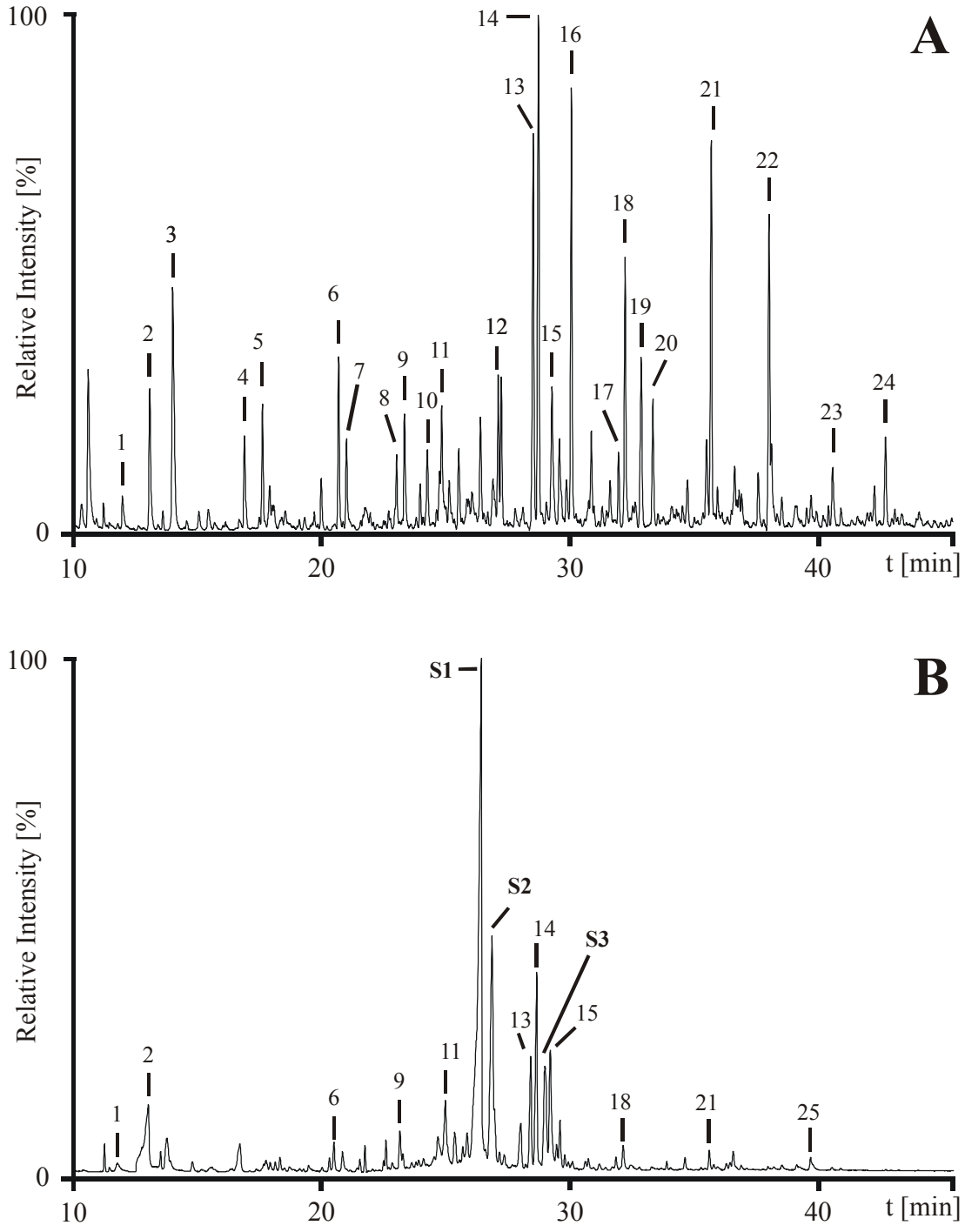

Figure 2-3. Thermochemogram of the HULIS fraction (**A**) and polar compound fraction (**B**) of filter U21 obtained with 2% TMAH. EI, full scan mode, mass range *m/z* 35-350, background subtracted (**A**: 100% = 3.0 x 10^6 counts, **B**: 100% = 8.6 x 10^6 counts). The compounds corresponding to the numbered signals are given in table 2-2.

Table 2-2. Summary of underivatised aliphatic and aromatic compounds found in the HULIS fractions of filters U1-U22 and M1-M6 and polar compound fractions of filters U10, U21 and M5. Matching factors of the library search are given (maximum = 100). Signal numbers correspond to the chromatographic signals in figure 2-3.

Compound	Matching factor	Signal-No.	Compound	Matching factor	Signal-No.
Nonanoic acid	93	5	Benzoic acid	83	3
Decanoic acid	85	7			
Dodecanoic acid	80	-	3-Hydroxybenzoic acid	85	9
Tetradecanoic acid	87	19	4-Hydroxybenzoic acid	88	11
Pentadecanoic acid	82	-	3,4-Dihydroxybenzoic acid	90	18
Hexadecanoic acid	91	28	3,4,5-Trihydroxybenzoic acid	92	21
Octadecanoic acid	90	24			
			1,2,3-Trihydroxybenzene	85	8
Hexadecenoic acid	87	-			
Octadecenoic acid	88	-	1,2-Benzenedicarboxylic acid	96	13
			1,3-Benzenedicarboxylic acid	93	15
Butanedioic acid	93	2	1,4-Benzenedicarboxylic acid	90	14
Pentanedioic acid	84	4	1,2,4-Benzenetricarboxylic acid	82	25
Hexanedioic acid	96	6			
Heptanedioic acid	88	10	4-Methylbenzoic acid	88	-
Octanedioic acid	92	12	4-(1-Methylethyl)-benzoic acid	82	-
Nonanedioic acid	93	16	4-Methyl-1,2-benzene-dicarb-oxylic acid	83	17
Decanedioic acid	83	-			
			2,2'-Biphenyldicarboxylic acid	88	23
2-Butenedioic acid	83	1	3,4,5-Trihydroxybenzaldehyde	90	20
2-Hexenedioic acid	86	-			
			3,4,5,6-Tetrahydroxy-tetrahydropyran	81	S1
2-Methyl-pentanedioic acid	81	-			
3-Methyl-pentanedioic acid	83	-	1,2,3,4,5,6-Hexahydroxy-cyclohexane	77	S2
1-Methylethyl-butanedioic acid	81	-			
3-Methyl-hexanedioic acid	89	-	1,2,3,4,5-Pentahydroxy-cyclopentane	70	S3
1,2,3-Propanetricarboxylic acid	83	-			

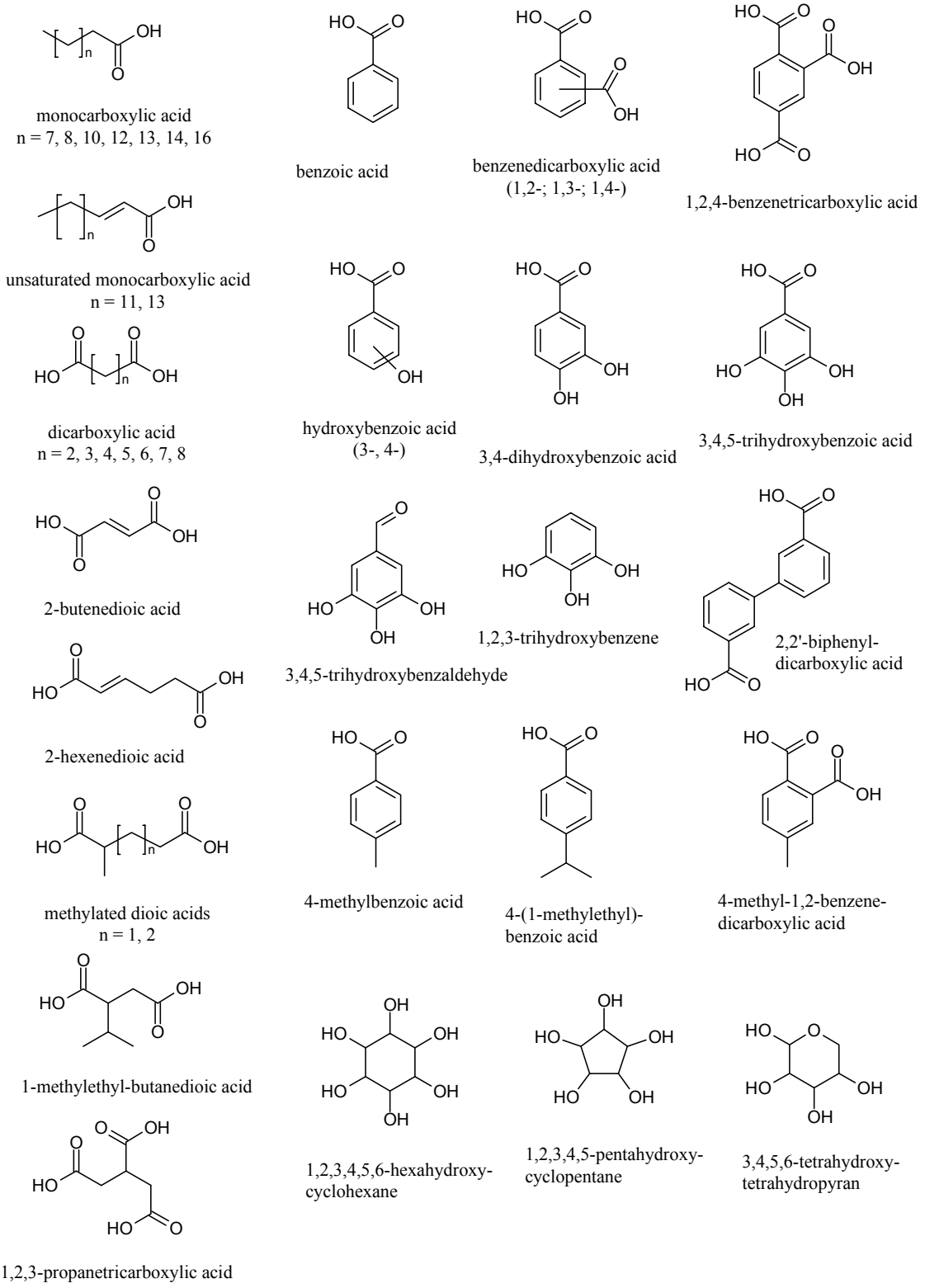

Figure 2-4. Structures of all underivatised aliphatic and aromatic compounds found in the HULIS fractions of filters U1-U22 and M1-M6 and polar compound fractions of filters U10, U21 and M5. The corresponding matching factors are listed in table 2-2.

Nearly all aliphatic compounds present in the HULIS fractions were aliphatic mono- and dicarboxylic acids. Monocarboxylic acids (fatty acids) with even numbered carbon chains such as dodecanoic acid, tetradecanoic acid, hexadecanoic acid and octadecanoic acid are common in biological material. Hexadecanoic acid and octadecanoic acid predominated in most filters. They belong to the most common fatty acids in plant and animal lipids (Steglich *et al.*, 1997). In most filters hexadecanoic acid was more abundant than octadecanoic acid as typical for vegetal lipids indicating their biogenic origin (Belitz and Grosch, 1992). Moreover, in some filters hexadecenoic acid and octadecenoic acid were identified. EI mass spectra do not allow to locate the double bond in a long aliphatic chain. However, these are probably palmitoleic acid and oleic acid. Both palmitoleic and especially oleic acid are present in vegetation (Belitz and Grosch, 1992) and support the biogenic origin of most of the aliphatic monocarboxylic acids. Fatty acids with an odd number of carbon atoms such as nonanoic acid and pentadecanoic acid were also identified. However, they are less common in biological material (Belitz and Grosch, 1992). They might not be of vegetal origin, but products of oxidation processes in the atmosphere.

Aliphatic dicarboxylic acids with chain lengths of C_4 to C_{10} (table 2-2) were present in the HULIS fraction of all filters. Dicarboxylic acids occur mainly in plants (Falbe and Regitz, 1996). Butanedioic acid is known to be an important metabolic intermediate (Stryer, 1999). Pentanedioic acid, hexanedioic acid, heptanedioic acid, octanedioic acid, nonanedioic acid and decanedioic acid may be oxidation products of fatty acids. Furthermore, methylated pentanedioic acid and hexanedioic acid were found. They either derive from oxidised isoprenoid precursors or from methylation of already existing non-methylated dicarboxylic acids.

2-Butenedioic acid and 2-hexenedioic acid were the only unsaturated dicarboxylic acids present in the HULIS fraction. 2-Butenedioic acid was detected in all filters. 2-Hexenedioic acid was only found occasionally. Both may be products of the oxidative degradation of aromatic compounds in the atmosphere. An approach is given by Guderian (2000).

1,2,3-Propanetricarboxylic acid is structurally very close to citric acid. However, conditions in the atmosphere are oxidative. Formation by reduction of citric acid is thus very unlikely. 1,2,3-Propanetricarboxylic acid is probably an oxidation product from a not fully oxidised precursor.

Moreover, a large number of carboxylated and hydroxylated aromatic compound was identified in the HULIS fraction. Benzoic acid and a series of mono-, di- and trihydroxy-benzoic acids were present in all filters. 1,2-Benzenedicarboxylic acid (phthalic acid), 1,3-benzenedicarboxylic acid and 1,4-benzenedicarboxylic acid were very abundant. Phthalic acid gave the most intensive chromatographic signal in nearly all filters. Moreover, N-methylphthalimide was found in filters U5, U6, U19 and M6 as the only nitrogen containing compound in the HULIS fraction. A detailed discussion is given in chapter 2.3.3. Aromatic dicarboxylic acids seemed to belong to the main constituents of the HULIS fraction. The rest of the aromatic compounds in table 2-2 were of lower abundance.

Many of the compounds in the polar compound fraction were the same as in the HULIS fraction. Aliphatic compounds such as 2-butenedioic, butanedioic acid and hexanedioic acid were identified. Moreover, aromatic compounds such as mono-, di- and trihydroxybenzoic acids, trihydroxybenzene and benzenedicarboxylic acids were detected (table 2-2).

However, characteristic for the polar compound fraction were polyhydroxylated cyclohexane, cyclopentane and tetrahydropyrane: 1,2,3,4,5,6-hexahydroxy-cyclohexane and 1,2,3,4,5-pentahydroxy-cyclopentane and 3,4,5,6-tetrahydroxy-tetrahydropyrane. They are structurally close to sugars. Moreover, they were the most intense chromatographic signals in the polar compound fraction of the filters investigated and might originate from cellulose or vegetal debris.

All aromatic compounds listed in table 2-2 originated possibly from vegetation or from combustion of vegetation. Benzoic acid and hydroxylated derivates are known to occur in plants (Lüttge *et al.*, 1999). Moreover, lignin consists of mainly aromatic moieties

(Steglich *et al.*, 1997). Comparison with thermochemolysis of lignin was carried out and discussed in chapter 2.3.2. Aromatic dicarboxylic acids are less present in vegetation (Falbe and Regitz, 1996). Phthalic acid may derive from anthropogenic sources. Alkylesters of phthalic acid such as dioctylphthalate are widely used as plasticisers. They may be cleaved during thermochemolysis yielding the phthalic acid methylester and the methylated 1-octanol. However, neither non-methylated nor methylated aliphatic alcohols were detected. Therefore, an anthropogenic source for phthalic acid is less likely.

Markers for wood combustion in the HULIS fraction

Diterpenoids such as dehydroabietic acid and its oxidised analogues 6-dehydrodehydroabietic acid and 7-oxodehydroabietic acid were identified (figure 2-5). They are released to the atmosphere mainly by combustion of wood. Abietic acid and its derivates are constituents of plant resins (Steglich *et al.*, 1997). Dehydroabietic acid is therefore regarded as a molecular marker for wood combustion (Simoneit and Mazurek, 1982). It was present in virtually all filters. Dehydroabietic acid probably oxidises in the atmosphere to 7-oxodehydroabietic acid. In addition, nicotinic acid was identified. Nicotinic acid is known to be an important component in plant metabolism (Lüttge *et al.*, 1999). However, its origin from cigarette smoke cannot be excluded.

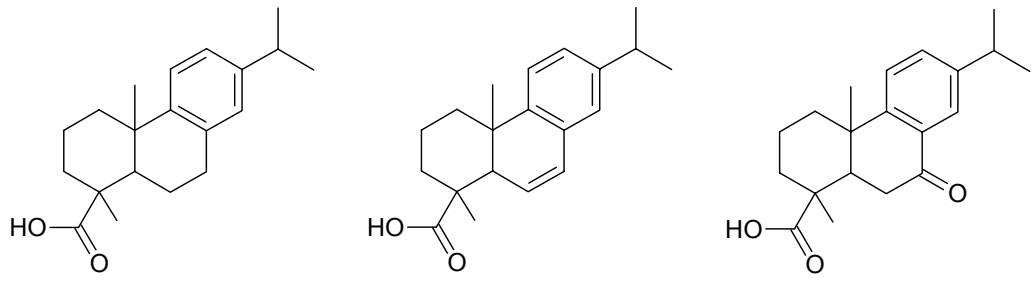

I **II** **III**

Figure 2-5. Molecular markers for wood combustion. Dehydroabietic acid (I), 6-dehydrodehydroabietic acid (II) and 7-oxodehydroabietic acid (III).

For most components identified in the HULIS fractions and the polar compound fractions (table 2-2) a biogenic origin was postulated. Szidat *et al.* (2004) made ^{14}C measurements of urban aerosols from Zürich (Switzerland) and showed, that 51-80% of the OC in aerosols were of biogenic origin. Furthermore, the amount of anthropogenic organic carbon strongly correlated with that of black carbon indicating that WINSOC is rather anthropogenic and WSOC rather biogenic. This supports the postulate of the organic compounds defined in the HULIS fraction and the polar compound fraction having mainly a vegetal origin.

Anthropogenic compounds in the HULIS fraction

Also typically anthropogenic compounds were found in the HULIS fraction. They are shown in figure 2-6. Substances with a di-*tert*-butylphenyl moiety (I-IV) are used as antioxidants and UV-stabilisers (Belitz and Grosch, 1992). Bisphenol A (V) is used in the production of epoxy resins and polycarbonate plastics. Moreover, triglyme (VI) was detected. It is widely used as an universal solvent. All these industrial substances are specific to human activities and were found mainly in winter filters. Cold temperatures might have favoured condensation of these substances onto atmospheric aerosols.

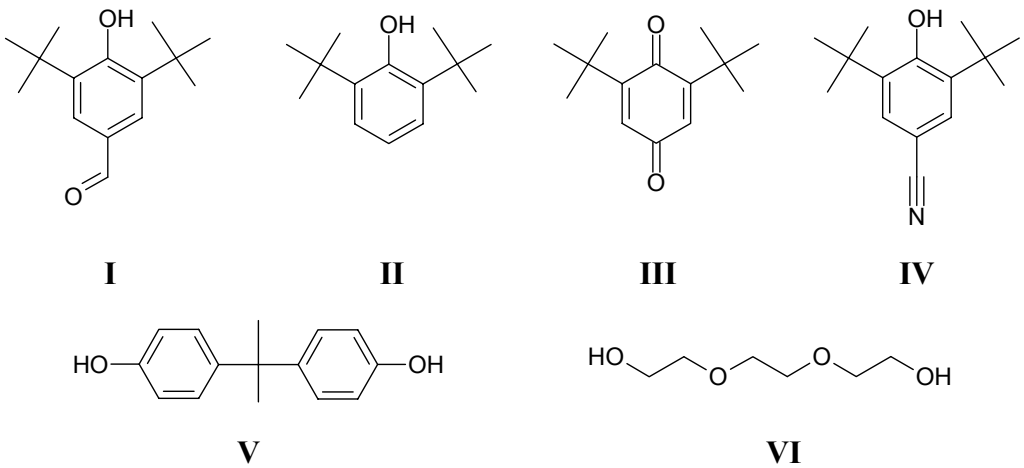

Figure 2-6. Anthropogenic compounds in HULIS fraction. 3,5-Di-*tert*-butyl-4-hydroxybenzaldehyde (I), 2,6-di-*tert*-butylphenol (II), 2,6-di-*tert*-butylcyclo-hexadiene-1,4-dione (III), 3,5-di-*tert*-butyl-4-hydroxy-benzonitrile (IV), bisphenol A (V) and triglyme (VI).

Volatile thermochemolytical products in the HULIS fraction

Most thermochemolytical products in the HULIS fraction eluted between 13 and 50 min (figure 2-3) and contained carbon, hydrogen and oxygen, but not nitrogen. The only nitrogen containing compounds were very volatile and eluted before 13 min. An exception is N-methylphthalimide, which appeared in some filters around 18 min. A more detailed discussion of its appearance is given in chapter 2.3.3. An adaptation of the temperature program of the chromatography was necessary to improve the separation of the most volatile compounds. 35 °C as starting temperature of method 1 was too high to trap and focus them on the separation capillary. Volatile compounds were sufficiently focussed with method 2 starting at 18 °C. The thermochemogram of U9 shows for example signals with little tailing between 4-5 min (figure 2-7). Tables 2-3 and 2-4 give a summary of all volatile compounds identified before 13 min in filters U8, U9, U12 and U14.

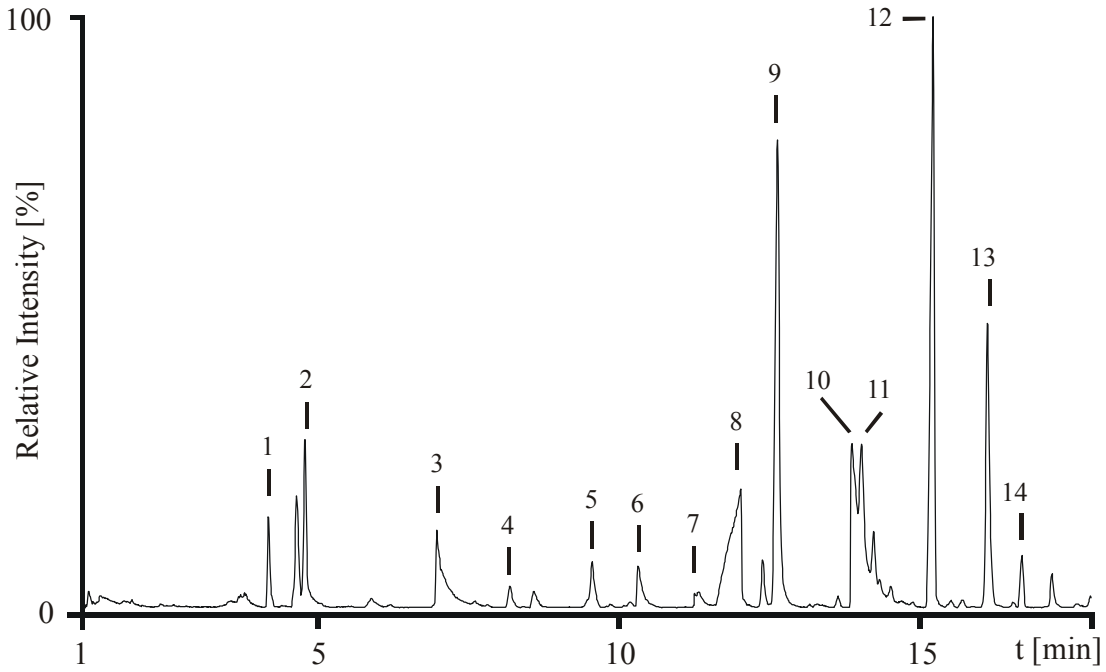

Figure 2-7. Thermochemogram of the HULIS fraction of filter U9 obtained with 2% TMAH and method 2. EI, full scan mode, mass range *m/z* 35-350, background subtracted (100% = 6.2 x 10^6 counts). The compounds corresponding to the numbered signals are given in tables 2-3 and 2-4.

Table 2-3. Summary of volatile aliphatic and aromatic compounds found in the HULIS fraction of filters U8, U9, U12 and U14. Matching factors of the library search are given (maximum = 100). Signal numbers correspond to the chromatographic signals in figure 2-7.

Compound	Matching factor	Signal-No.
4-Methyl-3-pentenoic acid	82	4
4-Methyl-4-pentenoic acid	89	5
4-Oxo-pentanoic acid	82	-
2-Hydroxy-propanoic acid	92	1
3-Furancarboxylic acid	93	9
2-Furancarboxylic acid	94	-
2,2-Dimethyl-1,3-dioxalane	81	6
Butenedioic acid	88	11
Butanedioic acid	90	12
Benzoic acid	83	13
2-Methyl-pentanedioic acid	81	14

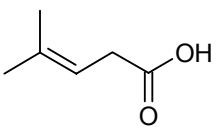

4-methyl-3-pentenoic acid

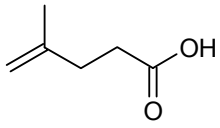

4-methyl-4-pentenoic acid

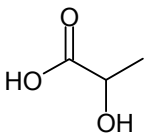

3-hydroxy-propanoic acid

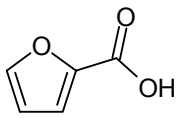

2-furancarboxylic acid

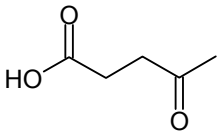

4-oxo-pentanoic acid

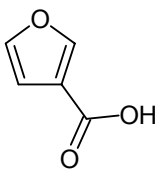

3-furancarboxylic acid

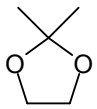

2,2-dimethyl-1,3-dioxalane

Figure 2-8. Structures of underivatised volatile compounds in the HULIS fraction. The corresponding matching factors are listed in table 2-3.

Table 2-4. Summary of volatile TMAH reaction products found in the HULIS fractions of filters U8, U9, U12 and U14. Matching factors of the library search are given (maximum = 100). Signal numbers correspond to the chromatographic signals in figure 2-7.

Compound	Matching factor	Signal-No.
Dimethylamino-acetonitrile	91	2
N,N-Dimethyl-formamide	90	3
Acetamide	90	-
N-Methyl-acetamide	91	8
N,N-Dimethyl-acetamide	91	-
Hexahydro-1,3,5-trimethyl-1,3,5-triazine	97	-
Guanidine	80	-
1-Methyl-1H-imidazole	91	10
N,N,N',N'-Tetramethyl-methanediamine	87	-

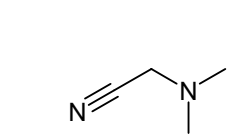

dimethylamino-acetonitrile

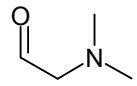

N,N-dimethyl-formamide

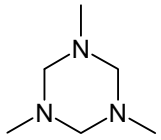

Hexahydro-1,3,5-trimethyl-1,3,5-triazine

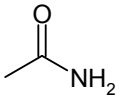

acetamide

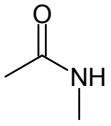

N-methyl-acetamide

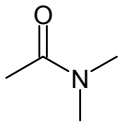

N,N-dimethyl-acetamide

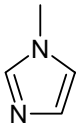

1-methyl-1H-imidazole

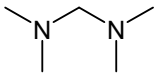

N,N,N',N'-tetramethyl-methanediamine

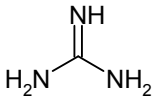

guanidine

Figure 2-9. Structures of volatile TMAH reaction products in the HULIS fraction. The corresponding matching factors are listed in table 2-4.

4-Methyl-3-pentenoic acid and 4-methyl-4-pentenoic acid have an isoprenoid-like side chain, which may indicate their vegetal origin. Furthermore, 4-oxo-pentanoic acid, 2-hydroxy-propanoic, 2,2-dimethyl-1,3-dioxalane as well as 2-furancarboxylic acid and 3-furancarboxylic acid were identified. A clear identification of their origin was not possible. However, a vegetal origin is likely. Butenedioic acid, butanedioic acid and benzoic acid eluted after 13 min and were already well detectable with method 1.

The nitrogen containing compounds are assumed to be reaction products of TMAH with other organic compounds or with itself. The HULIS fraction was dissolved in ACN and MeOH prior to thermochemolysis. Incomplete drying in the quartz tube might lead to reactions of TMAH with traces of solvent. Dimethylamino-acetonitrile is probably a reaction product of TMAH with traces of ACN. N,N-Dimethyl-formamide might be a reaction product of TMAH with MeOH or CO_2. Acetamide, N-methyl-acetamide and N,N-dimethyl-acetamide are likely reaction products of TMAH with acetic acid. Acetic acid was too volatile to be retained, but possibly detected indirectly as acetamide. Hexahydro-1,3,5-trimethyl-1,3,5-triazine, guanidine, 1-methyl-1H-imidazole and N,N,N',N'-tetramethyl-methanediamine were probably reaction products of TMAH as well.

2.3.2 Thermochemolysis of reference compounds

Fulvic and humic acids are generated by oxidative decomposition of lignin by microorganisms in soil. They were chosen as reference compounds due to their similarity to HULIS in atmospheric aerosols. In addition, lignin as the precursor of fulvic and humic acids was also selected as reference compound. Thermochemolytical products of fulvic acids, humic acids and lignin were compared to those of HULIS.

Fulvic and humic acids

Experiments were carried out with a solution of 20% of TMAH, since 2% yielded almost no cleavage products. The resulting thermochemograms are shown in figure 2-10. The corresponding identified compounds are given in table 2-5. Structures of part of the identified compounds are given in figure 2-11.

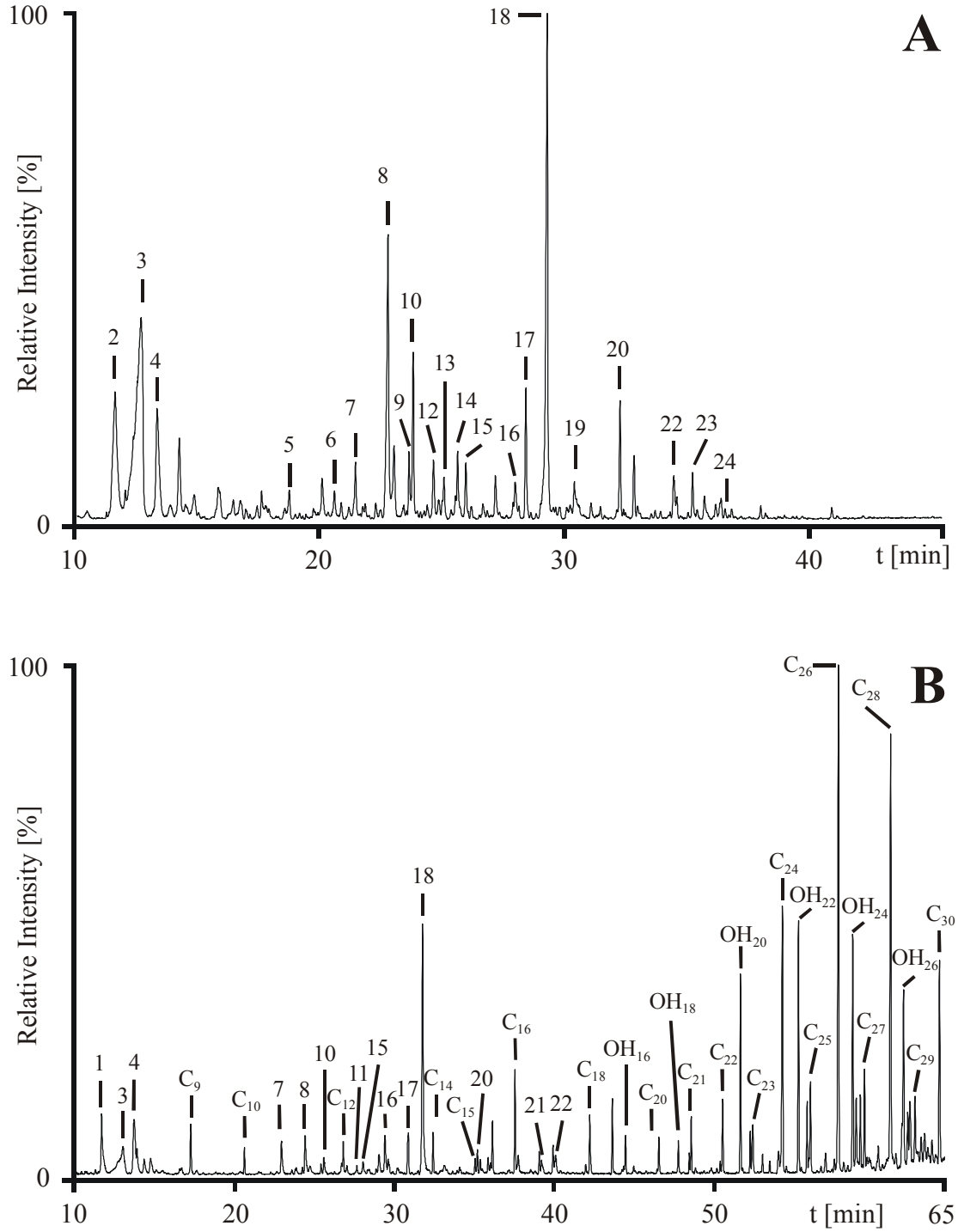

Figure 2-10. Thermochemogram of fulvic acids (**A**) and humic acids (**B**) obtained with 20% TMAH. EI, full scan mode, mass range *m/z* 35-350, background subtracted (**A**: 100% = 5.5 x 10^6 counts, **B**: 100% = 4.5 x 10^6 counts). The compounds corresponding to the numbered signals are given in table 2-5.

Table 2-5. A Summary of the presence of underivatised compounds in fulvic acids (FA) and humic acids (HA) is given and compared with compounds found in the HULIS fraction (HF). Matching factors of the library search are given (maximum = 100). Signal numbers correspond to the chromatographic signals in figure 2-10.

Compound	presence in FA, HA	presence in HF	Matching factor	Signal-No.
Phosphoric acid	HA	-	78	1
2-Butenedioic acid	FA	HF	86	2
Butanedioic acid	FA, HA	HF	86	3
Benzoic acid	FA, HA	HF	93	4
Ethylidenebutanedioic acid	FA	-	84	5
Hexenedioic acid	FA	HF	80	6
3-Hydroxybenzoic acid	FA, HA	HF	84	7
4-Hydroxybenzoic acid	FA, HA	HF	87	8
3-Hydroxy-4-methylbenzoic acid	FA	-	80	9
1,3,5-Trihydroxybenzene	FA, HA	HF	91	10
1,3,5-Trihydroxytoluene	HA	-	80	11
4-Hydroxybenzeneacetic acid	FA	-	82	12
1,3-Benzenedicarboxylic acid	FA	HF	78	13
1,2,3-Propanetricarboxylic acid	FA	HF	86	14
1,2-Benzenedicarboxylic acid	FA, HA	HF	87	15
3,4-Dihydroxybenzaldehyde	FA, HA	-	85	16
3,5-Dihydroxybenzoic acid	FA, HA	-	88	17
3,4-Dihydroxybenzoic acid	FA, HA	HF	92	18
3,4-Dihydroxybenzeneacetic acid	FA	-	85	19
1,2,4-Trihydroxybenzoic acid	FA, HA	HF	91	20
1,2,4-Benzenetricarboxylic acid	HA	HF	84	21
2,3,4-Trihydroxycinnamic acid	FA, HA	-	81	22
4-(2,4,6-Trihydroxyphenyl)-2-butanone	FA	-	75	23
2,3-Dihydroxycinnamic acid	FA	-	75	24
Aliphatic monocarboxylic acids *)	HA	HF ($<C_{18}$)	*)	C_9-C_{30}
Aliphatic alcohols **)	HA	-	**)	OH_{16}-OH_{26}

*) Homologue series deduced from several aliphatic monocarboxylic acids with a database matching of >82.

**) Series of homologues deduced from 1-eicosanol with a library matching factor of 85.

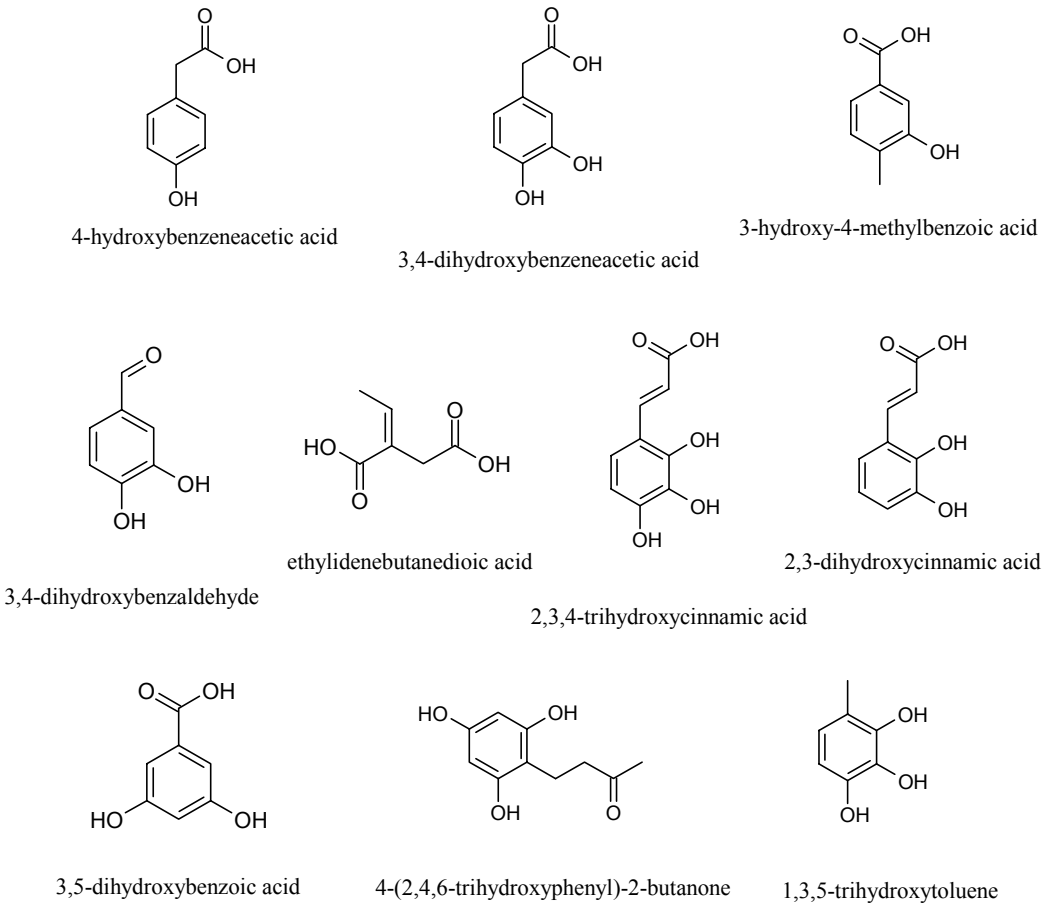

Figure 2-11. Structures of underivatised compounds formed from fulvic and humic acids not identified for HULIS. The corresponding matching factors are listed in table 2-5.

Hydroxylated aromatic carboxylic acids were detected in high yield. They were altogether the main fraction of compounds formed from fulvic and humic acids. In addition, benzoic acid, butanedioic acid, 1,3,5-trihydroxybenzene and 3,4-dihydroxybenzaldehyde were found to be in common. 2,3,4-Trihydroxycinnamic acid is typical for lignin (Lüttge *et al.*, 1999) and was detected in both fulvic and humic acid. This indicates lignin as their precursor.

Specific for fulvic acid were mono- and dihydroxylated benzeneacetic acid as well as ethylidenebutanedioic acid and 4-(2,4,6-trihydroxyphenyl)-2-butanone. Moreover, 2,3-dihydroxycinnamic acid was identified, which supports lignin as the precursor of fulvic acids.

For humic acids a signal series of long-chained aliphatic monocarboxylic acids (C_9-C_{30}) were most intense, which were absent in fulvic acid. Furthermore, a signal series of homologue unbranched aliphatic alcohols was possibly detected. One signal out of the signal series was proven to be 1-eicosanol (matching factor 85). The rest of the series was deduced from 1-eicosanol and abbreviated as OH_x, x corresponding to the chain length (OH_{16}-OH_{26}). This is consistent with the long-chained aliphatic alcohols in wood smoke found by Nolte *et al.* (2001).

The first eluting compound for humic acids was phosphoric acid, which occurs in plants as mono-, di- and triphosphate. Phosphoric acid was possibly bound to an hydroxyl group of a hydroxylated aromatic compound by means of an ester bond. During thermochemolysis cleavage occurred and phosphoric acid was detected as the corresponding trimethylester. However, not completely removed phosphate during the isolation process of humic acids could also be the reason.

Humic acids showed strong similarities to fulvic acid. Most of the compounds in humic acids were the same as in fulvic acid. However, long-chained aliphatic monocarboxylic acids (>C_{18}) and long-chained aliphatic alcohols (OH_{16}-OH_{26}) were not identified in fulvic acids. Aliphatic dicarboxylic acids such as 2-butenedioic acid and butanedioic acid were detected only in fulvic acids. Moreover, some more hydroxylated aromatic carboxylic acids were identified for fulvic acids (see table 2-7).

Differences were stated when comparing thermochemolytical products of fulvic acids and humic acids with HULIS. Aliphatic monocarboxylic acids with a chain length of C_9-C_{18} were found for HULIS. Aliphatic monocarboxylic acids in humic acid were longer (C_9-C_{30}), whereas none were detected in fulvic acids. Moreover, HULIS contained more aliphatic dicarboxylic acids than fulvic acids. Humic acids contained no dicarboxylic acids. Furthermore, no derivates of abietic acid were identified.

Despite the differences observed, humic acids and specially fulvic acids come chemically very close to HULIS. 50% of the compounds in fulvic and humic acid were the same as for HULIS (table 2-5). Moreover, all compound classes identified in HULIS were also detected in fulvic and humic acids. This might be an indication for the lignin origin of HULIS. Combustion products of lignin might get into the atmosphere, further oxidise and aggregate to HULIS. However, HULIS can also originate from oxidation of organic compounds emitted by vegetation.

Lignin

Lignin the precursor of fulvic and humic acid was also degraded by thermochemolysis. Lignin is composed by a series of typical alcohols and acids such as coniferyl, sinapyl, cumaryl, syringyl alcohol and coumaric, ferrulic and gallic acid (Lüttge *et al.*, 1999). These alcohols and acids are claimed to be linked together by ether bonds forming a supramolecular structure called lignin. The thermochemogram of lignin is shown in figure 2-12 and the corresponding identified compounds are listed in table 2-6.

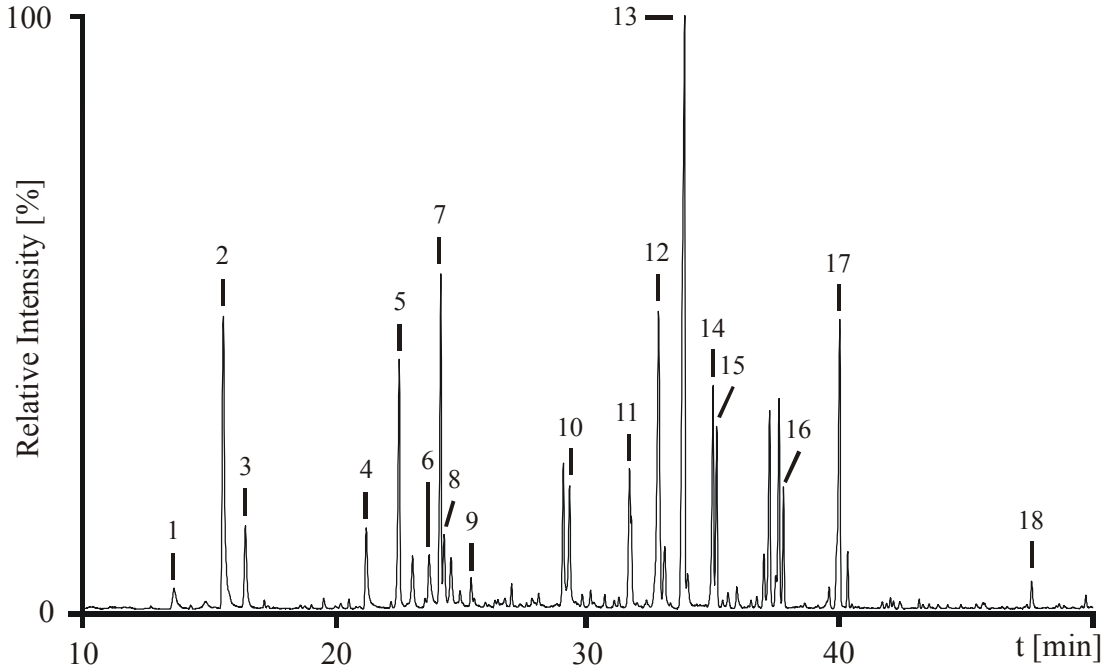

Figure 2-12. Thermochemogram of lignin obtained with 20% TMAH. EI, full scan mode, mass range *m/z* 35-350, background subtracted (100% = 5.0 x 10^6 counts). The compounds corresponding to the numbered signals are given in table 2-6.

Table 2-6. Summary of underivatised compounds present in lignin and a comparison with the compounds found in fulvic acids (FA), humic acids (HA) and in the HULIS fraction (HF) are given. Matching factors of the library search are shown (maximum = 100). Signal numbers correspond to the chromatographic signals in figure 2-12.

Compound	present in FA, HA, HF	compound class present in	Matching factor	Signal-No.
Benzoic acid	FA, HA, HF	-	81	1
1-Ethenyl-4-hydroxybenzene	-	-	91	2
1,2-Dihydroxybenzene	-	FA, HA, HF	88	3
4-Hydroxybenzaldehyde	-	FA, HA, HF	92	4
1,2,3-Trihydroxybenzene	HF	FA, HA	90	5
Ethenyloxybenzene	-	-	81	6
4-Ethenyl-1,2-dihydroxybenzene	-	-	91	7
4-Hydroxybenzoic acid	FA, HA, HF	-	82	8
1,2,3-Trihydroxytoluene	-	HA	86	9
3,4-Dihydroxybenzaldehyde	FA, HA	HF	93	10
3,4-Dihydroxybenzoic acid	FA, HA	HF	89	11
3,4,5-Trihydroxybenzaldehyde	HF	FA, HA	86	12
4-Hydroxycinnamic acid	-	FA, HA	94	13
1-(3,4,5-Trihydroxyphenyl)-ethanone	-	-	91	14
3,4,5-Trihydroxybenzoic acid	HF	FA, HA	93	15
1,2,3,4-Tetrahydroxy-5-(2-propenyl)-benzene	-	-	81	16
3,4-Dihydroxycinnamic acid	-	FA, HA	91	17
Dehydroabietic acid	HF	-	82	18

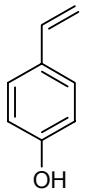

1-ethenyl-4-hydroxybenzene

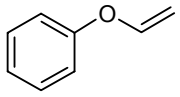

ethenyloxybenzene

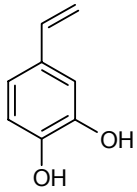

4-ethenyl-1,2-dihydroxybenzene

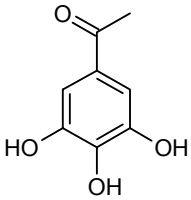

1-(3,4,5-trihydroxyphenyl)-ethanone

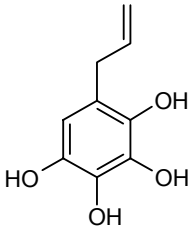

1,2,3,4-tetrahydroxy-5-(2-propenyl)-benzene

Figure 2-13. Structures of underivatised compounds in lignin not identified in fulvic acids, humic acids and HULIS. Matching factors are given in table 2-6.

The thermochemogram contained few cleavage products. Benzoic acid and 4-hydroxybenzoic acid are part of fulvic acids, humic acids and HULIS. Moreover, many compounds in lignin such as hydroxylated aromatic carboxylic acids, and hydroxylated benzaldehydes belonged to the same compound class as found in fulvic acids, humic acids and HULIS. Hydroxylated cinnamic acids are structurally very close to coumaric acid and ferrulic acid, which are components of lignin (Lüttge *et al.*, 1999). Dehydroabietic acid is a typical component of wood resins and was identified as well.

A series of hydroxylated benzene derivates substituted with vinyl and allyl (ethenyl and propenyl) groups were detected (figure 2-13). Vinyl and allyl groups might derive from ether cleavage as shown for 11-phenoxyundecanoic acid (VI) in chapter 2.3.3. This indicates the components in lignin being linked by ether bonds. However, no vinyl nor allyl and only few olefinic compounds such as 2-butenedioic acid and 2-hexenedioic acid were detected in the HULIS fraction. This is an indication that HULIS probably contain no ether but rather ester groups.

2.3.3 Thermochemolysis of model compounds

Thermochemolytical cleavage of esters or ethers was investigated with the model compounds shown in figure 2-14 in order to obtain more information about the cleavage behaviour and composition of HULIS.

Thermochemolysis of benzyl benzoate (I) and p-tolylbenzoate (II) gave the corresponding methylester and methoxy products. Didecylphtalate (III) formed phthalic acid dimethylester and decanol as cleavage products. Moreover, N-methylphthalimide was a reaction product of phthalic acid with TMAH. N-methylphthalimide was found in filters U5, U6, U19 and M6 (chapter 2.3.1). It was regarded as a thermochemolytical artefact. 4-Phenoxybenzoic acid (IV) reacted to 4-phenoxybenzoic acid methylester. The corresponding methylester and methoxy cleavage products were obtained in lower quantities. 4-Phenoxyphenol (V) was methylated to 1-methoxy-4-phenoxybenzene. Its methylester and methoxy cleavage products were obtained in lower quantities as well. Both 4-Phenoxybenzoic acid (IV)

and 4-Phenoxyphenol (V) formed in addition diphenylether as degradation product. 11-phenoxyundecanoic acid (VI) was methylated and produced undecenoic acid and methoxybenzene as cleavage products in low quantities. No thermochemolytical products were obtained for 2(3)-(tetrahydrofurfuryloxy)-tetrahydropyran (VII).

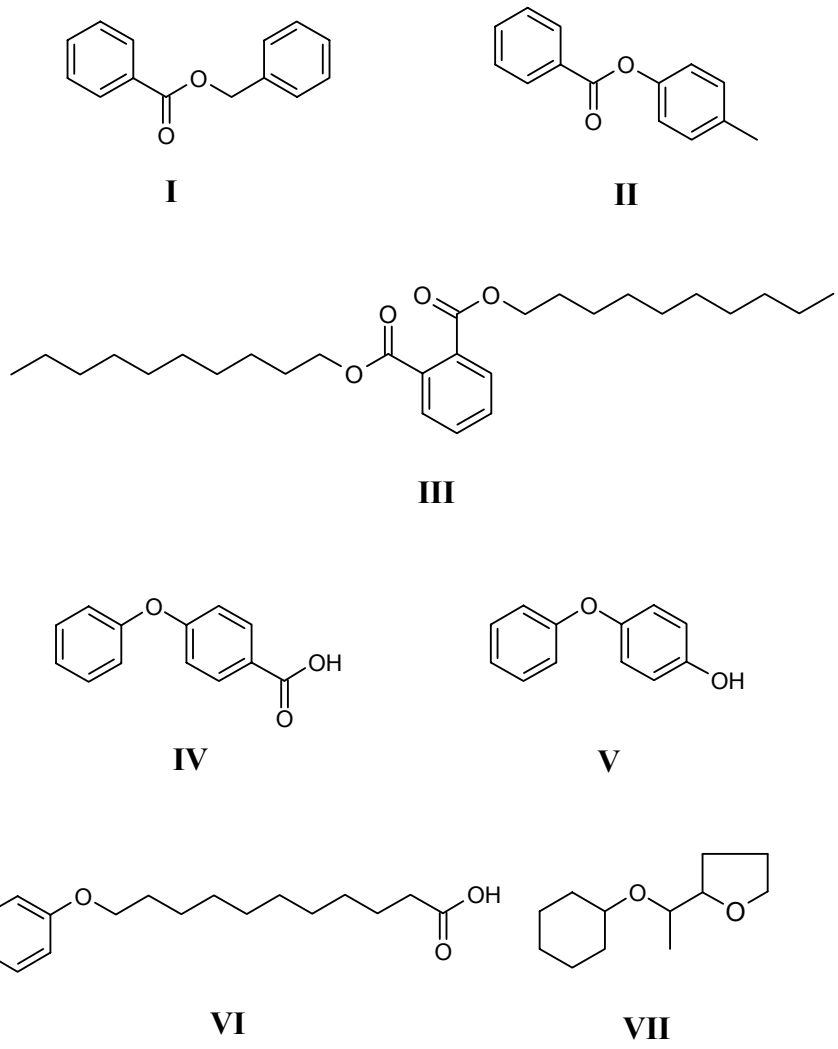

Figure 2-14. Model ester and ether compounds studied with thermochemolysis. Benzyl benzoate (I), 4-methylphenylester benzoic acid (II), didecylphtalate (III), 4-phenoxybenzoic acid (IV), 4-phenoxyphenol (V), 11-phenoxyundecanoic acid (VI), 2(3)-(tetrahydrofurfuryloxy)-tetrahydropyran (VII).

Investigations of model compounds showed that thermochemolysis of aromatic ester compounds was more efficient. The presence of aliphatic partial structures seemed to reduce the yield of ester cleavage. The same was valid for aromatic ethers. Aliphatic ethers did not show any reaction. Furthermore, it was observed that decarboxylation and dehydroxylation can occur during thermochemolysis even though at a lower degree.

2.3.4 Structure proposal for HULIS

Partial structure information about HULIS was obtained by thermochemolysis GC-MS (chapter 2.3.1, table 2-2). Aromatic carboxylic acids, hydroxylated aromatic carboxylic acids and aliphatic mono- and dicarboxylic acids were the most abundant substructures of HULIS.

However, after thermochemolysis of the HULIS, a dark brownish residue remained on the sample tube. Pyrolysis was performed of the residue at 600 °C, but only few chromatographic signals close to the detection limit were detected. The poor quality of the corresponding mass spectra did not allow any library search. The chemical composition of the residue remained unknown. Identification of some of the compounds would have given an indication of the composition of the brownish residue completing the list of the HULIS substructures.

Investigations on the thermochemolytical degradation of reference and model compounds (chapters 2.3.2 and 3.3.3) led to the conclusion that partial structures of HULIS are rather linked by ester than by ether bonds. Fulvic and humic acids formed very similar thermochemolytical products as HULIS. A major part of them were identical indicating the macromolecular nature of HULIS. Consequently, HULIS should consist of combinations of the substructures of table 2-2. Summarised substructures and general schematic structure proposals of HULIS are given in figure 2-15.

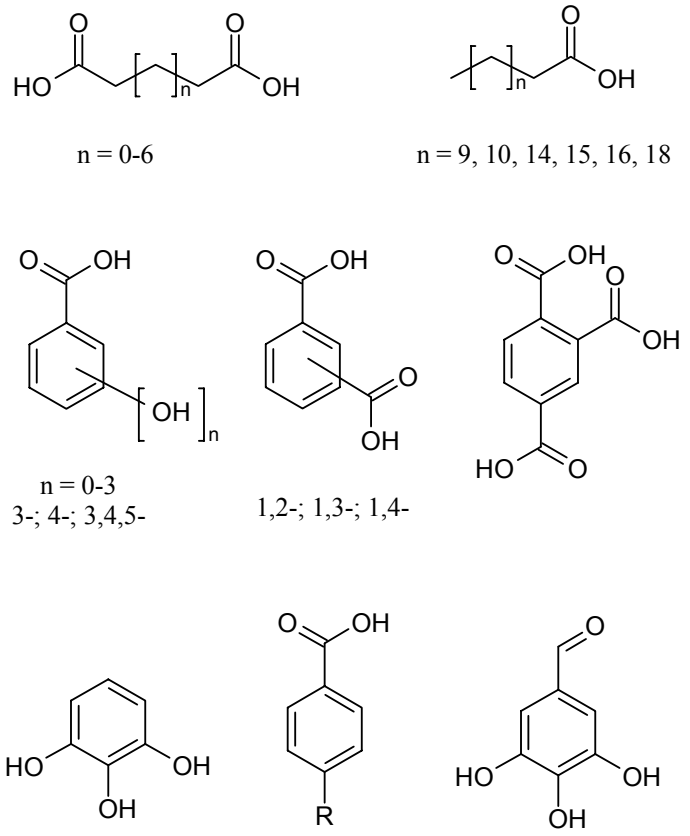

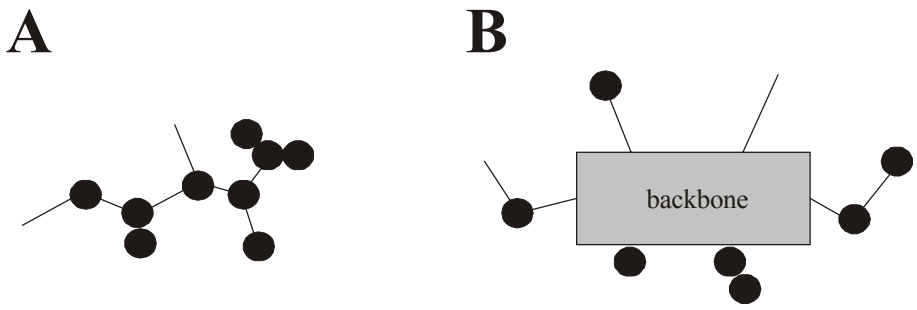

Figure 2-15. (Above) Summary of the 24 substructures identified by thermochemolysis GC-MS (chapter 2.3.1, table 2-2). (Below) Schematic structure proposals of HULIS without backbone (**A**) and with backbone (**B**). Aliphatic compounds are abbreviated as —— and aromatic compounds as ●.

Substructures with a carboxylic acid group can only bind to a substructure containing a hydroxylic group by means of a ester bond. This means, that hydroxylated aromatic substructures can be connected to each other. Moreover, aliphatic dicarboxylic acids can link to two hydroxylated aromatic substructures. Aliphatic monocarboxylic acids can only bind to one hydroxylated aromatic substructure. However, aliphatic carboxylic acids cannot link to each other, as they contain no hydroxyl groups. There are plenty of possibilities how substructures can be connected by ester bonds forming HULIS.

Part of the substructures of HULIS remained unresolved, since no further structural information could be retrieved from the brownish residue by pyrolysis. Therefore, it could not be excluded that HULIS are solely composed by the substructures given in table 2-2. The unresolved substructures might act as a backbone to which the elucidated substructures are attached to. A schematic example is given in figure 2-15.

2.3.5 Limitations of the method

A limitation of the method constitutes the isolation of HULIS from other organic compounds by solid phase extraction of the raw extract. Most HULIS were separated from other polar organic compounds. However, a complete isolation was difficult. The presence of other polar organic compounds in the HULIS fraction could not be excluded (chapter 2.3.1).

All carboxylic acids and hydroxyl groups were detected as their corresponding methylester and methoxy derivates with the method presented. It was not possible to differentiate between compounds already methylated before thermochemolysis and those methylated during thermochemolysis. An example was the detection of the fully methylated derivates of originally only partially methylated components of lignin such as synapyl acohol and methoxyphenol.

Despite of the good resolution of HR-GC (high resolution gas chromatography), coelution of two or more compounds occurred. Identification of the coeluting compounds was not always possible. Three abundant chromatographic signals (chapter 2.3.6, table 2-11) consisted of three coeluting compounds, which could not be identified. Only their aliphatic or aromatic nature was determined by interpretation of their sum fragment spectra.

2.3.6 Multivariate statistical pattern comparison

Most sample thermochemograms of the HULIS fraction contained the same compounds. However, signal intensities varied strongly. A manual comparison of the complex signal patterns was impossible. However, multivariate statistical methods such as cluster analysis and principal component analysis allowed to evaluate similarities and differences in the signal patterns of the thermochemograms.

Fingerprinting

Information was extracted as fingerprint patterns from the thermochemograms. For this purpose 20 identified compounds (S1-S20), which occurred in all thermochemograms were chosen (table 2-7). Three unknown compounds (S8, S12 and S14) had to be included, since they were abundant and thus relevant. Their aromatic or aliphatic nature was determined from interpretation from their mass spectra (chapter 2.3.5). The information in a thermochemogram was reduced to a fingerprint pattern containing the relative distribution of the signal intensities of the 20 relevant compounds. Since the area of the chromatographic signal was difficult to integrate due to interfering signals of low intensity, signal intensities were used instead for fingerprinting. Only sharp chromatographic signals were chosen for fingerprinting. The first two signals in the thermochemograms were omitted. Their signal intensities did not reflect the correct abundance of the corresponding compounds as they showed signal broadening (figure 2-16).

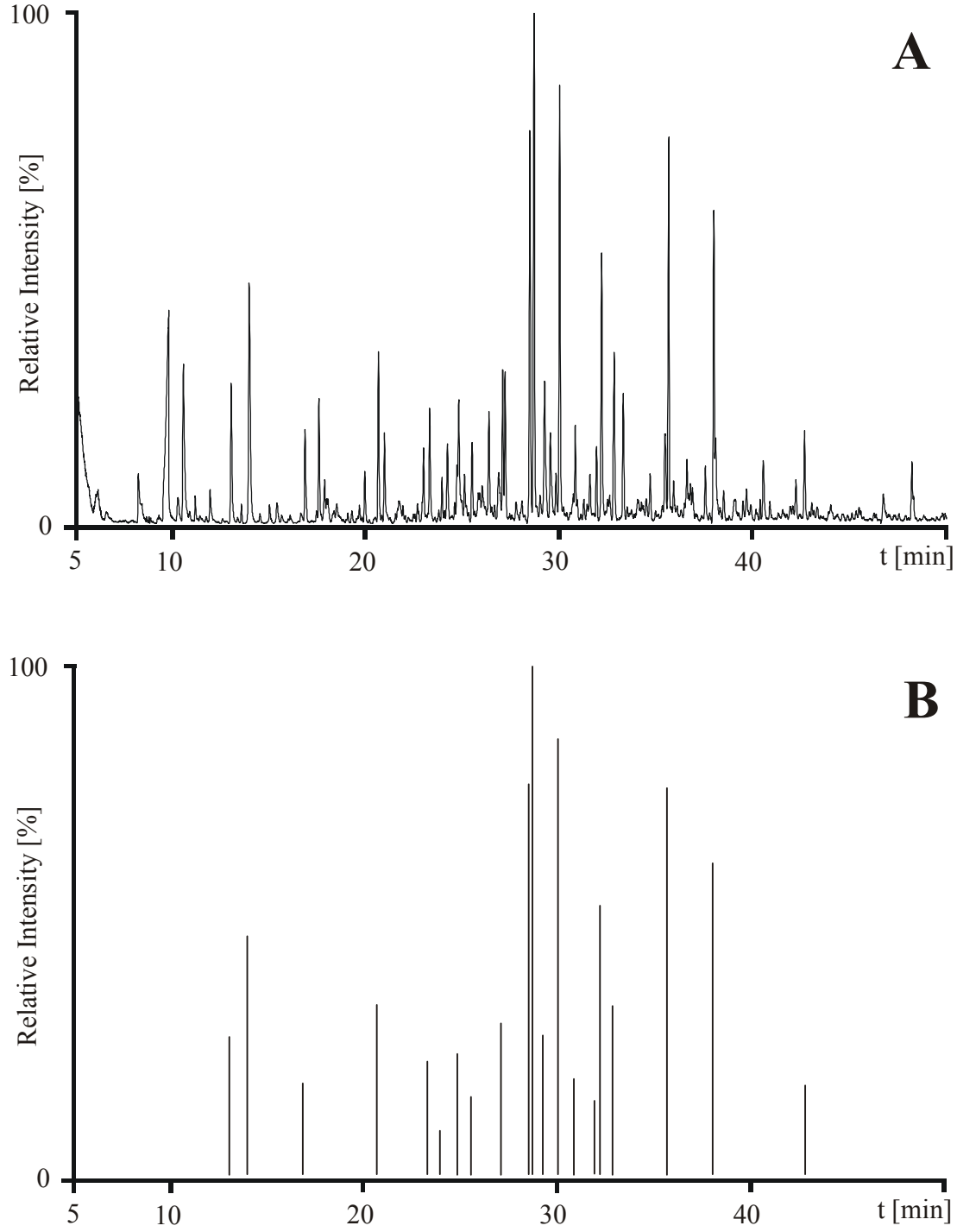

Figure 2-16. (**A**) Thermochemogram of the HULIS fraction of filter U21 obtained with 2% TMAH. EI, full scan mode, mass range *m/z* 35-350, background subtracted (100% = 3.0 x 10^6 counts). (**B**) Fingerprint pattern containing the relative distribution of the intensities of 20 relevant chromatographic signals of A.

Table 2-7 List of 20 underivatised compounds (S1-S20) selected for fingerprinting (see figure 2-16 for an example).

	Compounds for fingerprint pattern
S1	Butanedioic acid
S2	Benzoic acid
S3	Pentanedioic acid
S4	Hexanedioic acid
S5	3-Hydroxybenzoic acid
S6	Heptanedioic acid
S7	4-Hydroxybenzoic acid
S8	Unknown 1 (aliphatic)
S9	Octanedioic acid
S10	1,2-Benzenedicarboxylic acid
S11	1,4-Benzenedicarboxylic acid
S12	Unknown 2 (aromatic)
S13	Nonanedioic acid
S14	Unknown 3 (aliphatic)
S15	4-Methyl-1,2-Benzenedicarboxylic acid
S16	3,4-Dihydroxybenzoic acid
S17	Tetradecanoic acid
S18	3,4,5-Trihydroxybenzaldehyde
S19	Hexadecanoic acid
S20	Octadecanoic acid

Fingerprint patterns as shown in figure 2-16 were extracted from each thermochemogram recorded from filters U1-U22. Differences were found in the fingerprint patterns. The biggest differences were stated between winter and summer filter samples. Figure 2-17 shows the fingerprint patterns of a winter and summer sample. However, despite the data reduction a manual comparison was still very difficult. A differentiated comparison of the fingerprint patterns was only possible by multivariate statistical methods such as cluster analysis and principal component analysis. Therefore, a normalisation of the intensities in the fingerprint patterns was performed.

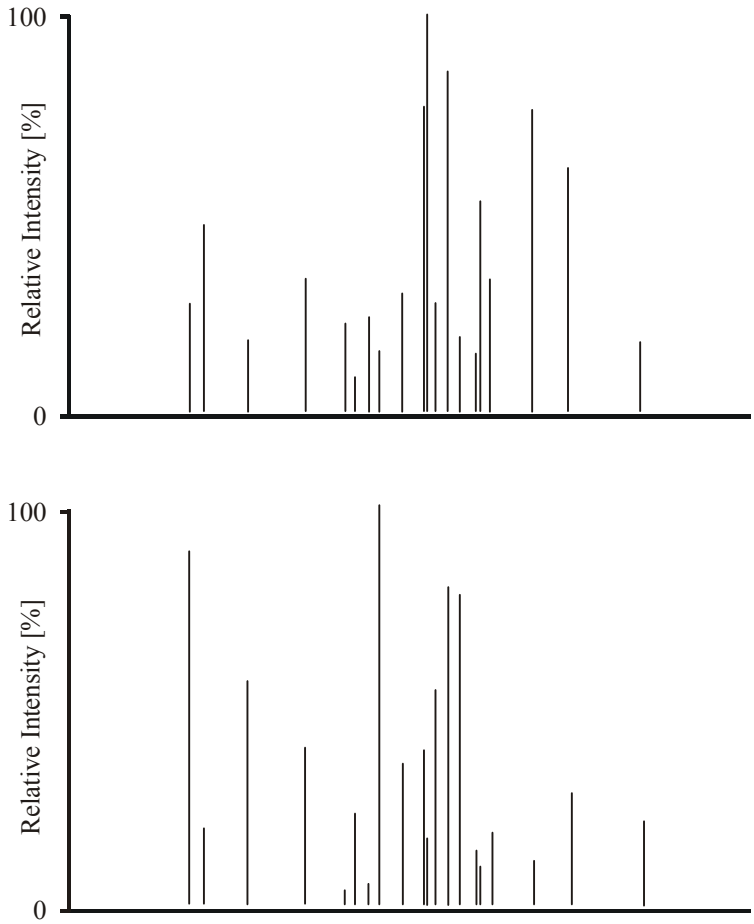

Figure 2-17. Relative distribution of the 20 signal intensities (S1-S20) of a winter filter (U21, December, above) and a summer filter (U12, August, below).

1,2-Benzenedicarboxylic acid (S10) was chosen for abundance normalisation, because it appears in the centre of the thermochemogram (29 min) and is the most intense signal in most filters. The intensity of each of the 20 signals was normalised by the intensity of 1,2-Benzenedicarboxylic acid as shown below (normalisation scale 0-1):

$$\frac{intensity\ of\ compound\ \ X}{intensity\ of\ compound\ S10} = \ normalised\ intensity\ X$$

X: Compounds S1-S9 and S11-S20

Since compound S10 gave a value of 1 when normalised by itself, it was not taken into consideration. The matrix used for cluster analysis and factor analysis was of 22 samples times 19 normalised intensities, thus containing 418 items.

To check the reproducibility of thermochemolysis and the correct performance multivariate analysis, control measurements were implemented. Thermochemolysis of the HULIS fraction of filter U9 was carried out four times (parallels A-D). The 19 normalised intensities in the parallels A-D had an average standard deviation of 14%. In addition, the similarities between A-D were investigated by multivariate analysis.

Cluster analysis

The above described matrix was submitted to different calculation methods and distance measures commonly used in cluster analysis. Most significant clustering of the filters was obtained by the Ward method. Euclidic distances enabled a good visualisation of the clusters. The resulting dendrogram is shown in figure 2-18.

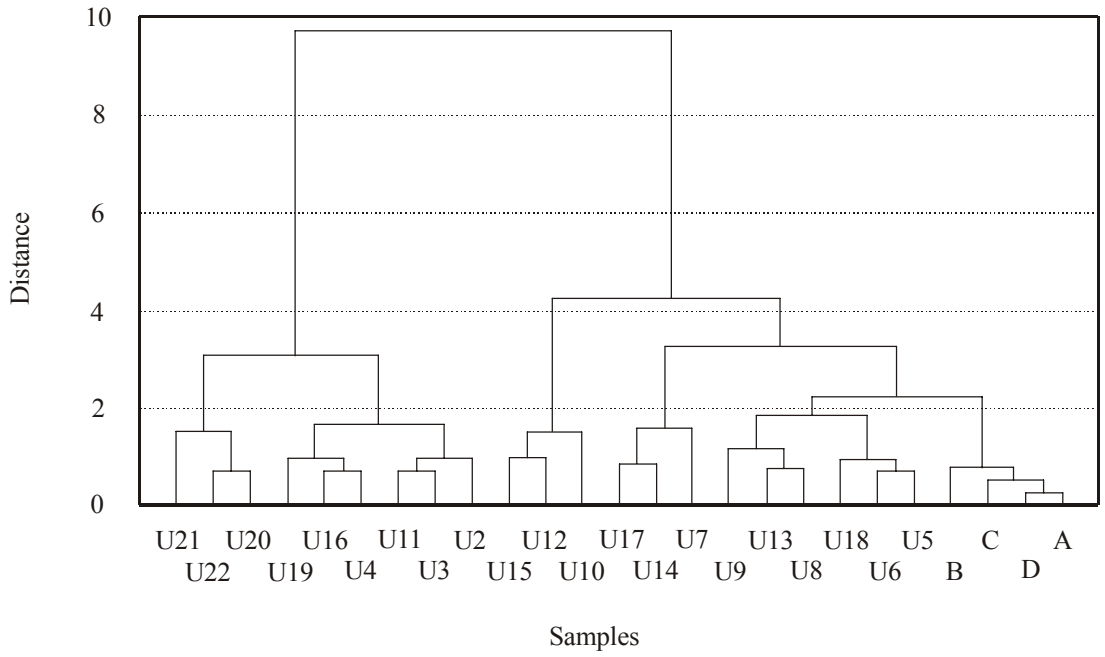

Figure 2-18. Dendrogram generated by cluster analysis with the Ward method and Euclidic distances for urban samples U2-U22 and the parallels A-D.

Cluster analysis gave two main clusters with a distance of 9.5. The left one contained all winter and two autumn filters. U11 (July) was the only seasonal exception in this cluster. The clustering inside the right main cluster seemed not to follow any order, as spring, summer and autumn filters were distributed randomly. Cluster analysis allowed a first differentiation between winter samples and the rest. However, factor analysis should provide more significant clustering.

The four parallels A-D of sample U9 formed a subcluster with distances of 0.3-0.8 on the very right side of right main cluster. The short distances additionally proved the reproducibility of thermochemolysis and the functionality of cluster analysis.

Principal component analysis

Principal component analysis (PCA) was performed with the matrix described above. Principal components (PC) were extracted without rotation. Three factors of a minimal eigenvalue >1 were found: PC 1 = 7.8 (41% of variance), PC 2 = 4.5 (24% of variance) and PC 3 = 3.0 (16% of variance). Therefore, a 3D- plots would reflect the complete information. However, such a visualisation is difficult. Therefore, 2D plots are shown.

The 2D-loading plot of PC 1 against PC 2 (figure 2-19) showed the clusters. The first one contained the winter samples and the second one those from spring and autumn. Summer samples were in the third cluster. There was no sharp separation between the three clusters. However, the warmer the season, the more the samples shifted towards higher PC1 values. U11 (July) was the only exception. The parallels A-D were close together, which again stated the good reproducibility of thermochemolysis.

2D-loading plots of PC 1 against PC 3 and PC 2 against PC 3 showed one cluster containing the winter samples and a second one containing the randomly distributed spring, summer and autumn samples. Not much information was retrieved from these plots.

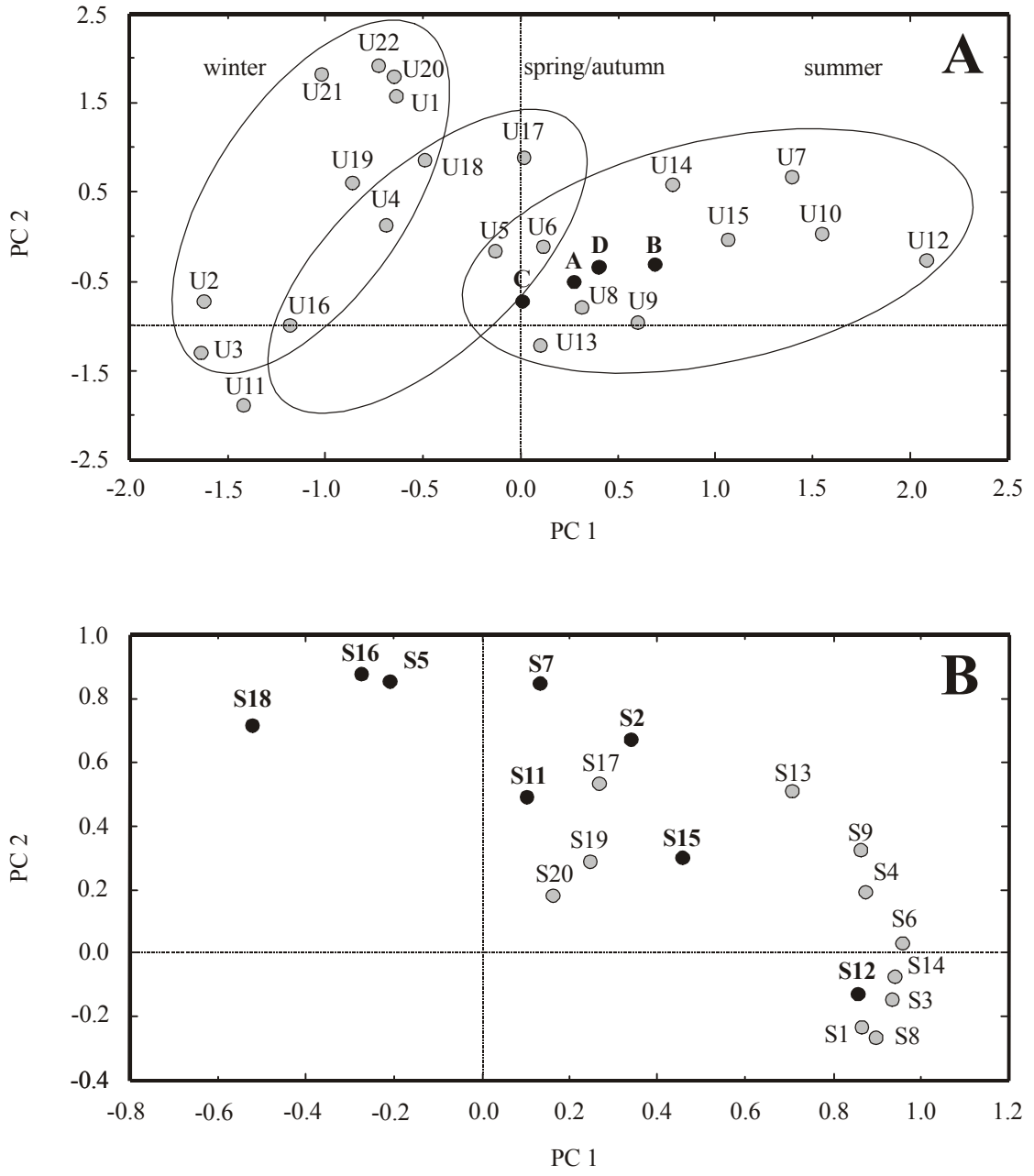

Figure 2-19. Loading plot of PC1 and PC2 (**A**) as well as the score plot (**B**) of the urban samples U1-U22 and the parallels A-D. Black dots are aromatic and grey dots aliphatic compounds.

The comparison of the loading plot and the score plot enabled a correlation between seasonal differences in the chemical composition of HULIS and the corresponding responsible compounds. Aromatic compounds were characteristic for winter samples, especially 3-hydroxybenzoic acid (S5), 3,4-dihydroxybenzoic acid (S16) and 3,4,5-trihydroxybenzaldehyde (S18). Unknown 2 (S12) was the only aromatic compound typical for the summer samples. Benzoic acid (S2), 4-hydroxybenzoic acid (S7) and 1,4-benzenedicarboxylic acid (S11) were characteristic aromatic compounds for spring and autumn samples. Generally, aliphatic compounds such as butanedioic acid (S1), pentanedioic acid (S3), hexanedioic acid (S4), heptanedioic acid (S6), octanedioic acid (S9) and the aliphatic unknown 1 (S8) were typical for summer samples. Nonanedioic acid (S13), tetradecanoic acid (S17), hexadecanoic acid (S19) and octadecanoic acid (S 20) were characteristic for spring and autumn samples.

Hydroxylated aromatic carboxylic acids and benzoic acid seemed to be characteristic for the winter months such as November (U19, U20), December (U21, U22), January (U1) and February (U2, U3). Their strong correlation of these compounds with the cold season indicates wood combustion and fossil fuel burning for heating as a main source for these substructures in HULIS. Aliphatic dicarboxylic acids dominated in the samples of the warm seasons and may have a vegetal origin. However, anthropogenic precursors cannot be excluded.

2.4 Conclusions

Thermochemolysis GC-MS allowed to cleave HULIS into substructures and to identify their methylated analogues. HULIS were mainly composed of substructures such as hydroxylated aromatic carboxylic acids, and aliphatic mono- and dicarboxylic acids. Moreover, a dark brownish residue remained, which indicated that not all substructures of HULIS were detected by thermochemolysis. However, no further substructures could be identified by pyrolysing the residue. This implies the existence of substructures to which the hydroxylated aromatic carboxylic acids, and aliphatic mono- and dicarboxylic acids might be attached to.

Thermochemolytical degradation was carried out with reference compound such as humic acids, fulvic acids and lignin. The investigations showed that part of the substructures of HULIS are the same as those of the reference compounds. Most other substructures of HULIS belonged to compound classes also present in the reference compounds. The strong similarities to the reference compounds indicates lignin as one probable precursor of HULIS. Oxidised lignin substructures are possibly directly emitted on wood smoke aerosols into the atmosphere during combustion of wood. They might further oxidise and aggregate to HULIS. However, fossil fuel burning could not be excluded as a source for these substructures.

From the investigations on thermochemolytical degradation of model compounds it was concluded that HULIS probably contain aromatic esters, and esters with aliphatic and aromatic partial structures. Aromatic ethers were less likely to be present, since no intact aromatic ethers were detected in the HULIS fraction. Ethers with aliphatic and aromatic partial structures were also less probable, since almost no olefinic compounds were identified in the HULIS fraction. Furthermore, aliphatic esters were unlikely, as no aliphatic alcohols were identified.

Signal patterns in the thermochemograms were compared by principal component analysis. The clusters observed could be attributed to different seasons. Chemical composition of spring, summer and autumn samples seemed to be similar. However, filter samples from November, December, January and February were completely separated from the rest, indicating a bigger difference in the chemical composition. Investigations showed that hydroxylated aromatic carboxylic acids were more abundant in these filter samples. Aliphatic dicarboxylic acids seemed to be typical for spring, summer and autumn samples. It was concluded, that aromatic substructures are typical for the winter filters, indicating combustion of heating oil and wood as possible source. Aliphatic substructures are characteristic for spring summer and autumn samples, which points to isoprenoid compounds emitted by vegetation as possible source.

2.5 References

Belitz, H.-D. and Grosch, W., 1992: *Lehrbuch der Lebensmittelchemie*, Springer-Verlag, Berlin.

Challinor, J., M., 2001: Review: the development and applications of thermally assisted hydrolysis and methylation, *J. Anal. Appl. Pyrolysis* **61**, 3-34.

Davies, A. N., Kuckuk, R., Hill, W., Nolte, J. and Burba, P., 2001: A comparison of various pyrolysis experiments for the analysis of reference humic substances, *J. Anal. Appl. Pyrolysis* **60**, 145-157.

Falbe, J. and Regitz, M., 1996: *Römpp Lexikon Chemie*, Georg Thieme Verlag, Stuttgart, New York.

Frazier, S. W., Nowack, K. O., Goins, K. M., Cannon, F. S., Kaplan, L. A. and Hatcher, P. G., 2003: Characterization of organic matter from natural waters using tetramethylammonium hydroxide thermochemolysis GC-MS, *J. Anal. Appl. Pyrolysis* **70**, 99-128.

Fuzzi, S., Facchini, M. C., Decesari, S., Matta, E. and Mircea, M., 2002: Soluble organic compounds in fog and cloud droplets: what have we learned over the past few years?, *Atmos. Environ.* **64**, 89-98.

Gelencser, A., Meszaros, E., Blazso, M., Kiss, G., Krivacsy, Z., Molnar, A. and Meszaros, E., 2000: Structural Characterisation of Organic Matter in Fine Tropospheric Aerosol by Pyrolysis-Gas Chromatography-Mass Spectrometry, *J. Atmos. Chem.* **37**, 173-183.

Guderian, R., (Ed.), 2000. Band 1A: Atmosphäre. In: Handbuch der Umweltveränderungen und Ökotoxikologie, Berlin, Springer-Verlag.

Lüttge, U., Kluge, M. and Bauer, G., 1999: *Botanik*, Wiley-VCH Verlag, Weinheim.

Martin, F., del Rio, J. C., Gonzalez-Vila, F. J. and Verdejo, T., 1995: Pyrolysis derivatisation of humic substances 2. Pyrolysis of soil humic acids in the presence of tetramethylammonium hydroxide, *J. Anal. Appl. Pyrolysis* **91**, 75-83.

Martin, F., Gonzalez-Vila, F. J., del Rio, J. C. and Verdejo, T., 1994: Pyrolysis derivatization of humic substances 1. Pyrolysis of fulvic acids in the presence of tetramethylammonium hydroxide, *J. Anal. Appl. Pyrolysis* **28**, 71-80.

Mukai, H. and Ambe, Y., 1986: Charaterization of a humic acid-like brown substance in airborne particulate matter and tentative identification of its origin, *Atmos. Environ.* **20**, 813-819.

Nolte, C. G., Schauer, J. J., Cass, G. R. and Simoneit, B. R. T., 2001: Highly Polar and Organic Compounds Present in Wood Smoke and in the Ambient Atmosphere, *Environ. Sci. Technol.* **35**, 1912-1919.

Saxena, P. and Hildemann, L. M., 1996: Water-Soluble Organics in Atmospheric Particles: A Critical Review of the Literature and Application of Thermodynamics to Identify Candidate Compounds, *J. Atmos. Chem.* **24**, 57-109.

Simoneit, B. R. T. and Mazurek, M. A., 1982: Organic matter of the troposphere. II. Natural background of biogenic lipid matter in aerosols over the rural western United States, *Atmos. Environ.* **16**, 2139-2159.

Steglich, W., Fugmann, B. and Lang-Fugmann, S., (Ed.), 1997. Naturstoffe. In: Römpp Lexikon, Stuttgart/New York, Georg Thieme Verlag.

Stryer, L., 1999: *Biochemie*, Spektrum Akademischer Verlag, Heidelberg.

Szidat, S., Jenk, T. M., Gäggeler, H. W., Synal, H.-A., Fisseha, R., Baltensperger, U., Kalberer, M., Samburova, V., Reimann, S., Kasper-Giebl, A. and Hajdas, I., 2004: Radiocarbon (^{14}C)-deduced biogenic and anthropogenic contributions to organic carbon (OC) of urban erosols from Zürich, Switzerland, *Atmos. Environ.* **38**, 4035-4044.

Varga, B., Kiss, G., Ganszky, I., Gelencser, A. and Krivacsy, Z., 2001: Isolation of water-soluble organic matter from atmospheric aerosol, *Talanta* **55**, 561-572.

3 STRUCTURE ELUCIDATION OF THE WSOC FRACTION BY LC-MS

3.1 Introduction

Atmospheric aerosols have an important effect on atmospheric processes. They can act as cloud condensation nuclei and control transmission of light through the atmosphere by scattering and absorbing light. A considerable effort has been undertaken to characterise the chemical composition of atmospheric aerosols. Many non-polar compounds of the water-insoluble fraction have already been characterised (Jacobson *et al.*, 2000). However, little is known about polar and water-soluble organic carbon (WSOC), which account for 20 to 70% of the total organic carbon (Saxena and Hildemann, 1996). HULIS constitute around one quarter of the WSOC and are thus largely involved in cloud condensation processes.

Besides polar and water-soluble organic compounds also inorganic salts, especially sulphate, are responsible for the cloud condensation effect of atmospheric aerosols (Novakov and Penner, 1993; Seinfeld and Pandis, 1998). The content of sulphate in atmospheric aerosols can reach 39% of all water-soluble species (Kiss *et al.*, 2000). Sulphate is directly emitted or generated by oxidation of sulphur dioxide (SO_2) (Brimblecombe, 1996). Dominant natural sources include weathering of rocks and soil, volatile biogenic sulphur emissions from land and oceans as well as volcanoes. Combined natural sources are estimated to release globally between 80-120 x 10^6 t of SO_2. In 1995 global anthropogenic SO_2 emissions were estimated to 142 x 10^6 t (UNEP, 2002). Furthermore, around 175 x 10^6 t of sulphate are transferred annually from the oceans to the continents (Brimblecombe, 1996).

Liquid chromatography coupled with mass spectrometry (LC-MS) constitutes a sensitive and selective analytical tool for characterisation and quantification of polar organic compounds occurring in the environment. Ion trap mass spectrometry (IT) allows to detect a series of consecutive fragment ion spectra (MS^n). They are suited for structure elucidation of unknown polar organic substances. Quadrupole mass

spectrometers are more sensitive in single ion monitoring (SIM) and MS-MS and thus preferably used for quantification and monitoring of polar organic and inorganic compounds.

Molecular weight distributions of HULIS were investigated by a quadrupole mass spectrometer (Feng and Möller, 2004; Kiss *et al.*, 2003). Furthermore, identification of single polar compounds in fog water was attempted by comparing MS-MS fragment spectra of HULIS with model compounds (Cappiello *et al.*, 2003). However, hitherto information about the chemical composition HULIS in atmospheric aerosols by means of LC-MS^n is scarce. More details about the chemical composition of HULIS and investigations on the reciprocal interaction of sulphate and HULIS in atmospheric aerosols by means of qualitative and quantitative LC-MS would lead to a better understanding of the effect of atmospheric aerosols in cloud condensation processes.

3.2 Experimental

3.2.1 Chemicals and solvents

Octyl sulphate (Fluka, Switzerland), 2-hydroxy-5-sulphobenzoic acid (Fluka, Switzerland), 2-hydroxy-5-nitrophenyl sulphate (Aldrich, Switzerland) and 5-bromo-4-chloro-3-indolyl sulphate (Acros, Belgium) were used as model compounds and were of ≥95% quality. Ammonium sulphate was obtained from Fluka (Switzerland). Humic acid, Nordic aquatic fulvic acid, ACN, MeOH and processed water were the same as described in chapter 2.2.1. D_2O was purchased from Cambridge Isotope Laboratories Inc. (USA). Helium of 99.996% (Carbagas, Switzerland) was used as damping gas for the ion trap mass spectrometer. Nitrogen (99.5% purity) from a high-purity nitrogen generator (NM30L; Peak Scientific Instruments, UK) was used for nebulising gas, drying gas, sheath gas and auxiliary gas for mass spectrometry.

3.2.2 Aerosol filter samples

Sampling conditions and settings were the same as described in chapter 2.2.2. Filters listed in table 2-1 (chapter 2.2.2) were used for quantification of organosulphates and inorganic sulphate. Filter QF 34 exposed at Feldbergstrasse (chapter 2.2.2) on

23.12.2003 (17 mg of PM_{10} collected), filters QF 92 (24.1 mg of PM_{10}, 19.10.2001), QF 99 (8.7 mg of PM_{10}, 26.10.2001), QF 116 (23.6 mg of PM_{10}, 14.10.2001), QF 117 (21.9 mg of PM_{10}, 15.10.2001) and QF 119 (23.1 mg of PM_{10}, 17.10.2001) sampled in Laufen (Switzerland, 47° 25' N, 7° 30' E) were used for qualitative measurements.

3.2.3 Sample preparation

Raw extracts of filters QF 34, QF 92, QF 99, QF 116, QF 117 and QF 119 were obtained as described in chapter 2.2.3 and directly used for analysis. Further preparation of the raw extracts was not necessary. The raw extracts of QF 117 and QF 119 were combined, evaporated to dryness and re-dissolved in D_2O.

3.2.4 Instrumentation

Chromatography

Two HPLC columns BioBasic-18 (C_{18} phase, 5 µm particle size and 300 Å pore size, Thermo Electron, USA) were used for qualitative (250 x 4 mm) and quantitative (150 x 3 mm) measurements. A gradient composed of A (H_2O) and B (50+50 v/v, ACN/MeOH) was employed as follows: 0-3 min 10% B, 3-4 min up to 90% B, 4-6 min 90% B, 6-7 min down to 10% B and 7-20 min 10% B. The flow rate was 450 µl/min for qualitative and 300 µl/min for quantitative measurements.

Mass spectrometry

An ion trap mass spectrometer (LCQ classic, ThermoFinnigan, USA) was used for qualitative measurements. Electrospray ionisation was employed as a soft ionisation method in the negative mode (ESI(-)). The following parameters were applied: sheath gas flow 60 arbitrary units (arb), auxiliary gas 0 arb, spray voltage 4.5 kV, heated capillary temperature 230 °C, capillary voltage -10.5 V and maximal ion time 500 ms. Samples were injected by a PAL autosampler (CTC Analytics, Switzerland). The injected volume was 20 µl in the partial loop mode. The mobile phase was previously degassed with a HP 1050 series degasser unit (Hewlett Packard, USA). A Rheos 2000

low pressure gradient HPLC pump (Flux Instruments, Switzerland) was used for eluent pumping.

An time-of-flight mass spectrometer (TOF) (LCT, Waters-Micromass, UK) was used in the ESI(-) mode for accurate mass measurements. The measurements were performed by flow injection (10 µl loop) to 50+50 (v/v) H_2O/ACN at a flow rate of 200 µl/min. The parameters were applied as follows: capillary voltage 3 kV, sample cone voltage 40 V, and source temperature 80 °C, desolvation temperature 100 °C, nebuliser gas flow 90 l h^{-1} and desolvation gas flow 470 l h^{-1}. Phosphate and its dimer and trimer were used as lock masses.

A triple quadrupole (1200L, Varian, USA) was used for quantification in the ESI(-) mode. The following parameters were applied: Spray voltage 4.0 kV, nebulising gas 4.1 bar, drying gas 1.2 bar, drying gas temperature 200 °C, shield voltage -600 V, capillary voltage -80 V. Samples were injected with a Triathlon autosampler (Spark Holland, The Netherlands) in the partial loop mode. The injected volume was 5 µl. The mobile phase was previously degassed with a degasser unit (Degassit, MetaChem Technologies, USA). A high pressure gradient HPLC system composed of two ProStar 210 HPLC pump units (Varian, Australia) was used for eluent pumping.

Data treatment

Results obtained by the ion trap in the full scan mode were processed by Xcalibur software (Thermo Electron, USA). Data from accurate mass measurements were obtained by MassLynx software (Waters, Great Britain). Quantification data were processed by MS Workstation software (Varian, USA).

3.3 Results and discussion

3.3.1 Chromatography of the WSOC

Common stationary phases used for reverse phase HPLC have a pore size of 100 Å. They showed poor separation and strong irreversible adsorption of the WSOC contained in the raw extract. Therefore, a HPLC column containing a C_{18}-phase with 300 Å pore size was used in this work. The wide pores provided a larger interaction surface, which allowed separation of the WSOC into several fractions partly according to the molecular size and polarity. Preseparation by solid phase extraction (SPE) as described in chapter 2.3.1 or by Limbeck and Puxbaum (1999) and Varga *et al.* (2001) was not necessary for LC-MS.

The HPLC method allowed the separation of inorganic species from WSOC. Moreover, WSOC was separated into three to four polar fractions (fractions I-IV) and one less polar fraction (fraction V). Detection in the ESI(+) mode yielded chromatographic signals of very poor intensity. Therefore, detection in the ESI(-) mode was performed for all measurements.

An example of the separation of the WSOC and their detection in the ESI(-) mode is shown by the total ion chromatogram of sample QF 34 in figure 3-1 A. A total of five signal ranges for fractionation (I-V) were visible between 5.6-16 min for most samples. Only few samples lacked fractions III and IV. Fractions I-IV eluted isocratically at 5% MeOH/ACN. They contained very polar and probably also ionic organic compounds. Inorganic sulphate eluted before fractions I-IV between 3.6-6.7 min. Some samples contained higher amounts of inorganic sulphate, which coeluted with fraction I. The most abundant fraction I had a signal at 6.4 min, fraction II at 7.0 min, fraction III at 7.5 and fraction IV at 8.2 min approximately.

Fraction V eluted between 12.4-16.4 min using a steep gradient from 5 to 95% MeOH/ACN within 1 min. Compounds of fraction V were less polar compared to those of fractions I-IV. The same fraction was isolated by C_{18} SPE and used as HULIS fraction for thermochemolysis GC-MS as discussed in chapter 2.3.1.

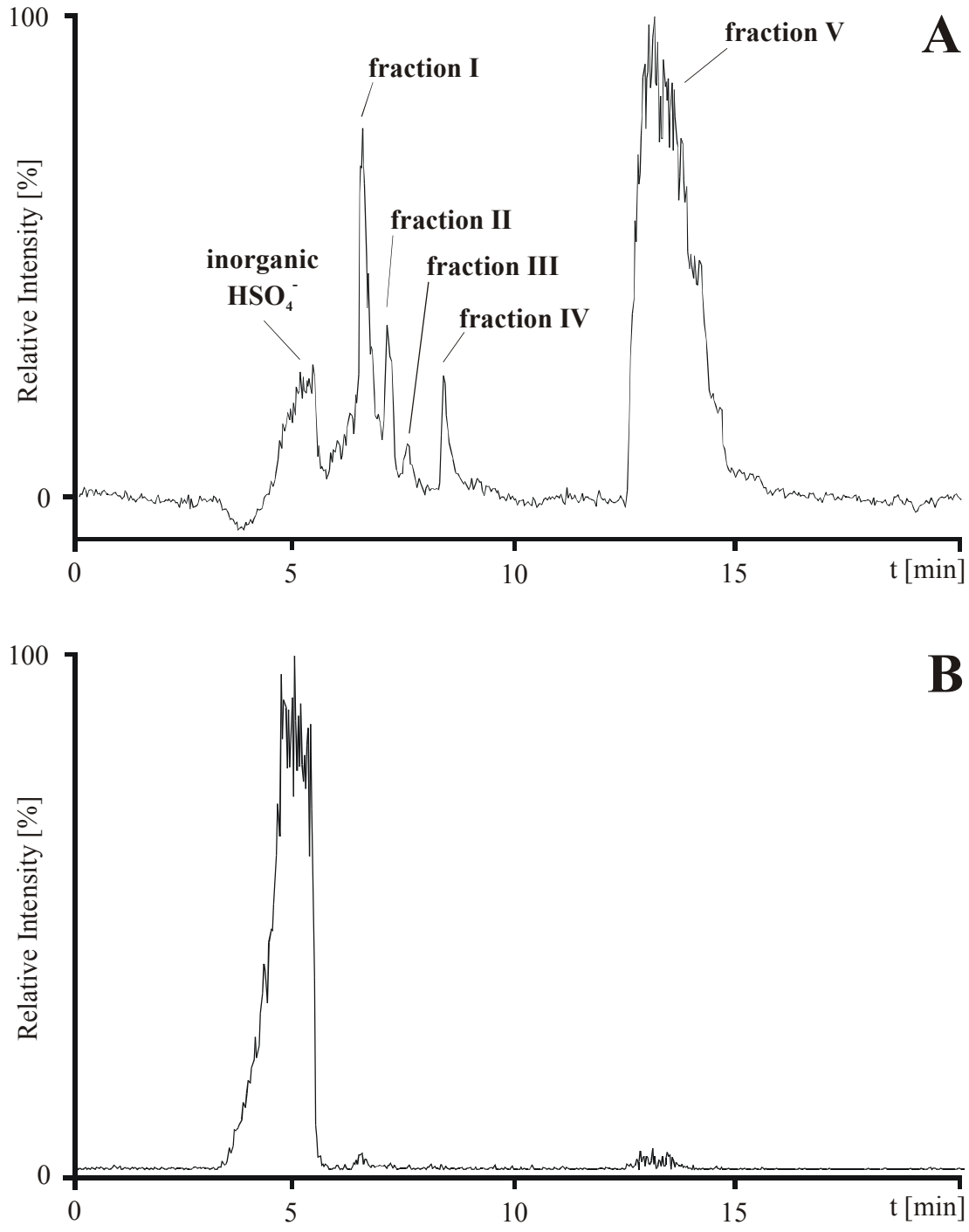

Figure 3-1. A IT-ESI(-) total ion chromatogram of filter QF34, mass range *m/z* 93-1000, (100% = 1.6 x 10^7 counts) showing inorganic sulphate and fraction I-V. **B** Extracted ion chromatogram of *m/z* 97 (HSO_4^-) (100% = 9.3 x 10^5 counts). Full scan spectra of fraction I and V are shown in figure 3-2 A and B respectively.

3.3.2 Mass distribution of HULIS

Full scan mass spectra of fractions I-IV showed a mass distribution starting at *m/z* 100 and ending at *m/z* 400. The mass signal pattern consisting of more intense odd than even mass signals was characteristic for HULIS. The intensity maximum of the mass signal pattern of HULIS was around *m/z* 240 (figure 3-2 A). A more detailed discussion about the mass signal pattern of HULIS is given in chapter 3.3.3.

Fractions I and II contained additionally single abundant masses. Many of them could be attributed to compounds identified by thermochemolysis GC-MS in the polar compound fractions and the HULIS fractions (chapter 2.3.3). Examples were the base ion *m/z* 165 corresponding to the deprotonated molecular ion of benzenedicarboxylic acid. This component was also abundant in the thermochemolysis experiments. The deprotonated molecular ions of the following compounds were also identified: benzenetricarboxylic acid (*m/z* 209), hydroxydicarboxylic acid (*m/z* 181), dihydroxycarboxylic acid (*m/z* 153), hydroxycarboxylic acid (*m/z* 137) and butanedioic acid (*m/z* 117) (figure 3-2 A). The identity of the compounds were confirmed by their corresponding MS^2 fragment spectra.

Fraction V showed a mass distribution starting at *m/z* 100 and ending at ca. *m/z* 900 (figure 3-2 B). The maximum was around *m/z* 500. The mass signal pattern of HULIS was hardly recognisable between *m/z* 100-400. Single abundant masses could not be attributed to any of the compounds found by thermochemolysis GC-MS. Compared to fractions I-IV the maximum of the mass signal pattern of HULIS shifted towards higher masses.

According to the chromatographic and mass spectrometric information discussed above, HULIS could be classified into two groups. Polar HULIS eluted first and were of lower mass (low mass HULIS, fractions I-IV). Less polar HULIS eluted later and were of higher mass (high mass HULIS, fraction V). Measurements of the raw extract by flow injections showed a mass distribution (figure 3-2 C) comparable to the sum of combined fractions I-V (figures 3-2 A and B).

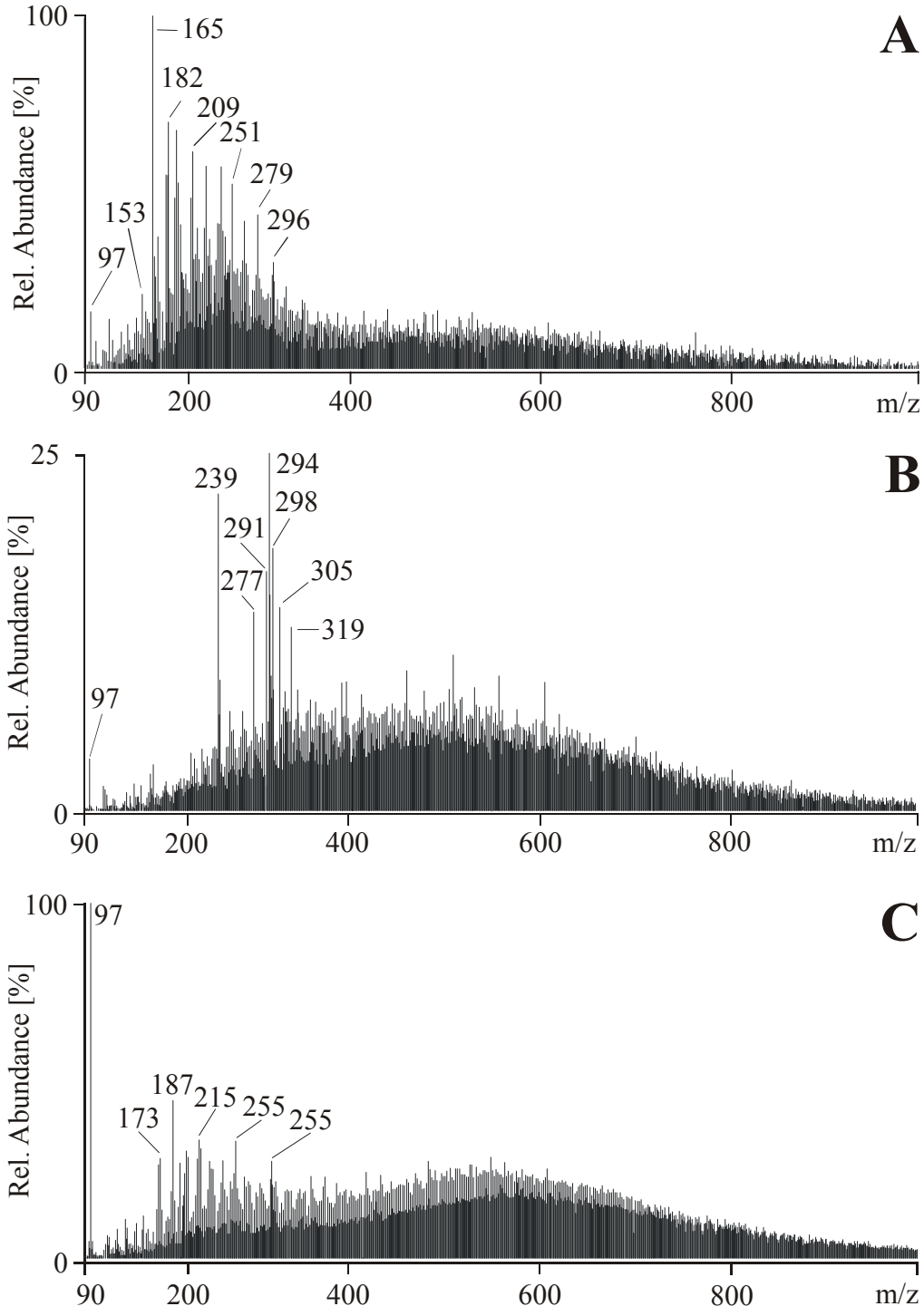

Figure 3-2. IT-ESI(-) full scan mass spectra (*m/z* 90-1000). **A** Fraction I of filter QF 34 (100% = 1.4 x 10^5 cps). **B** Fraction V of filter QF 34 (100% = 1.5 x 10^5 cps). **C** WSOC of filter QF 92 (100% = 3.1 x 10^5 cps) obtained by flow injection.

The maxima of the mass distributions in the full scan spectra were found to vary considerably with the voltages applied to the lenses in the low vacuum area after the ion inlet. They accelerate ions towards the mass filter and decluster analyte-solvent adducts. However, these lens voltages may also induce fragmentation of labile analytes. This kind of fragmentation at the entrance of the mass spectrometer is called "source fragmentation". HULIS were found to be sensitive to source fragmentation. The maximum of the mass distribution of the HULIS shifted towards lower *m/z* when applying higher lens voltages. In this work the voltage was set as low as possible to avoid source fragmentation. Moreover, the same voltage was used for all measurements allowing a relative comparison between fractions and samples.

The possibility of source fragmentation requires caution when interpreting molecular weight of HULIS obtained by mass spectrometry. Too low molecular weights might be estimated. Therefore, precise statements about the molecular weight of HULIS were avoided, since source fragmentation could not be completely excluded.

Chromatograms taken between *m/z* 1000-4000 showed signals of low intensity at the retention time of HULIS. The full scan mass spectra showed an intensive noise. It was difficult to ascertain, whether the high intensity noise between *m/z* 1000-4000 was an artefact or real. Molecular mass measurements of HULIS by mass spectrometry (Feng and Möller, 2004), by capillary electrophoresis (Havers *et al.*, 1998) and by ultrafiltration (Havers *et al.*, 1998) confirmed a maximal molecular weight for HULIS of 1000 u. Based on these results, the noise between *m/z* 1000-4000 was probably an artefact due to adduct or cluster formation during electrospray ionisation.

Comparison with mass distributions of fulvic and humic acid

Similarities between HULIS and fulvic and humic acid were obvious when comparing their corresponding full scan spectra (figures 3-2 C and figure 3-3 A and B). All full scan spectra showed a mass distribution between *m/z* 150-450 with a maximum at around *m/z* 300. However, the second maximum in the mass distribution of fulvic and humic acids was shifted towards higher masses at around *m/z* 800. Furthermore, the

mass distribution exceeded *m/z* 1000 for fulvic acid and humic acids, which indicates larger structures than for HULIS.

The mass signal pattern pointed to a similar chemical composition of fulvic acid, humic acid and HULIS. This could be proven by thermochemolysis GC-MS (chapters 2.3.3 and 2.3.7). However, thermochemolysis GC-MS could not provide any information about the molecular size of fulvic acid, humic acid and HULIS.

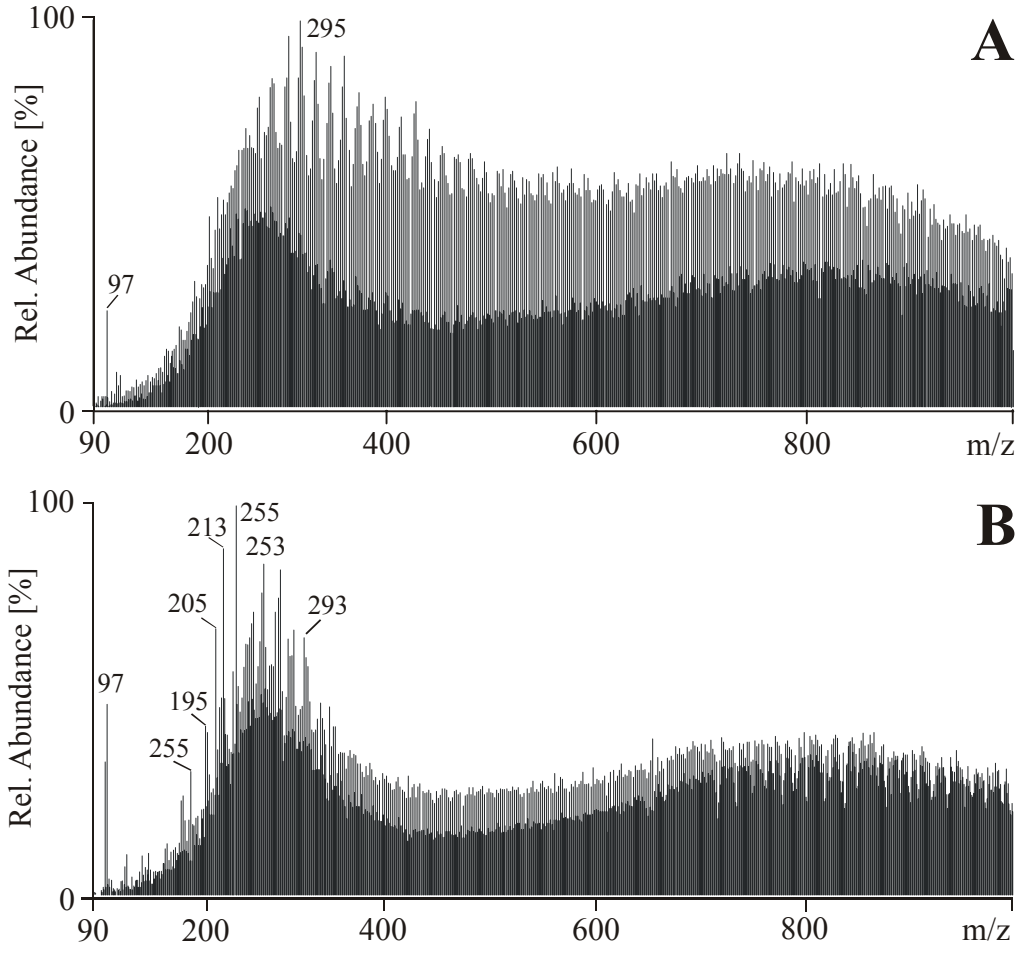

Figure 3-3. IT-ESI(-) full scan spectra (*m/z* 90-1000) of **A** fulvic acid reference (100% = 2.5 x 10^5 cps) and **B** humic acid standard (100% = 3.3 x 10^5 cps) recorded by flow injection.

3.3.3 Mass signal pattern of HULIS

As mentioned above, the signal pattern of HULIS consisted of a mass distribution between *m/z* 150-350 containing more intense uneven than even mass signals. An expanded view is given in figure 3-4 A. According to the "nitrogen rule", ESI(-) even masses contain an odd number of nitrogen atoms, and uneven masses either contain no nitrogen or an even number of nitrogen atoms. The signal pattern of HULIS was mainly composed by uneven masses, indicating that the corresponding compounds contained mainly C, H and O and no nitrogen. This was in good agreement with the the fragment spectra obtained by MS^2 and MS^3 (chapter 3.3.4). Furthermore, all compounds identified in the polar compound fractions and the HULIS fractions by thermochemolysis GC-MS contained no nitrogen (see tables 2-2, 2-3 and 2-4).

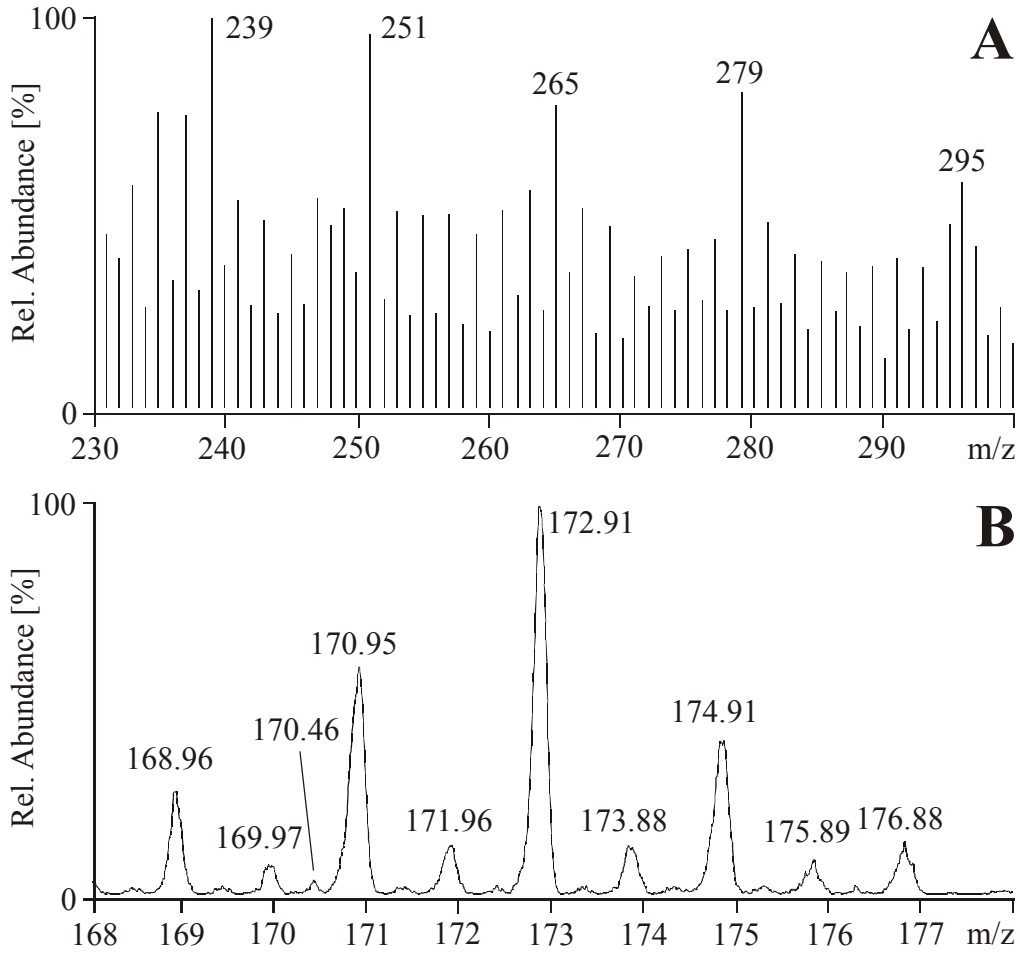

Figure 3-4. Mass signal pattern of HULIS recorded with IT-ESI(-). **A** Expanded full scan spectrum of spectrum A in figure 3-2 (*m/z* 230-300, 100% = 7.3 x 10^4 cps). **B** Zoom scan spectrum of filter QF 34 (*m/z* 168-178, 100% = 3.6 x 10^4 cps).

Uneven masses of the signal pattern of HULIS showed a maximum every 14 u (figure 3-4 A). This suggested that HULIS contained aliphatic moieties of different chain length such as aliphatic mono- and dicarboxylic acids as also found by thermochemolysis GC-MS (table 2-5). The chain lengths of aliphatic carboxylic acids differed by CH_2 units, which resulted in repetitive maxima every 14 u. Moreover, odd masses were recorded every 2 u (figure 3-4 A and B), indicating a variable saturation degree of HULIS.

Enhanced resolution measurements (zoom scan) were performed by ion trap mass spectrometry to investigate the charging state of the ions, which composed the mass signal pattern of HULIS. An example for a zoom scan spectrum is shown in figure 3-4 B. Most ions were single-charged (z = 1), as mainly odd and even integer masses were detected. However, between the odd and even integer masses, half masses of low intensity were observed (e.g. *m/z* 170.46). This means that few of the ions of the mass signal pattern of the HULIS are double-charged (z = 2), indicating that the corresponding structures contain at least two functional groups such as carboxyl and hydroxyl, each of them being able to stabilise a negative charge.

3.3.4 Fragmentation of HULIS

Fragmentation behaviour of low mass HULIS

Fragmentation of several single uneven masses of the signal pattern of HULIS was performed to obtain information about the chemical structure. Masses such as *m/z* 283, 279, 229, 201, 197 and 173 were selected as precursor masses for MS^2 fragmentation. MS^2 spectra of *m/z* 279 for fractions I-V are shown in figure 3-5 as an example for the typical fragmentation behaviour of low mass HULIS. The rest of the investigated masses showed a very similar fragmentation behaviour.

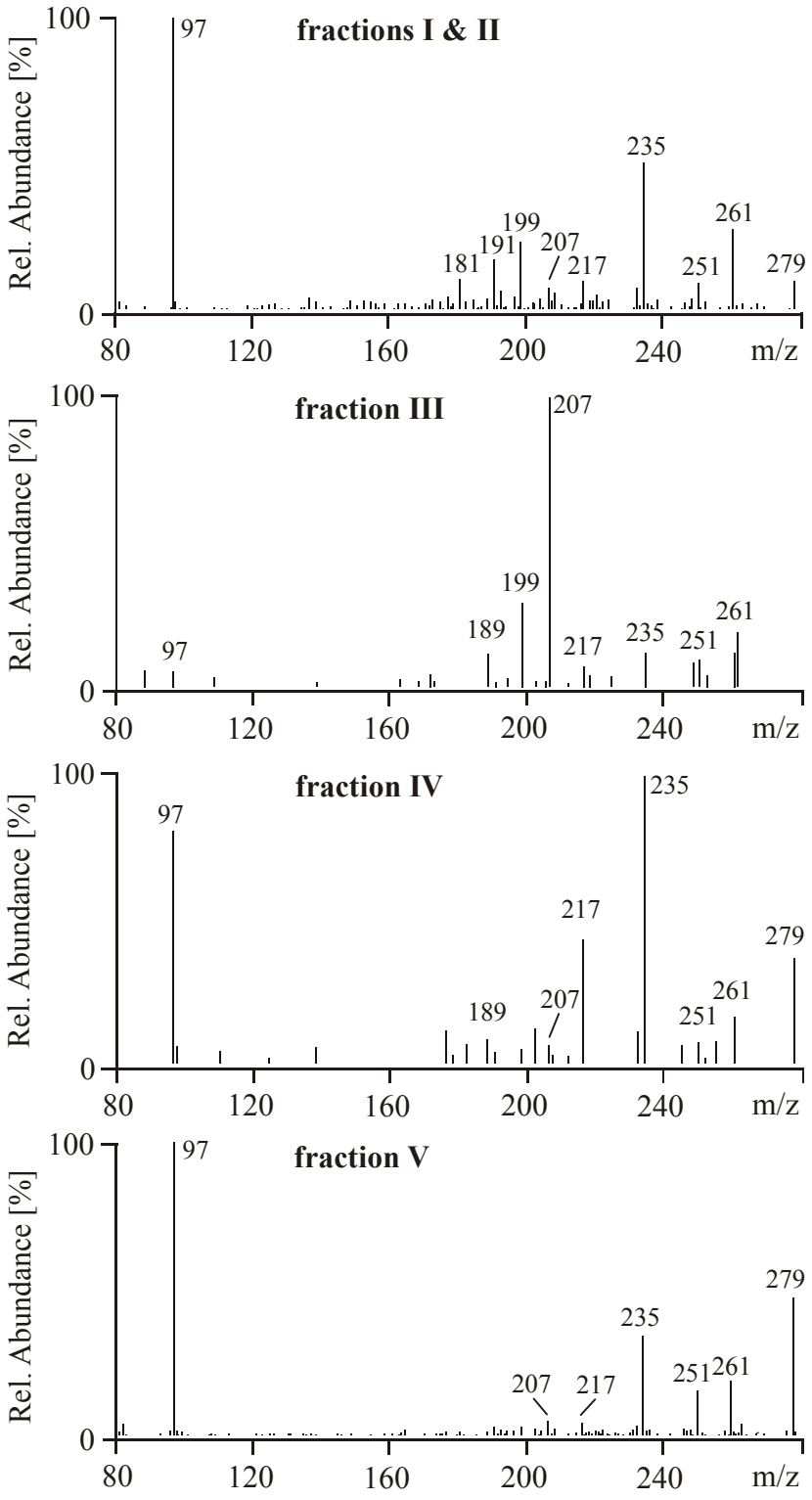

Figure 3-5. IT-ESI(-) MS^2 fragment spectra of *m/z* 279 (*m/z* 80-280) in sample QF 92 at 30% relative collision energy. The fragment spectra of combined fractions I and II (100% = 1.0 x 10^4 cps), fraction III (100% = 8.6 x 10^3 cps), fraction IV (100% = 5.5 x 10^3 cps) and fraction V (100% = 3.2 x 10^4 cps) are shown.

Fragment *m/z* 261 corresponded to the loss of OH as water (-18 u). Fragments *m/z* 251 and *m/z* 235 corresponded to the loss of CO (-28 u) and CO_2 (-44 u) from carboxylic acids. Further losses of H_2O could be assigned to fragment ions *m/z* 217, 199 and 181. Fragment *m/z* 191 corresponded to a further loss of CO_2 (-44 u) from *m/z* 235. In fraction III fragment *m/z* 207 was assigned to the loss of CO (-28 u) from *m/z* 235. Fragment *m/z* 207 in turn lost OH as water (-18 u). Some precursor masses lost 22 u, which corresponds to the loss of CO_2 when both precursor and fragment ion are doubly charged. This indicates the presence of more than one carboxylic group in the structure. Moreover, almost all fragment spectra showed fragment *m/z* 97. A more detailed discussion about fragment *m/z* 97 is given in chapter 3.3.5.

Fragmentation behaviour differed little between fractions I-IV and the masses chosen as precursor ions. The losses of 18 u, 28 u and 44 u and the corresponding fragments were predominantly present in all MS^2 and MS^3 fragment spectra. Figure 3-6 shows a fragmentation scheme containing combined MS^2 and MS^3 product ions of the precursor mass *m/z* 299. The fragmentation behaviour in figure 3-6 is representative for all masses in all fractions and filters investigated. Differences were only observed in the intensity of the fragment ions.

Even mass signals such as *m/z* 294 and *m/z* 196 showed a very similar fragmentation behaviour. MS^2 fragment spectra contained mainly losses of 18 u and 44 u as observed for uneven masses. Fragment *m/z* 97 was also frequently detected. Furthermore, typical losses for nitrated organic compounds such as NO (-30 u) and NO_2 (-46 u) were observed. However, the corresponding fragment masses were of low intensity. MS^3 fragment spectra could not be recorded, as even masses occurred at low intensities. After MS^2 fragmentation the amount of the resulting ions was not large enough to yield MS^3 fragment spectra.

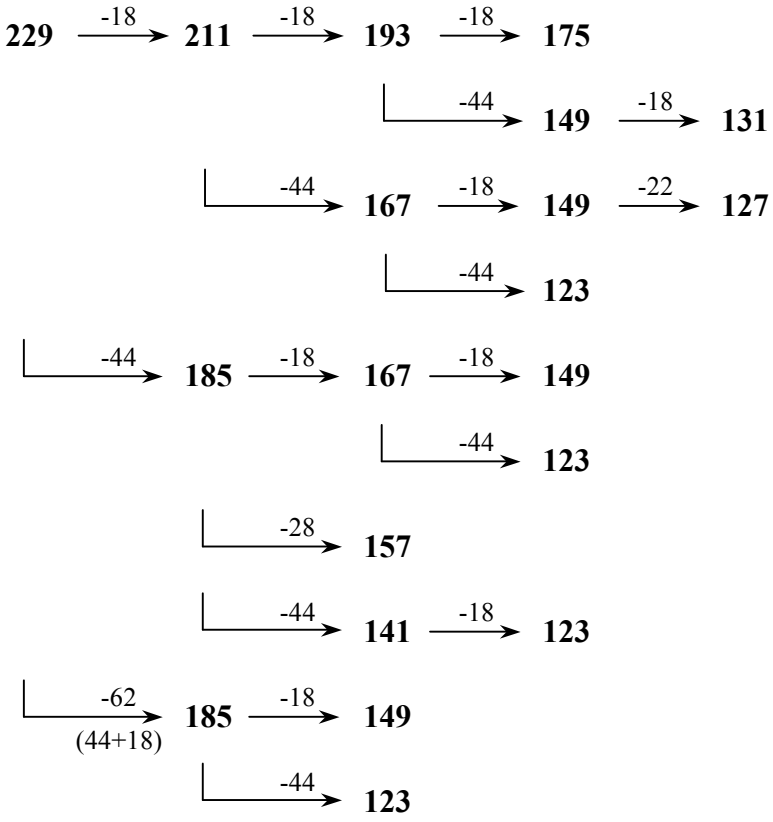

Figure 3-6. Scheme of combined product ions of MS^2 and MS^3 fragment spectra of the precursor ion *m/z* 229 of filter QF 92. Mass losses are given in u above the arrows and product ions are given in *m/z*. This fragmentation behaviour is representative for all masses in all fractions and filters investigated.

Fragmentation behaviour of high mass HULIS

MS^2 fragment spectra of the high mass HULIS present in fraction V showed little fragmentation. Investigated masses such as *m/z* 409, 517, 632 and 814 yielded few fragments ions. The MS^2 fragment spectra of *m/z* 409 and 814 are shown in figure 3-7. Fragmentation of *m/z* 409 resulted in *m/z* 391 (-18 u), *m/z* 365 (-44 u) and a series of losses of -18 u (*m/z* 347, 329 and 311). The precursor ion *m/z* 813 formed *m/z* 795 (-18 u) and *m/z* 769 (-44 u), which fragmented further to *m/z* 751 (-18 u) and *m/z* 707 (-44 u).

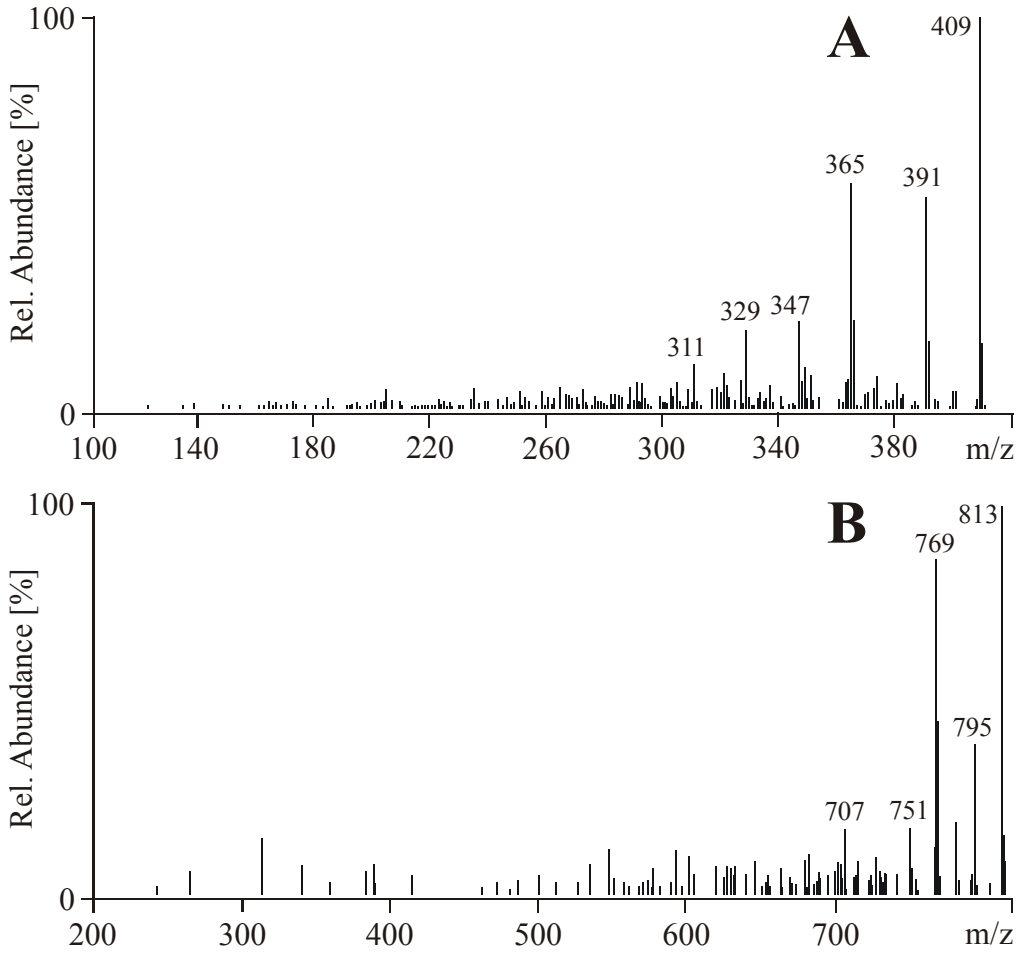

Figure 3-7. IT-ESI(-) MS^2 fragment spectra of *m/z* 409 (**A**, *m/z* 120-420, 100% = 2.4 x 10^4) and *m/z* 813 (**B**, *m/z* 220-820, 100% = 2.7 x 10^3) at 30% relative collision energy of filter QF 99.

Presence of low mass fragments in MS^2 spectra

Many of the recorded MS^2 spectra contained conspicuous low mass fragments with a mass pattern similar to the one of HULIS in full scan spectra. An example is shown in figure 3-8 for *m/z* 187. The expanded fragment spectrum (figure 3-8 B) shows four mass groups with mass difference of 14 u in between. The masses within the groups were 2 u apart. The first group contained the masses *m/z* 57, 59 and 61, the second one *m/z* 69, 71 and 73, the third one *m/z* 83, 85 and 87 and the fourth one *m/z* 95, 97, 99 and 101.

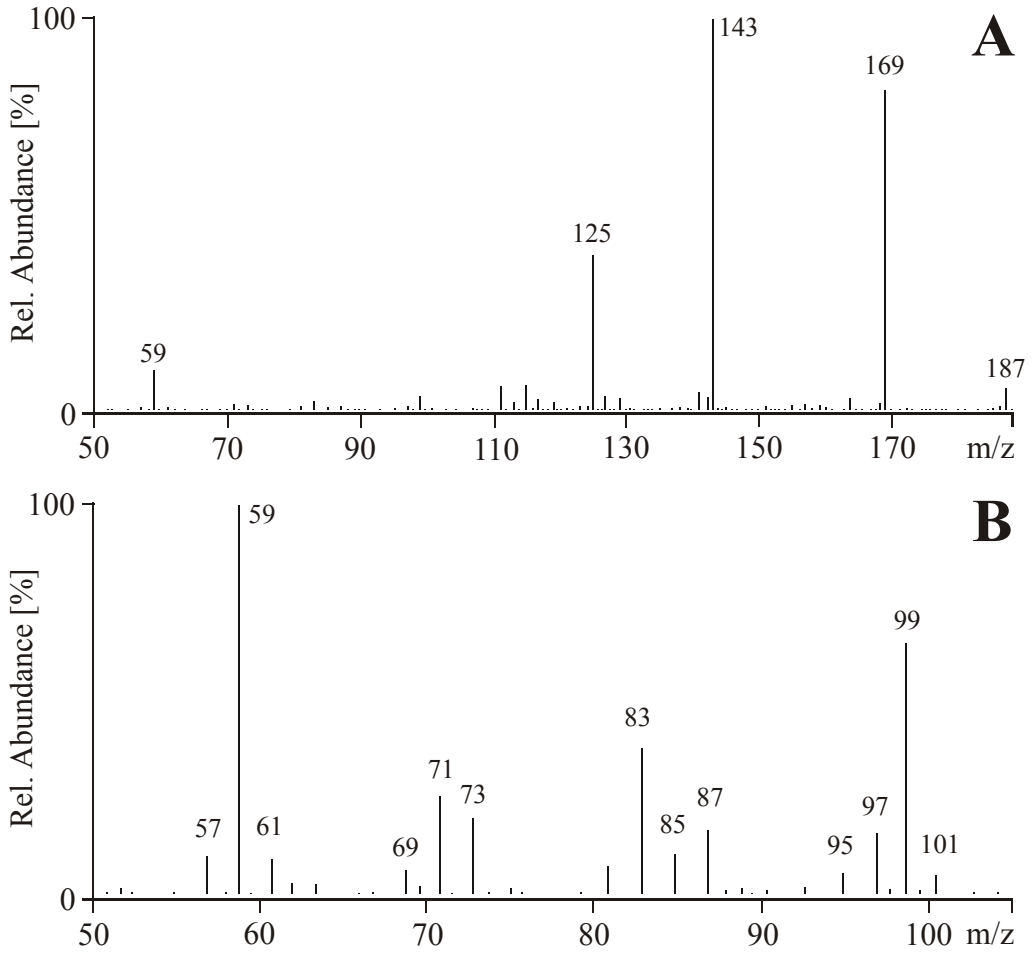

Figure 3-8. IT-ESI(-) MS^2 fragment spectra of *m/z* 187 at 30% relative collision energy of filter QF 116. **A** (*m/z* 50-190, 100% = 5.6 x 10^5) and **B** expanded spectrum (*m/z* 50-105, 100% = 4.4 x 10^4).

Chemical structures could be proposed for each of the low mass fragments, since HULIS are known to contain mainly the elements C, O and H (Kiss, 2002). Furthermore, fragments have to contain a chemical moiety stabilising the negative charge. The only O containing moieties fulfilling this requirement are hydroxyl or carboxyl groups. In addition, the possibilities of elemental composition is limited for such low masses. Therefore, only few structure proposals remained, which are presented in figure 3-9.

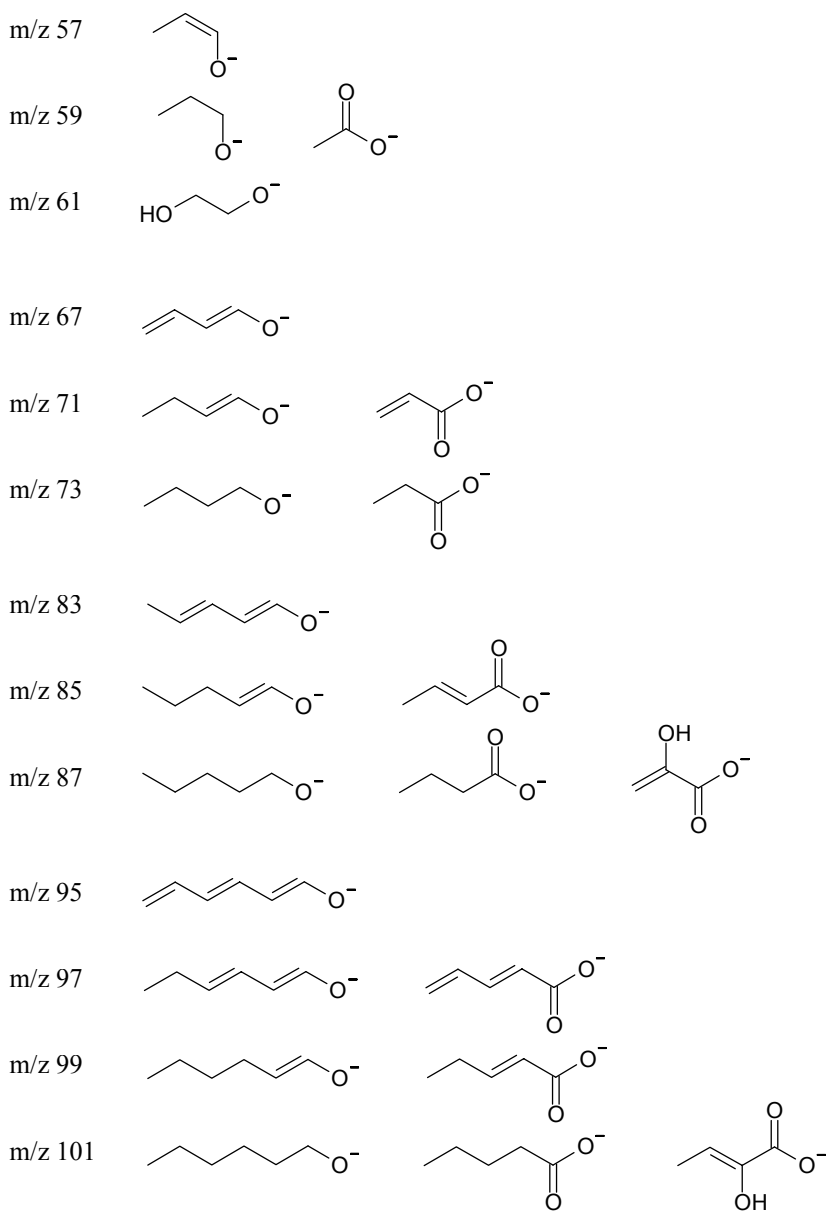

Figure 3-9. Structure proposals for low mass fragments (*m/z* 57-101) present in the MS^2 fragment spectrum of *m/z* 187.

Generally, aliphatic carboxylic acids and aliphatic alcohols with a varying degree of saturation degree are most likely. This is in good agreement with the results obtained by thermochemolysis GC-MS (chapter 2.3.3) and reported by Nolte *et al.* (2001). Only one structure proposal was possible for each of the fragments *m/z* 57, 61, 67, 83 and 95. However, three could be made for fragments *m/z* 87 and 101. Hydroxylated unsaturated carboxylic acids were less likely to be part of HULIS since no comparable

compounds were found by thermochemolysis GC-MS. Moreover, unsaturated alcohols do not stabilise well a negative charge. Therefore, aliphatic carboxylic acids are the most probable structures of fragments *m/z* 87 and *m/z* 101.

A precursor mass such as *m/z* 187 cannot contain all structural components proposed in figure 3-9. However, they all occur in the same fragment spectrum. This is due to the mass resolution of the ion trap mass spectrometer. Ion trap mass spectrometers are operated at unit mass resolution, which implies that masses having the same nominal mass are isolated together for fragmentation. As a consequence the obtained fragment spectrum is composed by several superimposed fragment spectra of the different precursor ions with the same nominal mass. High resolution measurements of fulvic acid by fourier transform ion cyclotron resonance mass spectrometry showed that one mass signal at unit resolution could consist of up to fifteen monoisotopic mass signals (Stenson *et al.*, 2003) (figure 3-10).

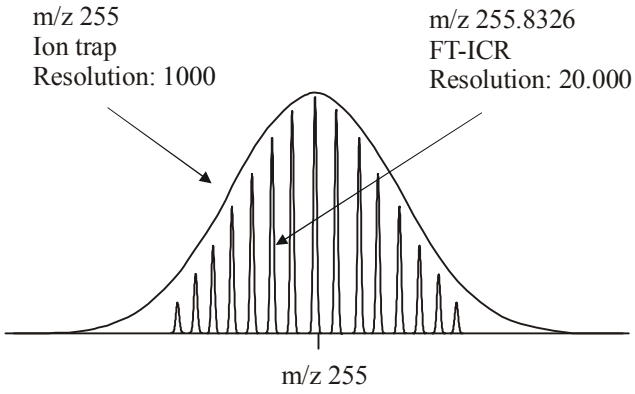

Figure 3-10. Unit resolution of an ion trap mass spectrometer versus high resolution of a fourier transform ion cyclotron resonance mass spectrometer (FT-ICR). One mass signal at unit resolution was resolved into fifteen monoisotopic masses for fulvic acid by FT-ICR.

An indication for superimposed fragment spectra are the numerous mass signals of low intensity present in all MS^2 fragment spectra (figures 3-6 and 3-9 A). MS^3 fragment spectra contained much less fragments of low intensity indicating a higher selectivity due to the isolation process in the ion trap. Nevertheless, information obtained by MS^2 and MS^3 fragment spectra could not be assigned to one single precursor ion or to one

single structure. In conclusion, the low resolution of ion traps are a drawback for the elucidation of single structures of HULIS.

3.3.5 Organosulphates

Fragment *m/z* 97 was detected in the MS^2 and MS^3 fragment spectra of most of the precursor ions (chapter 3.3.4). In addition, *m/z* 97 was even base ion in many of the recorded fragment spectra (figure 3-4, fractions I and V). Its relevance for structure elucidation is clearly underlined by its frequent occurrence and high abundance. Therefore, more detailed investigations were carried out.

Detection and fragmentation of organosulphates

The presence of mass *m/z* 97 after the elution of HSO_4^- (figure 3-2 A and B) was first interpreted as an organic compound with the same mass. TOF experiments gave an exact mass of *m/z* 96.9647. This allowed to exclude organic compounds such as C_4HO_3, $C_5H_5O_2$ or C_6H_9O. Only $H_2PO_3^-$ and HSO_4^- with the calculated monoisotopic masses of 96.9691 u (45 ppm off) and 96.9596 u (53 ppm off) were valuable options. However, a clear distinction between $H_2PO_3^-$ and HSO_4^- was not possible.

Therefore, the mass change in D_2O was studied using continuous-flow-injection with a syringe pump. This mode gave slightly different but well recognizable mass spectra compared to the chromatographic separation. Exchange of H by D should result in *m/z* 97 ($H_2PO_3^-$), 98 ($HDPO_3^-$) and 99 ($D_2PO_3^-$) for $H_2PO_3^-$ and was confirmed by ammonium phosphate with relative abundances of 100% for $HDPO_3^-$, and 50% for $H_2PO_3^-$ and $D_2PO_3^-$. However, the full scan spectrum (figure 3-11 A) showed only *m/z* 98 (DSO_4^-, base ion) and *m/z* 97 (HSO_4^-, 90%). At *m/z* 99 only background noise was present. Moreover, MS^2 and MS^3 fragmentations (figure 3-11 B and C) of *m/z* 299 as a typical HULIS mass formed both *m/z* 97 (HSO_4^-) and *m/z* 98 (DSO_4^-). This proved the identity of *m/z* 97 as HSO_4^- formed by fragmentation from WSOC.

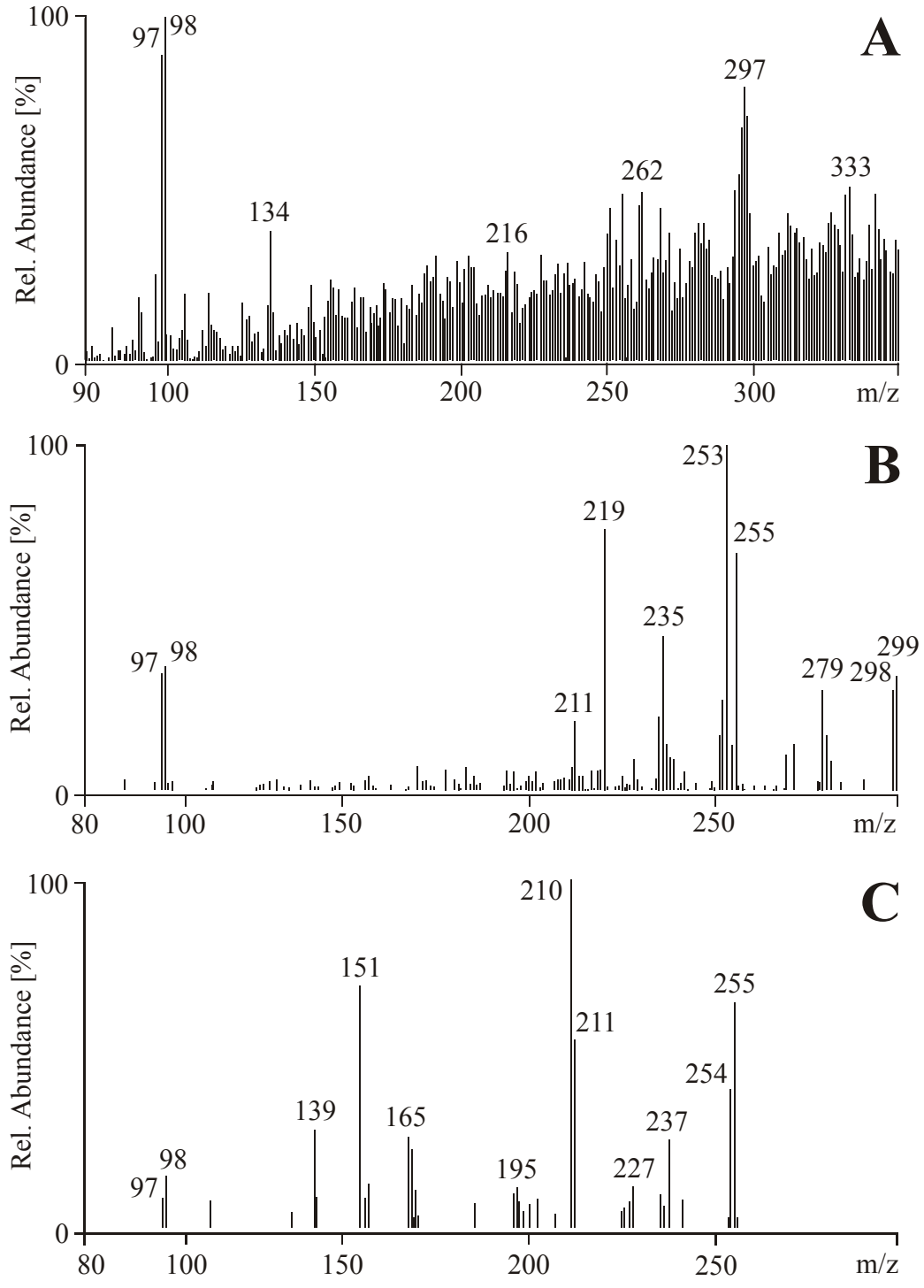

Figure 3-11. IT-ESI(-) mass spectra recorded by continuous flow injection of WSOC in the combined extracts of filters QF 117 and 119 dissolved in D_2O. **A** Full scan spectrum (*m/z* 70-350, 100% = 7.1 x 10^5 cps). **B** MS^2 fragment spectrum of *m/z* 299, *m/z* 80-300 (isolation width 1.5 u, collision energy 30%, 100% = 3.0 x 10^4 cps). **C** MS^3 fragment spectrum of *m/z* 299 → *m/z* 255, *m/z* 80-300 (isolation width 2.0 u, collision energy 30%, 100% = 1.3 x 10^4 cps).

The indication that sulphated compounds are part of WSOC, was studied further by fragmenting additional masses belonging to the main part of the mass signal pattern of HULIS (*m/z* 230-300, see figure 3-4 A). A fragmentation as for *m/z* 299 was observed for many of them (chapter 3.3.4). Therefore, more detailed investigation was carried out with this single mass.

The MS^2 spectrum of *m/z* 299 (figure 3-12 A) showed the typical fragmentation behaviour of HULIS. Fragment *m/z* 281 corresponded to the loss of OH as water (-18 u) and *m/z* 255 of CO_2 from carboxyl groups. The fragment *m/z* 219 was base ion and resulted from the cleavage of 80 u (SO_3). Further losses of H_2O could be assigned to fragment ions of lower intensity (e.g. *m/z* 237 and 201). HSO_4^- (*m/z* 97) had a relative intensity of ca. 70%.

The fragments *m/z* 281, *m/z* 255 and *m/z* 219 were further dissociated and their MS^3 spectra recorded (figures 3-12 B, C and D). Sufficient selectivity was obtained by isolating and fragmenting *m/z* 299 (MS^2) as well as subsequent isolation and fragmentation of its product ions *m/z* 281, *m/z* 255 and *m/z* 219 (MS^3). Fragmentation of *m/z* 281 resulted in loss of H_2O (*m/z* 263), CO_2 (*m/z* 237) and again 80 u (*m/z* 201). Mass *m/z* 97 (HSO_4^-) was present at a relative intensity of 30%. The fragmentation behaviour of *m/z* 255 was similar to *m/z* 281 yielding as main fragments *m/z* 211 ($-CO_2$) and *m/z* 237 ($-H_2O$). Again, *m/z* 175 (-80 u) and *m/z* 97 (HSO_4^-) were observed.

However, the fragmentation behaviour of *m/z* 219 was significantly different. Only the losses of H_2O (*m/z* 201) followed by CO_2 (*m/z* 157) and CO_2 alone (*m/z* 175) were present. Cleavage of 80 u and the HSO_4^- fragment at *m/z* 97 were missing. This suggested that loss of 80 u and presence of HSO_4^- are linked together.

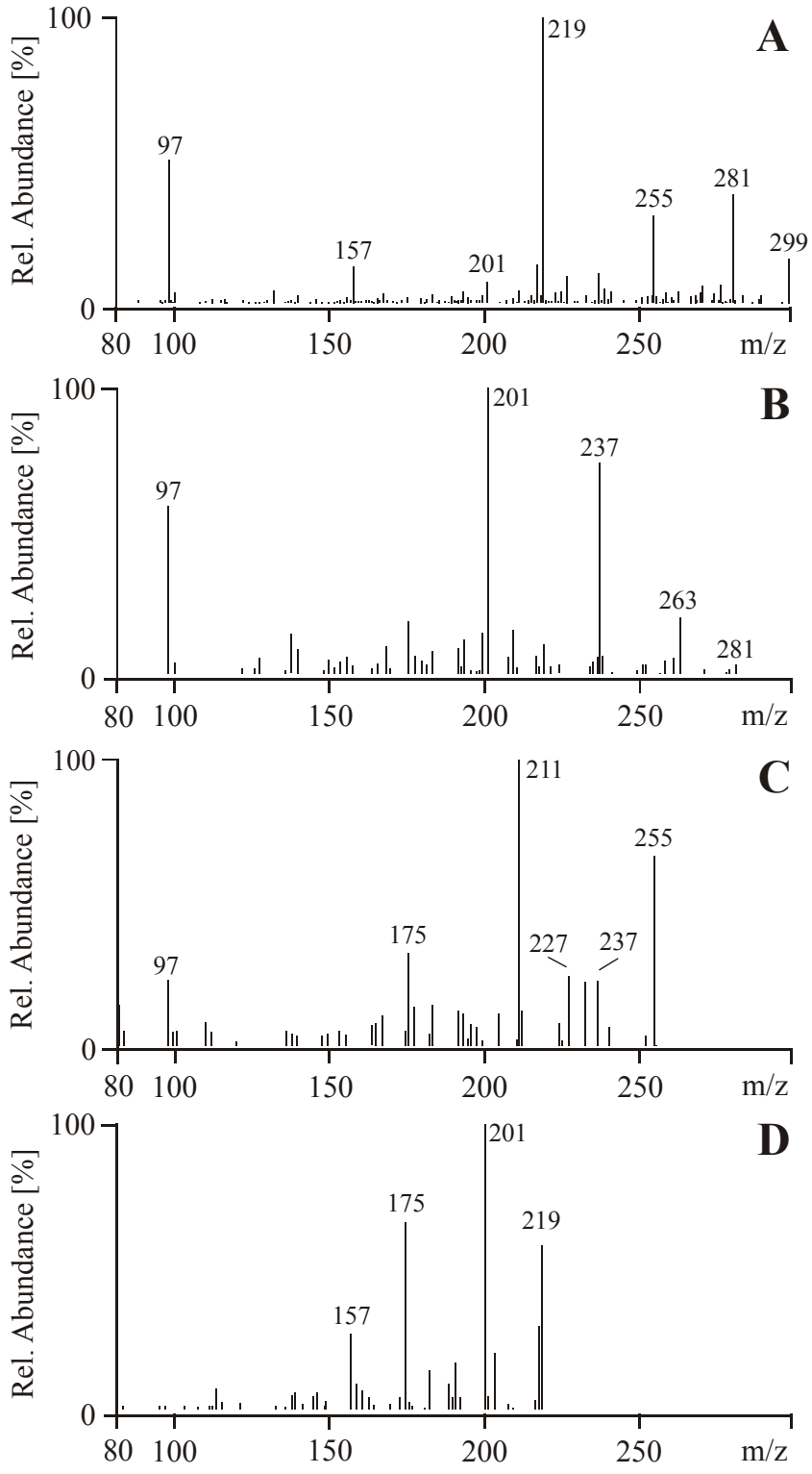

Figure 3-12. Fragment spectra from filter QF 92 (isolation width 1.5 u, collision energy 30%). **A** MS^2 fragment spectrum of *m/z* 299, *m/z* 80-300 (100% = 5.6 x 10^4 cps). **B** MS^3 fragment spectrum of *m/z* 299 → *m/z* 281, *m/z* 80-300 (100% = 3.2 x 10^3 cps). **C** MS^3 fragment spectrum of *m/z* 299 → *m/z* 255, *m/z* 80-300 (100% = 3.6 x 10^3 cps). **D** MS^3 fragment spectrum of *m/z* 299 → *m/z* 219, *m/z* 80-300 (100% = 4.3 x 10^3 cps).

To evaluate the presence and formation of *m/z* 97 further, the MS^2 spectra of *m/z* 299 present in humic and fulvic acid extracts were studied. They showed a very similar fragmentation as HULIS. However, the fragments *m/z* 219 and *m/z* 97 had a very low relative intensity of ca. 4% and 0.4%, respectively. Moreover, fulvic and humic acid solutions were spiked with 50 mM ammonium sulphate. No increase of the relative intensity of *m/z* 97 was observed. This allowed to exclude *m/z* 97 as an artefact by previous adduct formation with HSO_4^-. This demonstrated together with the MS^n experiments, that *m/z* 97 is a real fragment of HULIS and thus HSO_4^- covalently bound.

Model compounds

To confirm the observed fragmentation behaviour and to link it further to sulphated HULIS, the fragmentation of model compounds (table 3-1) was investigated. MS^2 fragmentation of octyl sulphate (1) gave the expected *m/z* 97 (HSO_4^-) fragment. Both 2-hydroxy-5-nitrophenyl sulphate (3) and 5-bromo-4-chloro-3-indolyl sulphate (4) lost 80 u (SO_3) and gave the fragments *m/z* 234 and *m/z* 324, respectively. The model compounds (1), (3) and (4) provided also an answer to the simultaneous appearance of *m/z* 97 (HSO_4^-) and -80 u (SO_3) in the MS^2 and MS^3 spectra of HULIS. A loss of -80 u (SO_3) was observed if sulphate was attached to a π-electron system containing electron withdrawing groups (see structures 3 and 4). A reason could be the stabilisation effect of the π-electron system on the sulphate group. The fragment *m/z* 97 (HSO_4^-) was only observed, if sulphate was attached to a purely aliphatic or aliphatic-behaving system, which was confirmed by (1). In this case no stabilisation of the sulphate rest occurred. 2-hydroxy-5-sulphobenzoic acid (2) showed only -80 u (SO_3) as expected for sulphonated organic compounds.

Apparently both -80 u and *m/z* 97 seem to be indicators for covalently bound sulphate. However, sulphonic acids as a further source for -80 u (SO_3) cannot be excluded. In addition, a combination of sulphonic acids losing -80 u and covalently bound sulphate yielding *m/z* 97 is theoretically possible but not very much likely.

Table 3-1. IT-ESI(-)-MS^n fragmentation of octyl sulphate (1), 2-hydroxy-5-sulphobenzoic acid (2), 2-hydroxy-5-nitrophenyl sulphate (3) and 5-bromo-4-chloro-3-indolyl sulphate (4).

Compound	$[M-H]^-$	MS^2 fragments	MS^3 fragments
(1) Octyl sulphate	*m/z* 209 →	*m/z* 97 (HSO_4^-)	-
(2) 2-Hydroxy-5-sulphobenzoic acid	*m/z* 217 →	*m/z* 171 (-46 u)	
	→	*m/z* 137 (-80 u)	→ *m/z* 93 (-44 u)
(3) 2-Hydroxy-5-nitrophenyl sulphate	*m/z* 234 →	*m/z* 154 (-80 u, $-SO_3$)	→ *m/z* 124 (-30, -NO)
(4) 5-Bromo-4-chloro-3-indolyl sulphate	*m/z* 324 →	*m/z* 244 (-80 u, $-SO_3$)	→ *m/z* 182 ($C_8H_5NO_2Cl$)
			→ *m/z* 79, 81 (^{79}Br, ^{81}Br)

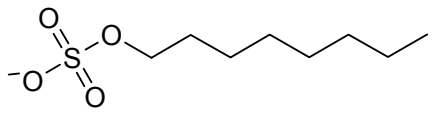

(1)

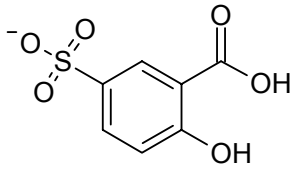

(2)

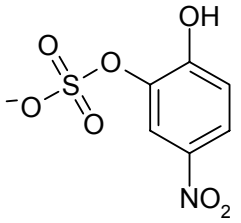

(3)

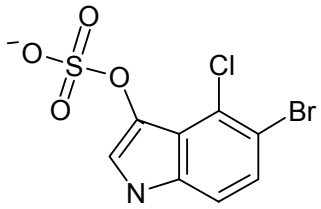

(4)

3.3.6 Quantification of organosulphates

Quantification method

Organosulphates are a large group of different compounds present in the WSOC fraction. They yield *m/z* 97 (HSO_4^-) as a common fragment (chapter 3.3.5). Quantification based on MS-MS fragmentation of single precursor masses and detection of *m/z* 97 as the common product ion discriminates most of the

organosulphates, since only a limited number of precursor masses can be processed simultaneously by a triple quadrupole. Therefore, quantification was performed by source fragmentation, by applying a higher voltage between the capillary and the skimmer located in the low vacuum area at the entrance of the quadrupole mass spectrometer. Organosulphates are accelerated in this electric field and collide with remaining air and eluent molecules. Simultaneous fragmentation of all organosulphates will occur. This yields the common fragment *m/z* 97, which is then detected by single ion monitoring (SIM). Integration of the chromatographic signals in the resulting mass chromatogram of *m/z* 97 allowed the quantification of the total amount of organosulphates.

Octyl sulphate was used as calibration standard. However, quantification could not be performed by internal standard calibration. Chromatography of octyl sulphate was not straightforward, due to its properties as a surfactant. Therefore, external calibration was performed by flow injection (5 µl loop). The linearity test using eight reference solutions containing octyl sulphate (0.02, 0.2, 1, 2, 5, 10, 15 and 20 ng/µl) showed a linear response (R^2=0.9997) over three orders of magnitude. The limit of quantification defined as signal-to-noise ratio (S/N) of 10:1 was at 10 pg on column.

Inorganic HSO_4^- was additionally quantified with the same method as for organosulphates. Calibration was performed externally and the reference solutions were injected on column (5 µl). The linearity test using five reference solutions containing ammonium sulphate (0.01, 0.1, 1, 10 and 100 ng/µl) showed a linear response (R^2=0.9984) over four orders of magnitude. Quantification limit defined as signal-to-noise ratio (S/N) of 10:1 was 50 pg injected compound.

Blank values for organosulphates were around the limit of quantitation. Inorganic sulphate showed blank values below the limit of detection. Concentrations in real samples were 10^4 times more abundant. Blank corrections were not needed. The repeatability was ± 1.5% for octyl sulphate and ± 3.5% for ammonium sulphate. Together with the repeatability of sample injection, precision of the pipettes, the precision of weighing, dilution and clean-up a total error of 12% was estimated for

both. Organosulphate concentrations were calculated in nmol/m^3. This allowed a mass independent evaluation of the concentrations, as the mass of the calibration standard octyl sulphate is 209 u and organosulphates can range up to 1000 u.

Quantification results

Inorganic sulphate eluted first between 1.5-3.5 min. It was followed by the sulphated low mass HULIS (fractions I-IV, 2.5-3.5 min). Sulphated high mass HULIS (fraction V) were detected at 7.0 min. An example of a SIM chromatogram of *m/z* 97 is shown in figure 3-13.

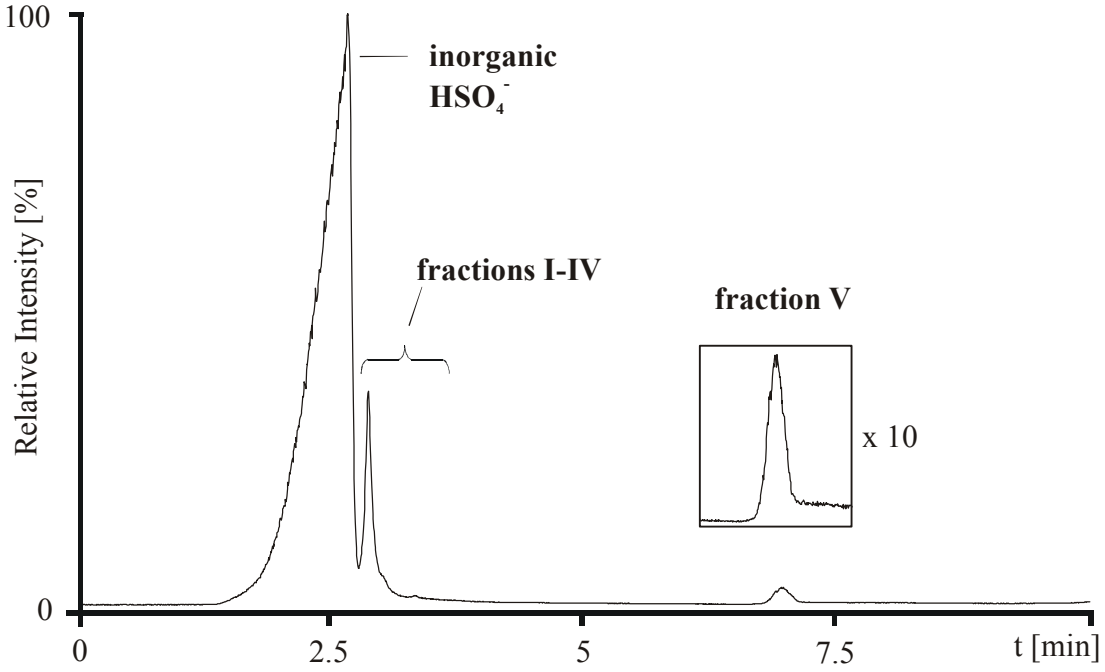

Figure 3-13. ESI(-) SIM chromatogram of *m/z* 97 obtained by source fragmentation of the raw extract of sample M6 (100% = 8.7 x 10^9 counts).

Coelution of inorganic sulphate with low mass HULIS in fraction I occurred in most of the samples. A quantification of sulphated low mass HULIS was hardly possible. However, values were obtained for samples U3, U5, U19, U22, M5 and M6, which showed a resolved chromatographic signal of fraction I. Concentrations were between 0.09 and 0.23 nmol/m^3.

Quantification of sulphated high mass HULIS (fraction V) was carried out for samples U1-U22 and M1-M6. Results are presented in table 3-2 and figure 3-14. Most concentrations in urban samples were between 0.01-0.05 nmol/m^3. Sample U15 had a particular high level of 0.11 nmol/m^3. Motorway concentrations were between 0.02-0.04 nmol/m^3 and were comparable to the urban samples.

Table 3-2. Quantitative data of organosulphates of fraction V (nmol/m^3) and inorganic sulphate (µg/m^3) for filters U1-U22 and M1-M6 measured by source fragmentation of the raw extract and detection of fragment *m/z* 97.

Filter-No.	**organosulphates in nmol/m^3**	**inorganic HSO_4^- in µg/m^3**
Urban filters		
U1	0.015	1.5
U2	0.064	4.8
U3	0.037	7.2
U4	0.029	0.9
U5	0.032	3.8
U6	0.029	4.6
U7	0.027	4.0
U8	0.021	4.2
U9	0.034	8.6
U10	0.035	3.8
U11	0.043	5.0
U12	0.042	7.4
U13	0.032	6.3
U14	0.024	2.8
U15	0.104	3.6
U16	0.017	1.5
U17	0.018	1.2
U18	0.045	1.4
U19	0.040	2.4
U20	0.031	1.9
U21	0.015	0.3
U22	0.036	4.4
Motorway filters		
M1	0.036	3.0
M2	0.023	10.8
M3	0.034	16.1
M4	0.029	10.6
M5	0.035	7.0
M6	0.036	8.5

Combined sulphated organosulphates of low and high mass HULIS were estimated to 0.05-0.2 nmol/m^3. Similar concentrations were found for single organic compounds such as aliphatic dicarboxylic acids and aromatic carboxylic acids in atmospheric aerosols by Rogge *et al.* (1993).

There appears to be a slight seasonal trend for the concentrations of sulphated high mass HULIS. Concentrations tended to be higher in the winter months November, December, January, February (U18-22 and U1-3) and in the summer months June, July and August (U9-13). Spring and autumn samples showed lower values. This trend might be explained with increased emission of SO_2 by heating in winter and by traffic in summer. However, the trend might be within the normal fluctuation of organosulphate concentrations. A higher number of samples need to be measured to prove the seasonal variations.

Concentrations of inorganic sulphate in urban samples were between 0.3-8.3 µg/m^3 (figure 3-14). No seasonal trend was observed. Concentrations in motorway samples were somewhat higher (3-16 µg/m^3). This might be due to SO_2 emissions from diesel engines powered by sulphur containing diesel fuel. The concentrations of inorganic sulphate were in good agreement with the concentrations found by Zappoli *et al.* (1999).

A correlation between inorganic sulphate and organosulphates was not observed. This suggests that the sulphatation reaction of HULIS is not only dependent on the amount of sulphate in the atmospheric aerosol. It probably also depends on other factors such as temperature, solar irradiation, acidity of other chemical components present in aerosols.

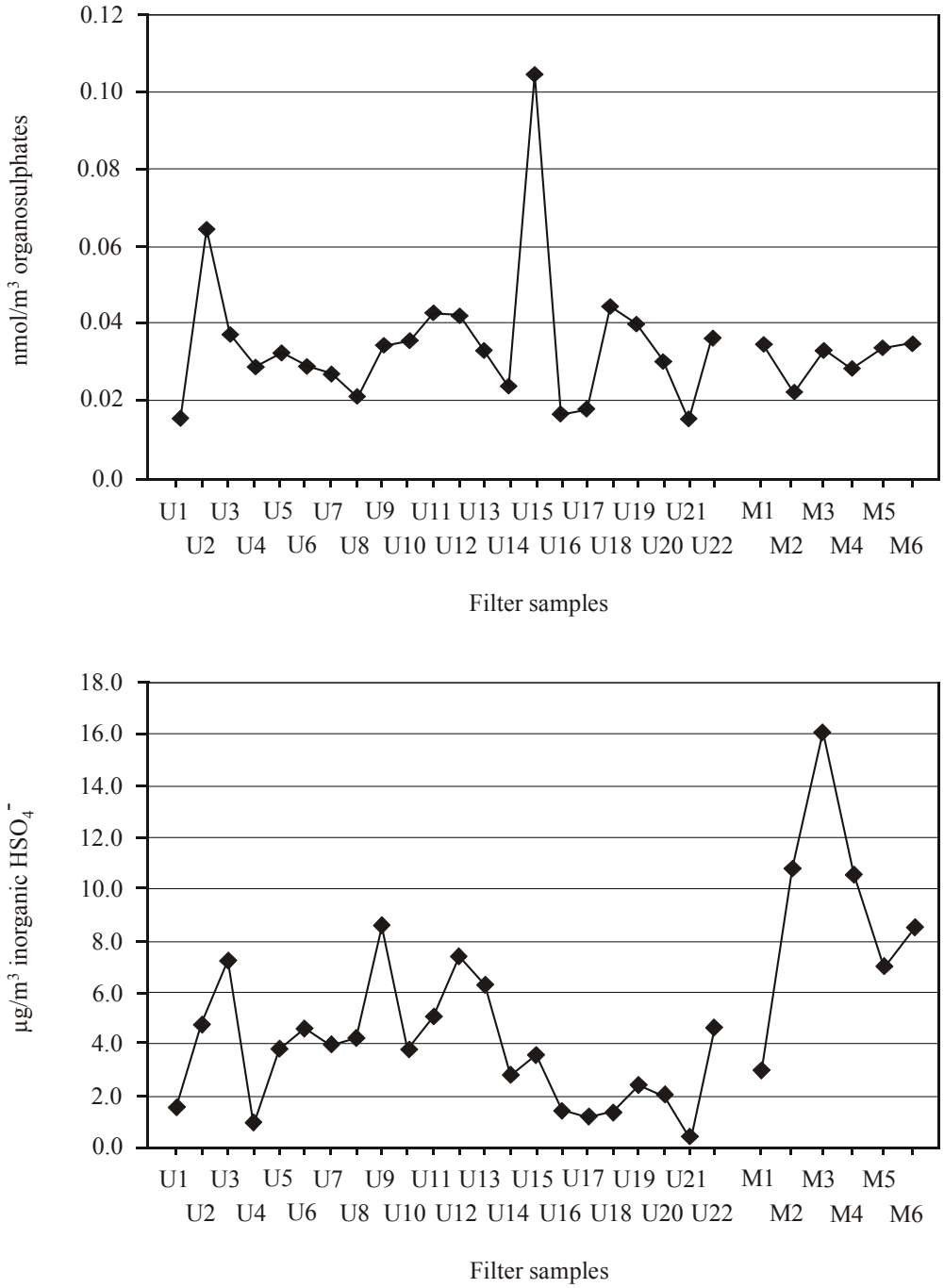

Figure 3-14. Graph of organosulphate (above) and inorganic sulphate (below) concentrations of fraction V measured in urban samples U1-U22 and motorway samples M1-M6 by source fragmentation of the raw extract and detection of *m/z* 97. Data are listed in table 3-2.

3.3.7 Structure proposal for HULIS

Structure proposals for HULIS were already discussed in chapter 2.3.4. The proposals were based on the substructures of HULIS found in the HULIS fraction by thermochemolysis GC-MS (table 2-2). Combinations of aromatic and aliphatic substructures by means of ester bonds yielding a branched structure with and without backbone were proposed as shown schematically in figure 3-15.

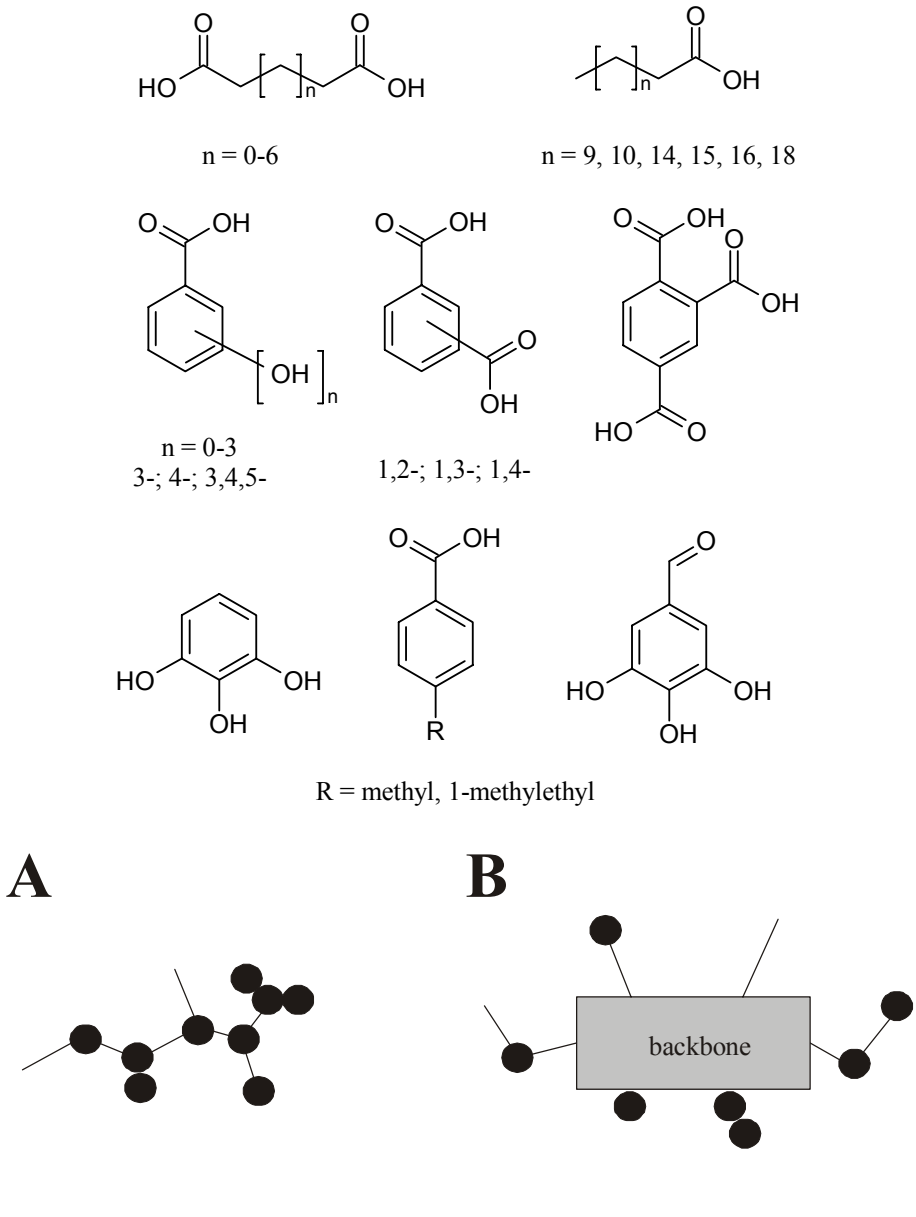

Figure 3-15. (Above) Summary of the 24 substructures identified by thermochemolysis GC-MS (chapter 2.3.4, table 2-2). (Below) Schematic structure proposals of HULIS without backbone (A) and with backbone (B). Aliphatic compounds are abbreviated as —— and aromatic compounds as ●.

The MS^2 and MS^3 fragment spectra did not reveal substantial new structural information except the existence of covalent bound sulphate. However, more precise structure proposals for HULIS were possible by combining the information about the mass distributions obtained by LC-MS and the substructures identified by thermochemolysis GC-MS.

The mass distribution of *m/z* 90-1000 allowed to propose structures consisting of 2-4 substructures linked by ester bonds. A total of 24 aliphatic and aromatic substructures (summarised in figure 3-15) were available resulting in a large number of combinations of possible HULIS structures with masses between *m/z* 220-840. Combinations of two substructures yielded 94 possible HULIS structures within *m/z* 220-420 and an intensity maximum at *m/z* 300 as schematically shown in figure 3-16 A. Combinations of three substructures gave 368 possible combinations between *m/z* 320-580 with a maximum at *m/z* 450. Finally, combinations of four substructures gave 1472 possible combinations between *m/z* 429-833 with a maximum at around *m/z* 600. The mass ranges of the combinations of 2-4 substructures are shown in figure 3-16 B.

The mass distributions of the combinations fitted well with that of fractions I-IV and V (figures 3-2 A and B and figure 3-15 B). HULIS of fractions I-IV are probably composed of 2-3 and those of fraction V of 3-4 substructures. Some examples of the proposed structures for HULIS are shown in figure 3-17. Mass signals below *m/z* 220 belong to the unlinked substructures identified by MS^2 (chapter 3.3.2).

HULIS of more than 4 or 5 substructures are principally possible. However, some of them might be non-polar enough to irreversibly adsorb on the C_{18}-phase of the chromatographic column thus remaining undetected. However, molecular weight measurements of HULIS by different methods such as mass spectrometry (chapter 3.3.2; Feng and Möller, 2004), capillary electrophoresis (Havers *et al.*, 1998) and ultrafiltration (Havers *et al.*, 1998) revealed a maximal molecular weight for HULIS of 1000 u. Therefore, HULIS of more than 4 or 5 units are rather unlikely.

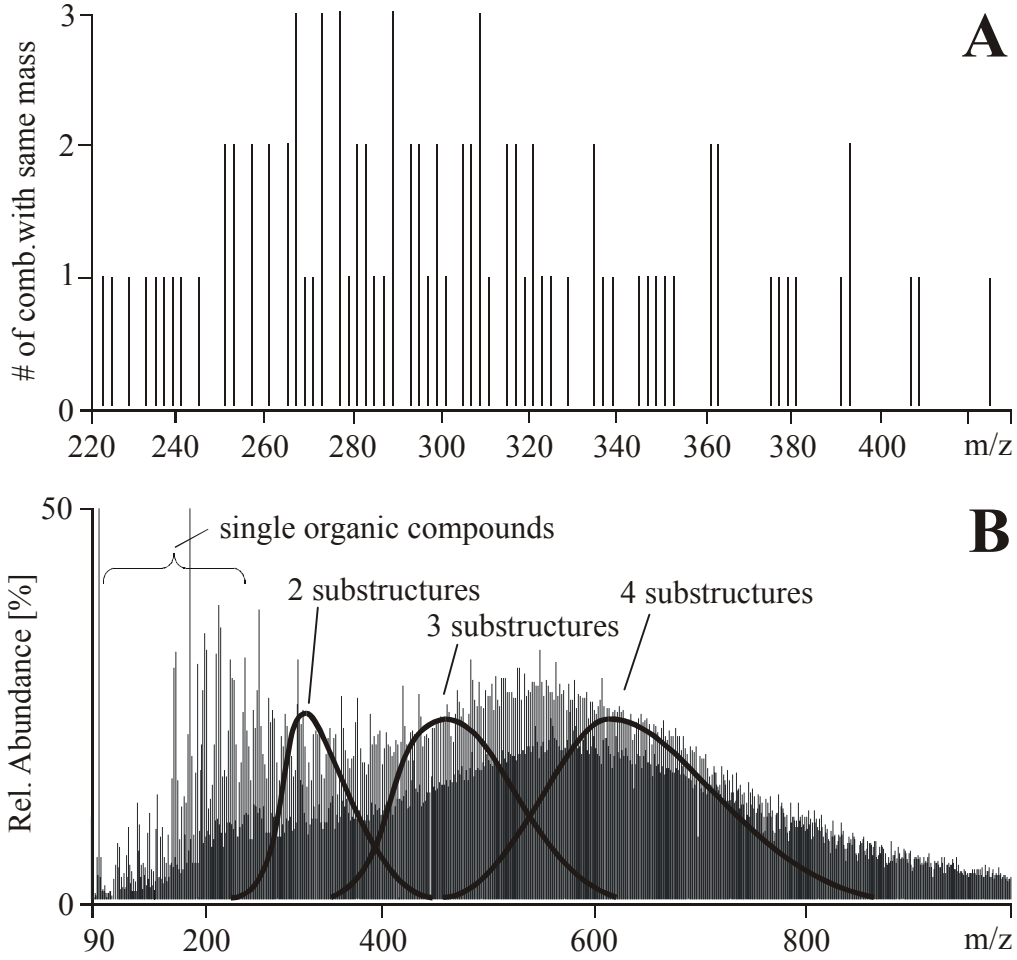

Figure 3-16. **A** Sheme of the mass distribution of HULIS composed of 2 substructures. Intensity corresponds to the number of combinations with the same mass. **B** ESI(-) full scan mass spectrum of WSOC of filter QF 92 by obtained by flow injection (*m/z* 90-900, 100% = 3.1 x 10^5 cps). The mass distributions of the combinations of 2, 3 and 4 substructures is overlaid.

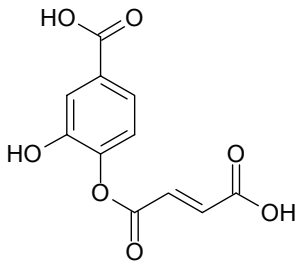

2 substructures (*m/z* 251)

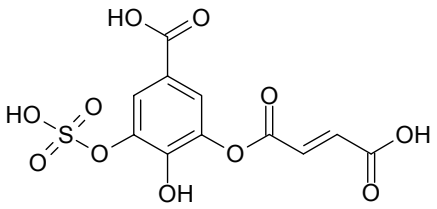

3 substructures with sulphate (*m/z* 347)

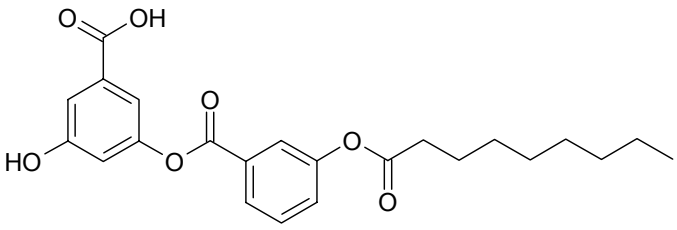

3 substructures (*m/z* 413)

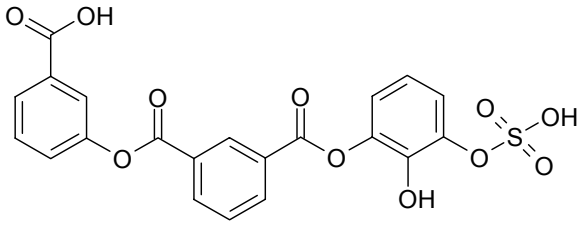

3 substructures with sulphate (*m/z* 473)

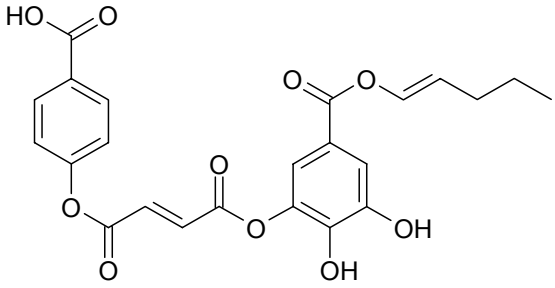

4 substructures (*m/z* 485)

Figure 3-17. Proposed structures of HULIS. Five examples containing 2, 3 and 4 substructures are presented. Their corresponding mass for ESI(-) is given in brackets. Proposed structures are combinations of the substructures summarised in figure 3-15. Two of the proposals contain covalently bound sulphate.

3.4 Conclusions

WSOC could be isolated from inorganic species and separated into five fractions by using a 300 Å pore size reversed stationary phase for HPLC. Chromatographic and mass spectrometric information revealed that HULIS present in fractions I-V consisted of polar lower mass compounds and less polar substances of higher mass. Polar HULIS had a mass distribution between *m/z* 100-400 with a maximum at *m/z* 240. Less polar HULIS showed a mass distribution between *m/z* 100-900 with a maximum at *m/z* 500. However, a precise estimation of the molecular weight was not possible due to unavoidable source fragmentation. LC-MS experiments could show that HULIS are composed by a large quantity of compounds of different polarity and size.

MS^2 and MS^3 fragmentation experiments proved that carboxylic and hydroxyl moieties were the predominant functional groups for HULIS. They may contribute decisively to the water solubility of HULIS. Furthermore, fragment *m/z* 97 was detected in almost all MS^2 and MS^3 fragment spectra. Mass determination by TOF-MS excluded an organic structure, and fragmentation with D_2O-solution provided the proof that *m/z* 97 is HSO_4^-. Altogether these facts make it very likely that HSO_4^- is covalently bound to HULIS. However, since both sulphonation and sulphatation of HULIS are possible in the atmosphere, -80 u (SO_3) could not be clearly associated to sulphonated or sulphated HULIS. Both sulphated and sulphonated compounds showed a loss of -80 u .

Moreover, it could be shown that sulphatation of HULIS is likely, but this study did not allow to differentiate between a sulphatation process of HULIS in the atmosphere, on the filter after collection or in the raw extract. Generally, sulphatation occurs either by addition of sulphuric acid to alkenes or by esterification of an alcohol with sulphuric acid. The possibility of enzymatic sulphatation is remote. Considering the chemical conditions for a sulphatation (water, sulphate/sulphuric acid and HULIS), the possibility of sulphatation in aerosol droplets in the atmosphere is real, but sulphatation can also be an artefact on the filter or in the raw extract.

Quantification of sulphate covalently bound to HULIS revealed concentrations similar to other polar organic compounds common in atmospheric aerosols. The presence of sulphated groups implies a higher water solubility of HULIS, which in turn results in a increased activity of atmospheric aerosols as cloud condensation nuclei. This should be taken into account for model calculations.

Structural information obtained by LC-MS and thermochemolysis GC-MS allowed to make concrete structure proposals for HULIS. Low mass HULIS consisting of 2-3 and high mass HULIS of 3-4 substructures could be proposed. The postulated mass distributions of 2, 3 and 4 substructures were in good agreement with the recorded full scan spectra of HULIS. However, single organic compounds (< *m/z* 220) were still predominant compared to HULIS.

The unit resolution of the applied ion trap mass spectrometer yielded superimposed fragment spectra. Only information about the functionalities of HULIS were obtained. However, more precise structural information should be determined by a fourier transform ion cyclotron mass spectrometer. Structure elucidation of single humic-like compounds would be possible by highly selective isolation of precursor ions and highly resolved scanning of the resulting fragment ions. This would allow a confirmation of the proposed structures.

Further investigations should be performed by sulphatation of model compounds in a reaction chamber. HULIS should be generated in a smog chamber in presence of SO_2/sulphate. Furthermore, the aging of HULIS should be studied, as there might be a correlation with the degree of sulphatation. The quantification of HULIS might be further improved by selecting quantification standards, which are structurally closer to HULIS. Moreover, more samples should be analysed to confirm the observed seasonal trend. Finally, a comparison of the content of covalently bound sulphate in atmospheric aerosols with rain water and fog would be of interest.

3.5 References

Brimblecombe, P., 1996: *Air composition & chemistry*, Cambridge University Press, Cambridge.

Cappiello, A., De Simoni, E., Fiorucci, C., Mangani, F., Palma, P., Trufelli, H., Decesari, S., Facchini, M. C. and Fuzzi, S., 2003: Molecular Characterization of the Water-Soluble Organic Compounds in Fogwater by ESI-MS/MS, *Environ. Sci. Technol.* **37**, 1229-1240.

Feng, J. and Möller, D., 2004: Characterization of Water-Soluble Macromolecular Substances in Cloud Water, *J. Atmos. Chem.* **48**, 217-233.

Havers, N., Burba, P., Klockow, D. and Klockow-Beck, A., 1998: Characterisation of Humic-Like Substances in Airborne Particulate Matter by Capillary Electrophoresis, *Chromatographia* **47**, 619-624.

Havers, N., Burba, P., Lambert, J. and Klockow, D., 1998: Spectroscopic Characterization of Humic-Like Substances in Airborne Particulate Matter, *J. Atmos. Chem.* **29**, 45-54.

Jacobson, M. C., Hansson, H.-C., Noone, K. J. and Charlson, R. J., 2000: Organic Atmospheric Aerosols: Review and State of the Science, *Rev. Geophys.* **38**, 267-294.

Kiss, G., 2002: Characterization of water-soluble organic matter isolated from atmospheric fine aerosol, *J. Geophys. Res.* **107**, 1-1-1-8.

Kiss, G., Gelencser, A., Hoffer, A., Krivacsy, Z., Meszaros, E., Molnar, A. and Varga, B., 2000: Chemical Characterisation Of Water Soluble Organic Compounds In Tropospheric Fine Aerosol, *Proc. Conf. on Nucleation and Atmospheric Aerosols*, 761-764.

Kiss, G., Tombácz, E., Varga, B., Alsberg, T. and Persson, L., 2003: Estimation of the average molecular weight of humic-like substances isolated from fine atmospheric aerosol, *Atmos. Environ.* **37**, 3783-3794.

Limbeck, A. and Puxbaum, H., 1999: Organic acids in continental background aerosols, *Atmos. Environ.* **33**, 1847-1852.

Nolte, C. G., Schauer, J. J., Cass, G. R. and Simoneit, B. R. T., 2001: Highly Polar and Organic Compounds Present in Wood Smoke and in the Ambient Atmosphere, *Environ. Sci. Technol.* **35**, 1912-1919.

Novakov, T. and Penner, J. E., 1993: Large contribution of organic aerosols to cloud-condensation-nuclei concentrations, *Nature* **365**, 823-826.

Rogge, W. F., Mazurek, M. A., Hildemann, L. M., Cass, G. R. and Simoneit, B. R. T., 1993: Quantification of urban organic aerosols at a molecular level: identification, abundance and seasonal variation, *Atmos. Environ.* **27A**, 1309-1330.

Saxena, P. and Hildemann, L. M., 1996: Water-Soluble Organics in Atmospheric Particles: A Critical Review of the Literature and Application of Thermodynamics to Identify Candidate Compounds, *J. Atmos. Chem.* **24**, 57-109.

Seinfeld, J. H. and Pandis, S. N., 1998: *Atmospheric Chemistry and Physics*, Wiley-Interscience, New York.

Stenson, A. C., Marshall, A. G. and Cooper, W. T., 2003: Exact Masses and Chemical Formulas of Individual Suwanee River Fulvic Acids from Ultrahigh Resolution Electrospray Ionization Fourier Transform Ion Cyclotron Resonance Mass Spectra, *Anal. Chem.* **75**, 1275-1284.

UNEP, 2002: *Global Environment Outlook 3 - GEO 2003*, Earthscan Publication Ltd, London.

Varga, B., Kiss, G., Ganszky, I., Gelencser, A. and Krivacsy, Z., 2001: Isolation of water-soluble organic matter from atmospheric aerosol, *Talanta* **55**, 561-572.

Zappoli, S., Andracchio, A., Fuzzi, S., Facchini, M. C., Gelencser, A., Kiss, G., Krivacsy, Z., Molnar, A., Meszaros, E., Hansson, H.-C., Rosman, K. and Zebühr, Y., 1999: Inorganic, organic and macromolecular components of fine aerosol in different areas of Europe in relation to their water solubility, *Atmos. Environ.* **33**, 2733-2743.

Eidesstattliche Erklärung

Ich erkläre, dass ich die Dissertation "Structure elucidation of the water-soluble organic carbon fraction in atmospheric aerosols by mass spectrometry" selbständig nur mit der darin angegebenen Hilfe verfasst und bei keiner anderen Fakultät der Universität Basel eingereicht habe.

Basel, 21. April 2006

Fernando Romero